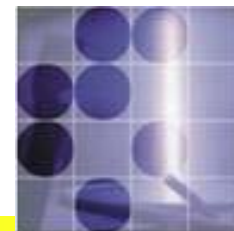


University of Ljubljana

“Jožef Stefan” Institute



High Intensity Frontier in Particle Physics (part 2/2)

Peter Križan

University of Ljubljana and J. Stefan Institute

Doctoral studies, Specialized Seminar on Experimental Physics

Peter Križan, Ljubljana



Contents of this course

- Lecture 1: Introduction, experimental methods, detectors, data analysis
- Lecture 2: Intensity frontier experiments

Contents

- Physics case for B factories / Super B factories
- Accelerator
- Detector

A little bit of history...

CP violation: difference in the properties of **particles** and their **anti-particles**
– first observed in 1964 in the decays of neutral kaons.

M. Kobayashi and T. Maskawa (1973): **CP violation** in the Standard model – related to the weak interaction **quark transition matrix**

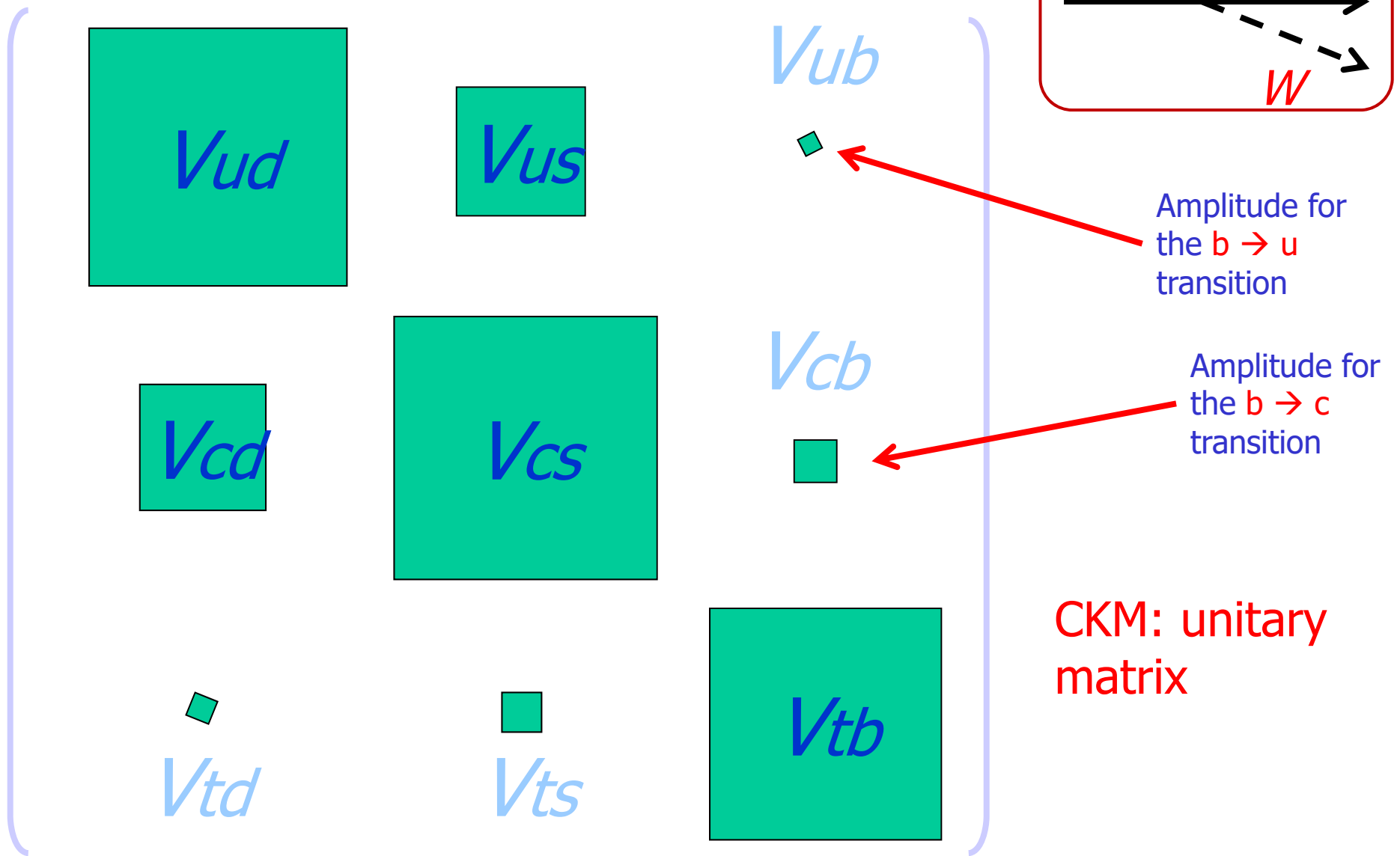
Their theory was formulated at a time when three quarks were known – and they requested the existence of three more!

The last missing quark was found in 1994.

... and in 2001 two experiments – Belle and BaBar at two powerful accelerators (B factories) - have further investigated CP violation and have indeed proven that it is tightly connected to the quark transition matrix

CKM - Cabibbo-Kobayashi-Maskawa (quark transition) matrix:

almost real and diagonal, but not completely!



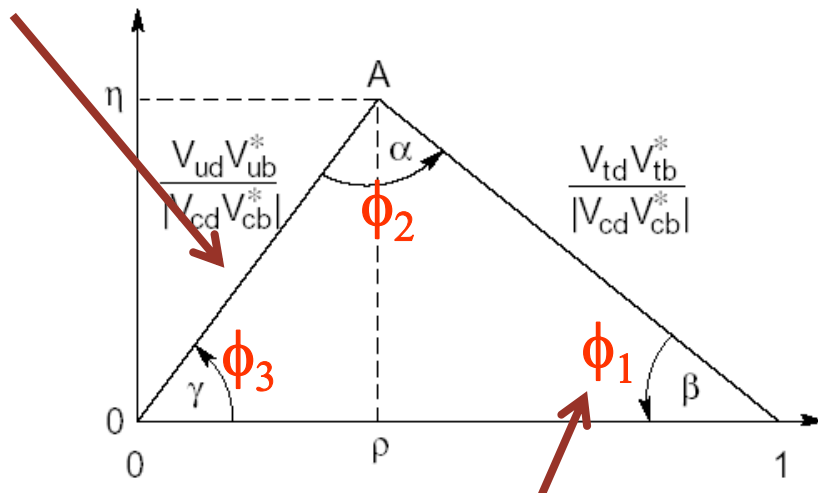
CKM matrix: determines charged weak interaction of quarks

Wolfenstein parametrisation: expand the CKM matrix in the parameter λ ($=\sin\theta_c=0.22$)

A, ρ and η : all of order one

$$V = \begin{pmatrix} 1 - \frac{\lambda^2}{2} & \lambda & A\lambda^3(\rho - i\eta) \\ -\lambda & 1 - \frac{\lambda^2}{2} & A\lambda^2 \\ A\lambda^3(1 - \rho - i\eta) & -A\lambda^2 & 1 \end{pmatrix} + O(\lambda^4)$$

determines probability of $b \rightarrow u$ transitions



determines CP violation in $B \rightarrow J/\psi K_S$ decays

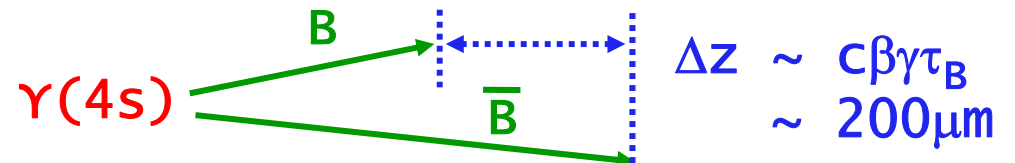
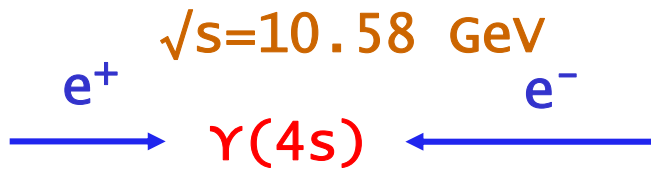
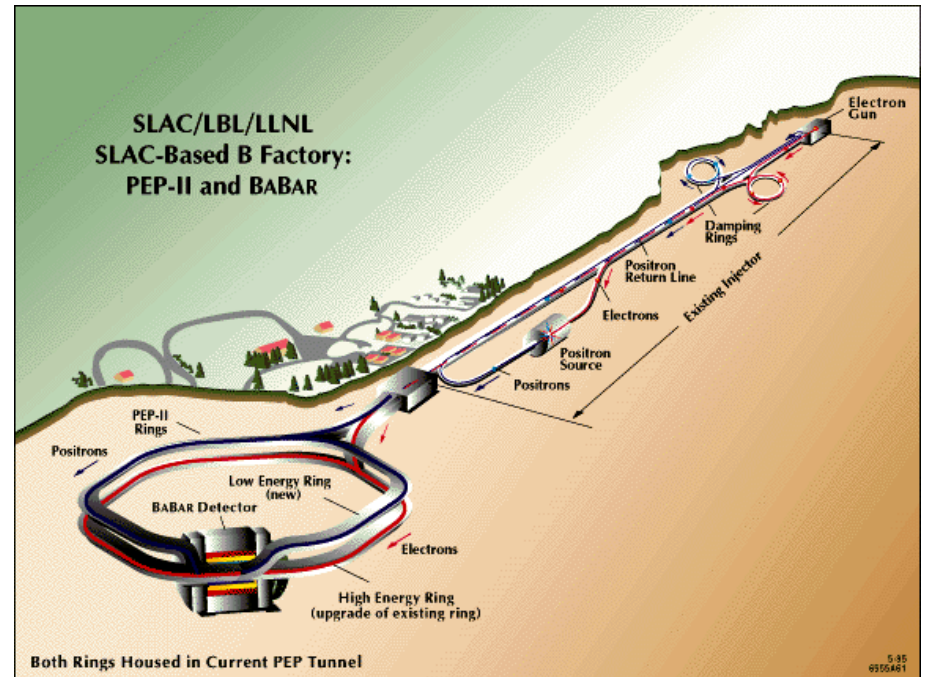
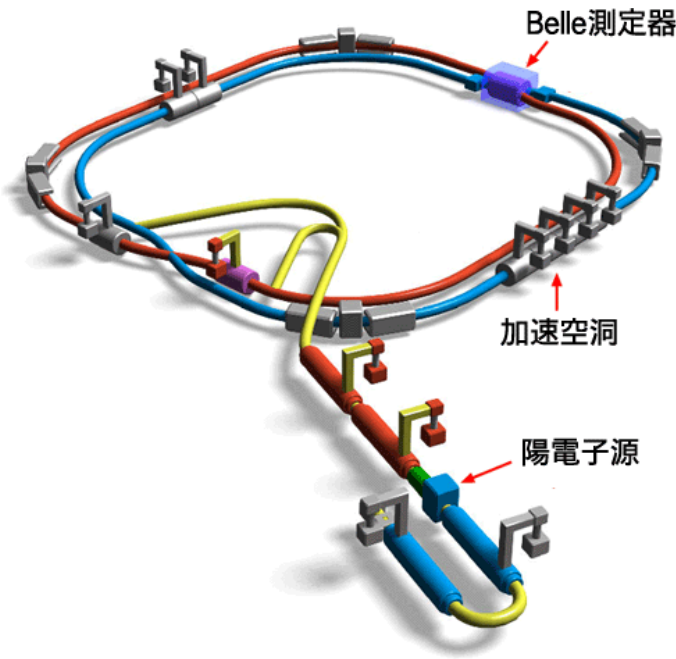
Unitarity condition:

$$V_{ud} V_{ub}^* + V_{cd} V_{cb}^* + V_{td} V_{tb}^* = 0$$



Goal: measure sides and angles in several different ways, check consistency \rightarrow

Asymmetric B factories



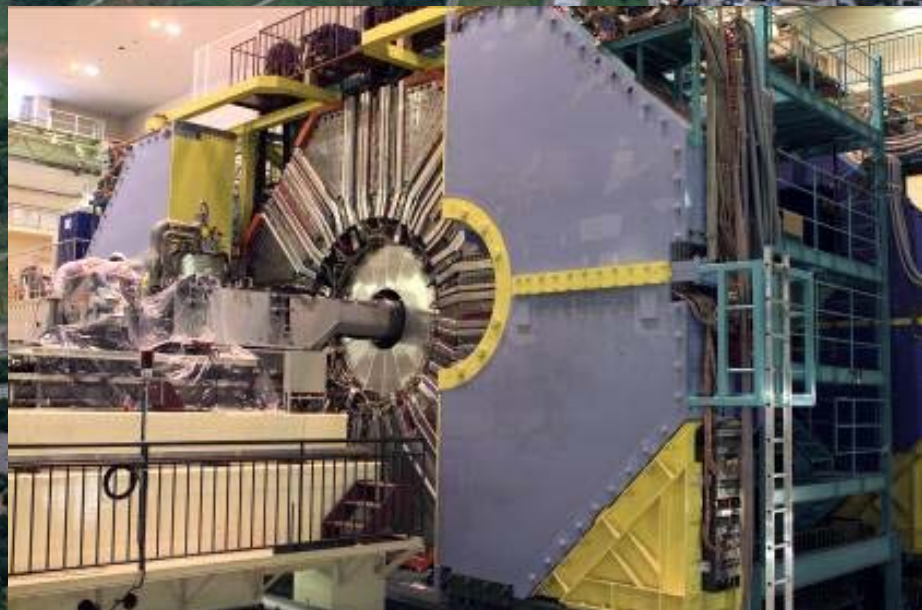
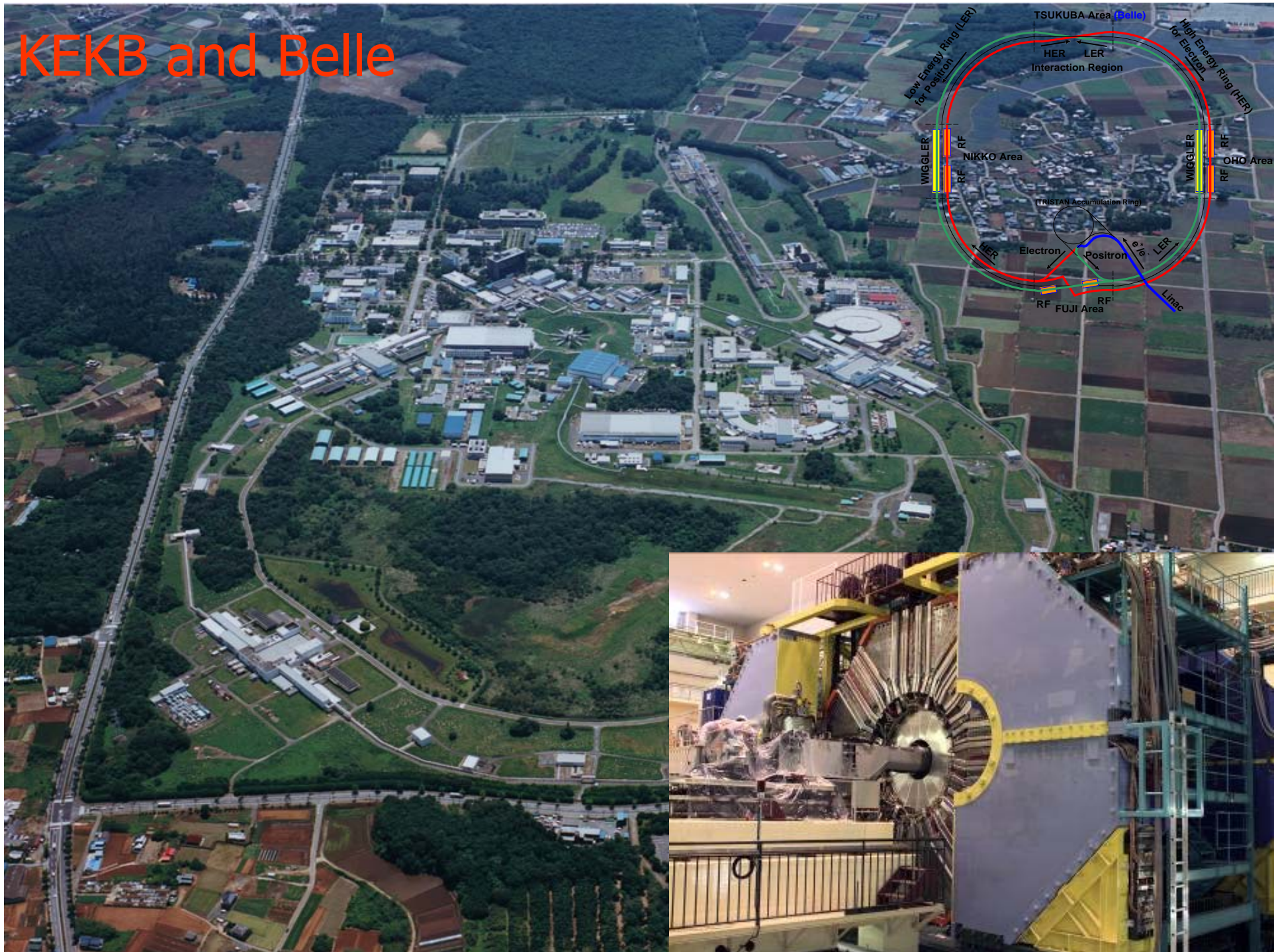
BaBar $p(e^-) = 9 \text{ GeV}$ $p(e^+) = 3.1 \text{ GeV}$

$\beta\gamma = 0.56$

Belle $p(e^-) = 8 \text{ GeV}$ $p(e^+) = 3.5 \text{ GeV}$

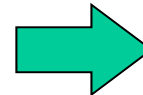
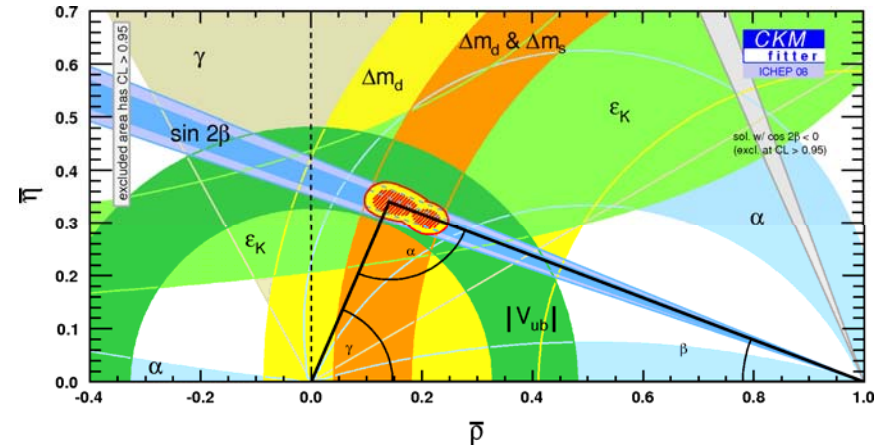
$\beta\gamma = 0.42$

KEKB and Belle



KM's bold idea verified by experiment

Relations between parameters
as expected in the Standard
model →

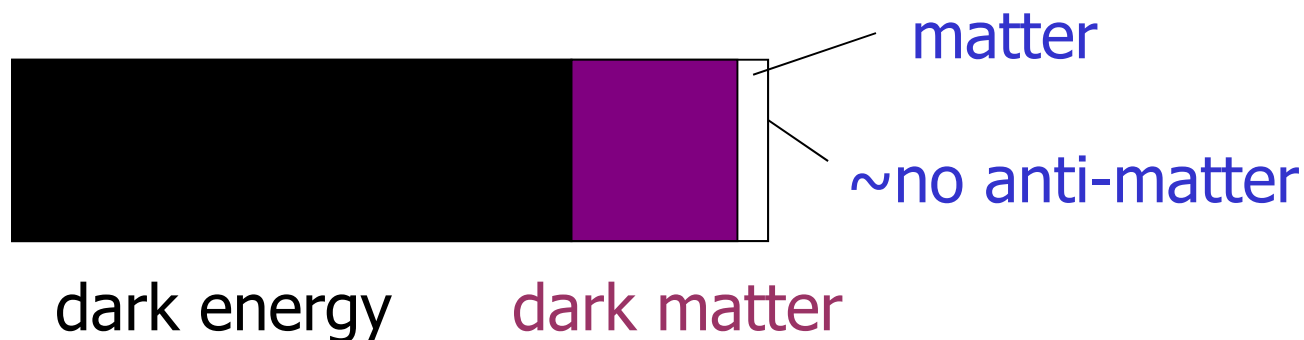


Nobel prize 2008!

→ With essential experimental confirmations by BaBar and Belle! (explicitly noted in the Nobel Prize citation)

The KM scheme is now part of the Standard Model of Particle Physics

- However, the CP violation of the KM mechanism is too small to account for the asymmetry between matter and anti-matter in the Universe (falls short by 10 orders of magnitude !)
- SM does not contain the fourth fundamental interaction, gravitation
- Most of the Universe is made of stuff we do not understand...



Are we done ? (Didn't the B factories accomplish their mission, recognized by the 2008 Nobel Prize in Physics ?)



*Из дарения С. Окубо
при большой температуре
для Вселенной сила слабо
но ее кривой фигуре*

НАРУШЕНИЕ CP-ИНВАРИАНТНОСТИ, C-АСИММЕТРИЯ
И БАРИОННАЯ АСИММЕТРИЯ ВСЕЛЕННОЙ

А.Д.Сазаров

Теория расширяющейся Вселенной, предполагающая сверхплотное начальное состояние вещества, по-видимому, исключает возможность макроскопического разделения вещества и антивещества; поэтому следует

**Matter - anti-matter
asymmetry of the Universe:
KM (Kobayashi-Maskawa)
mechanism still short by 10
orders of magnitude !!!**

Two frontiers

Two complementary approaches to study shortcomings of the Standard Model and to search for the so far unobserved processes and particles (so called New Physics, NP). These are the **energy frontier** and the **intensity frontier** .

Energy frontier : direct search for production of unknown particles at the highest achievable energies.

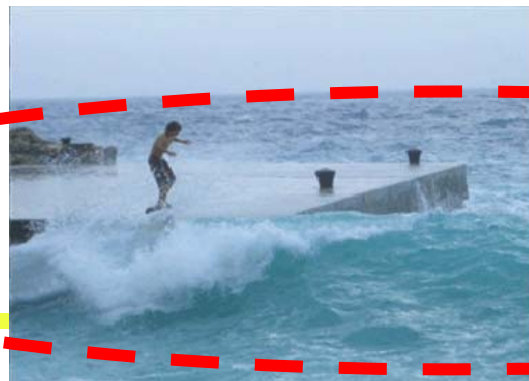
Intensity frontier : search for rare processes, deviations between theory predictions and experiments with the ultimate precision.

→ for this kind of studies, one has to investigate a very large number of reactions events → need accelerators with ultimate **intensity** (= luminosity)

Comparison of **energy** / **intensity** frontiers

To observe a large ship far away one can either use **strong binoculars** or observe **carefully the direction and the speed of waves** produced by the vessel.

Energy frontier (LHC)

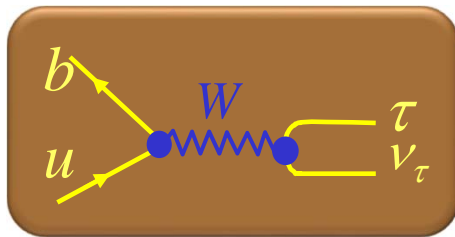


**Luminosity frontier
(Belle and Belle II)**

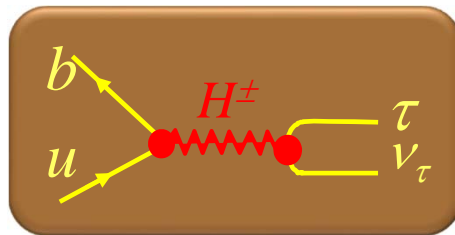
Peter Križan, Ljubljana

An example: Hunting the **charged Higgs** in the decay $B^- \rightarrow \tau^- \nu_\tau$

In addition to the Standard Model Higgs – as discovered at the LHC - in New Physics (e.g., in supersymmetric theories) there could also be a **charged Higgs**.



The rare decay $B^- \rightarrow \tau^- \nu_\tau$ is in SM mediated by the **W boson**

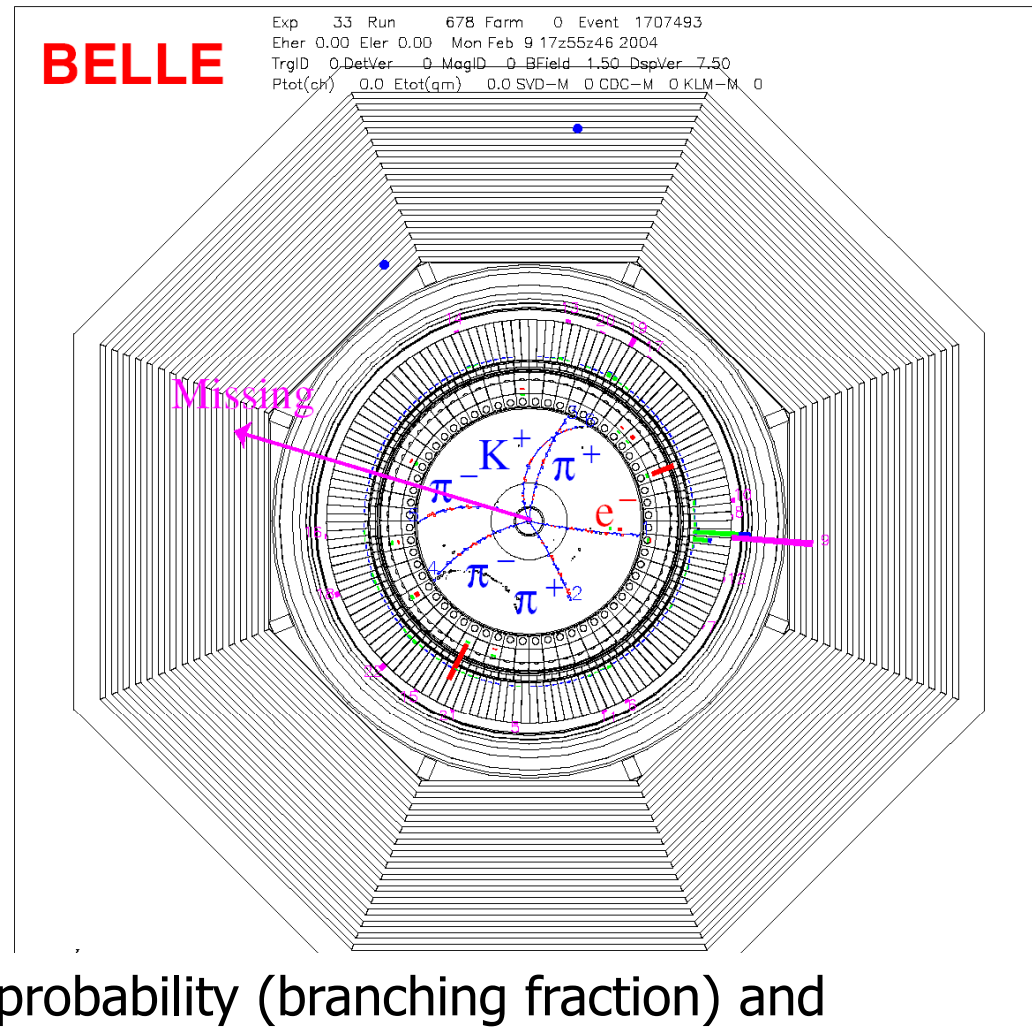


In some supersymmetric extensions it can also proceed via a **charged Higgs**

The **charged Higgs** would influence the decay of a B meson to a tau lepton and its neutrino, and modify the probability for this decay.

Missing Energy Decays: $B^- \rightarrow \tau^- \nu_\tau$

$$B^+ \rightarrow D^0 \pi^+ \\ (\rightarrow K \pi^- \pi^+ \pi^-) \\ B^- \rightarrow \tau (\rightarrow e \nu \bar{\nu}) \nu$$

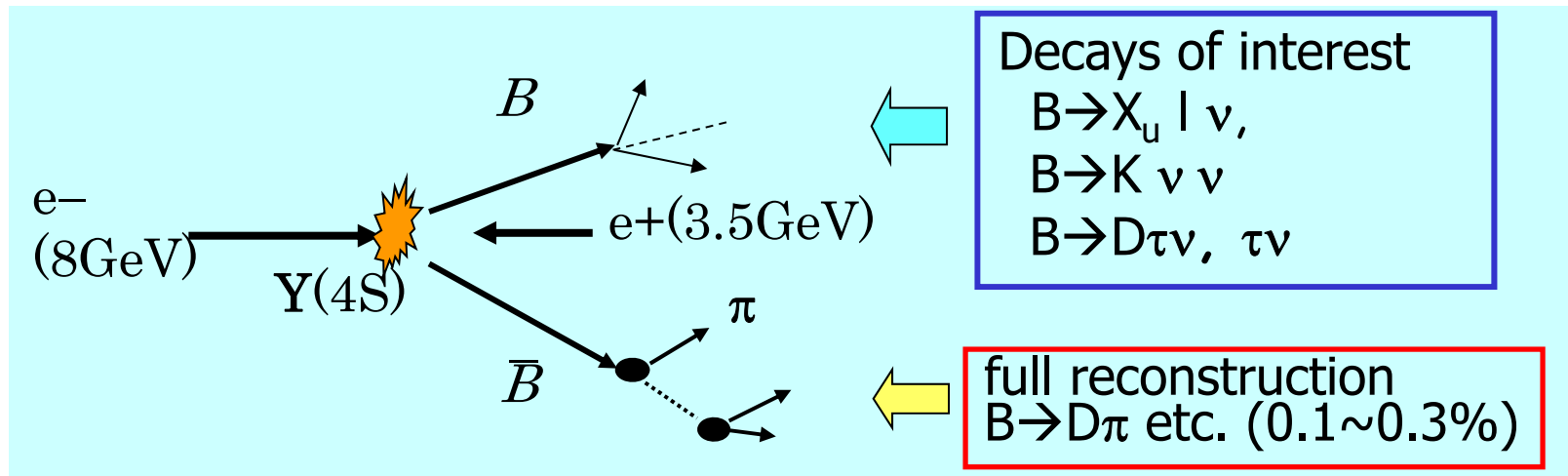


By measuring the decay probability (branching fraction) and comparing it to the SM expectation:

→ Properties of the charged Higgs (e.g. its mass)

Full Reconstruction Method

- Fully reconstruct one of the B's to
 - Tag B flavor/charge
 - Determine B momentum
 - Exclude decay products of one B from further analysis



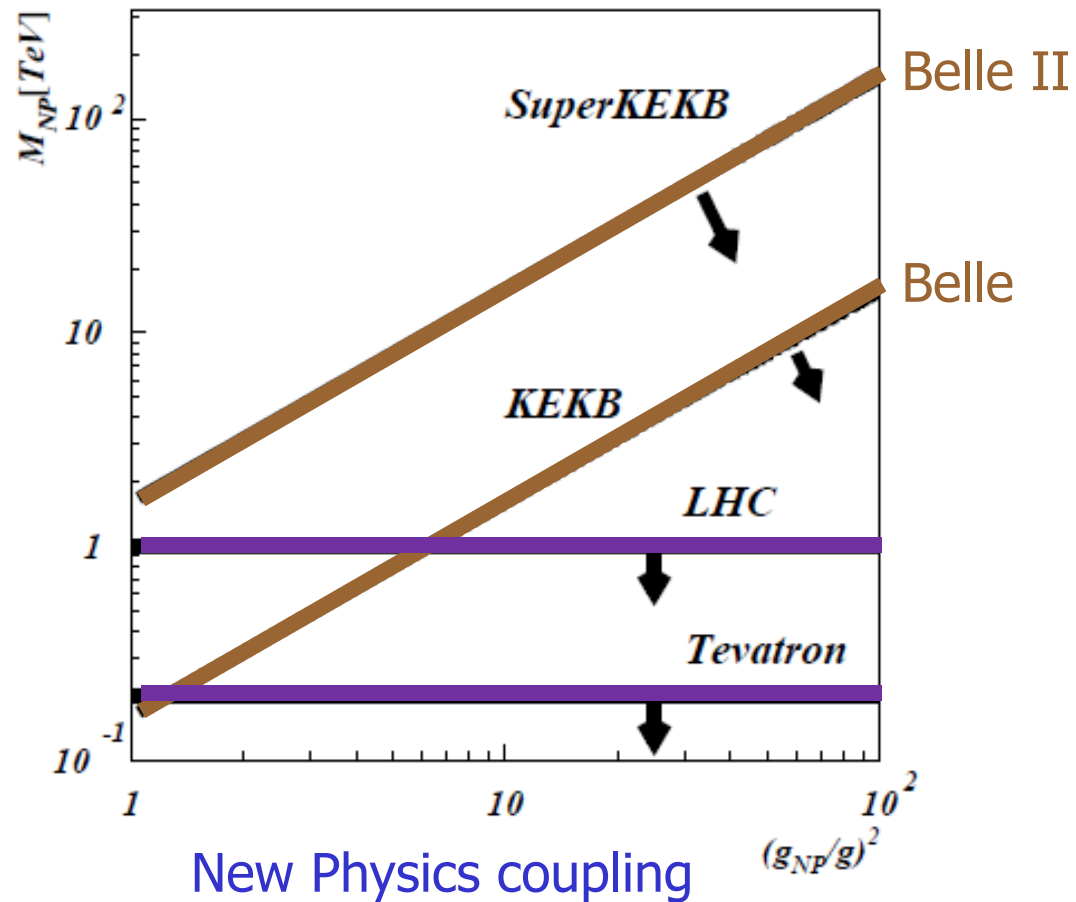
→ Offline B meson beam!

Powerful tool for B decays with neutrinos

New Physics reach

energy frontier vs. intensity frontier

New Physics mass scale (TeV)

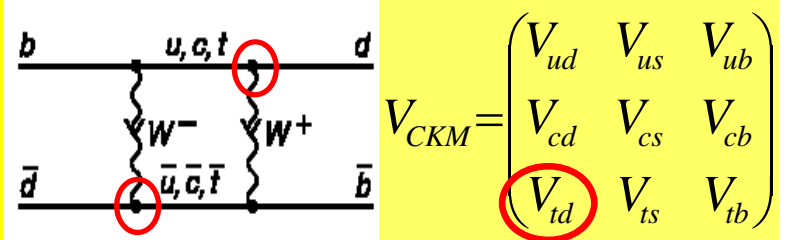


Super B Factory Motivation 2

- Lessons from history: the top quark

Physics of top quark

First estimate of mass: BB mixing → ARGUS
Direct production, Mass, width etc. → CDF/D0
Off-diagonal couplings, phase → BaBar/Belle



- Even before that: prediction of charm quark from the GIM mechanism, and its mass from K^0 mixing

Physics at a Super B Factory

- There is a good chance to see new phenomena;
 - **CPV in B decays from the new physics (non KM).**
 - **Lepton flavor violations in τ decays.**
- They will help to diagnose (if found) or constrain (if not found) new physics models.
- $B \rightarrow \tau \nu$, $D \tau \nu$ can probe the charged Higgs in large $\tan\beta$ region.
- **Physics motivation is independent of LHC.**
 - If LHC finds NP, precision flavour physics is compulsory.
 - If LHC finds no NP, high statistics B/ τ decays would be a unique way to search for the $> \text{TeV}$ scale physics (=TeV scale in case of MFV).

Physics reach with 50 ab^{-1} :

- Physics at Super B Factory (Belle II authors + guests)
hep-ex arXiv:1002.5012

Components of an experimental apparatus ('spectrometer')

- Tracking and vertexing systems
- Particle identification devices
- Calorimeters (measurement of energy)

Spectrometer design: what do we want to measure?

B factories: Time evolution in the B system

An arbitrary linear combination of the neutral B-meson flavor eigenstates

$$a|B^0\rangle + b|\bar{B}^0\rangle$$

with $a=a(t)$ and $b=b(t)$, is governed by a time-dependent Schroedinger equation

$$i\frac{d}{dt}\begin{pmatrix} a \\ b \end{pmatrix} = H\begin{pmatrix} a \\ b \end{pmatrix} = \left(M - \frac{i}{2}\Gamma\right)\begin{pmatrix} a \\ b \end{pmatrix}$$

M and Γ are 2x2 Hermitian matrices. CPT invariance $\rightarrow H_{11}=H_{22}$

$$M = \begin{pmatrix} M & M_{12} \\ M_{12}^* & M \end{pmatrix}, \Gamma = \begin{pmatrix} \Gamma & \Gamma_{12} \\ \Gamma_{12}^* & \Gamma \end{pmatrix}$$

diagonalize, solve \rightarrow

Time evolution of B's

Time evolution in the B^0 in \bar{B}^0 basis:

$$\begin{aligned} |B_{phys}^0(t)\rangle &= g_+(t)|B^0\rangle + (q/p)g_-(t)|\bar{B}^0\rangle \\ |\bar{B}_{phys}^0(t)\rangle &= (p/q)g_-(t)|B^0\rangle + g_+(t)|\bar{B}^0\rangle \end{aligned}$$

with

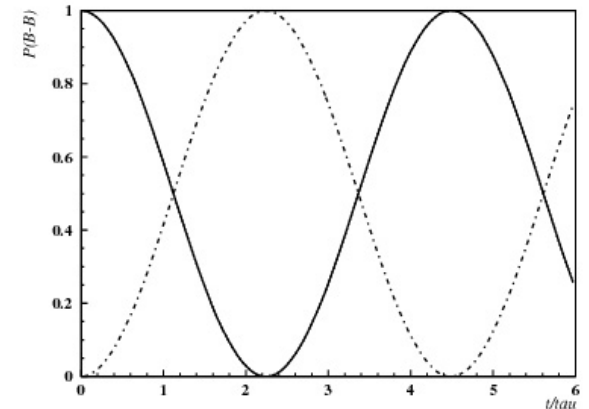
$$\begin{aligned} g_+(t) &= e^{-iMt} e^{-\Gamma t/2} \cos(\Delta mt / 2) \\ g_-(t) &= e^{-iMt} e^{-\Gamma t/2} i \sin(\Delta mt / 2) \end{aligned}$$

$$M = (M_H + M_L)/2$$

If B mesons were stable ($\Gamma=0$), the time evolution would look like:

$$g_+(t) = e^{-iMt} \cos(\Delta mt / 2)$$

$$g_-(t) = e^{-iMt} i \sin(\Delta mt / 2)$$



→Probability that a B turns into its anti-particle

→beat in classical mechanics

$$\left| \langle \bar{B}^0 | B_{phys}^0(t) \rangle \right|^2 = |q/p|^2 |g_-(t)|^2 = |q/p|^2 \sin^2(\Delta mt / 2)$$

→Probability that a B remains a B

$$\left| \langle B^0 | B_{phys}^0(t) \rangle \right|^2 = |g_+(t)|^2 = \cos^2(\Delta mt / 2)$$

→Expressions familiar from quantum mechanics of a two level system, neutrino mixing etc

CP violation: decay rate difference

Decay rate asymmetry:

$$a_{f_{CP}} = \frac{P(\bar{B}^0 \rightarrow f_{CP}, t) - P(B^0 \rightarrow f_{CP}, t)}{P(\bar{B}^0 \rightarrow f_{CP}, t) + P(B^0 \rightarrow f_{CP}, t)}$$

Decay rate: $P(B^0 \rightarrow f_{CP}, t) \propto \left| \langle f_{CP} | H | B_{phys}^0(t) \rangle \right|^2$

Decay amplitudes vs time:

$$\langle f_{CP} | H | B_{phys}^0(t) \rangle = g_+(t) \langle f_{CP} | H | B^0 \rangle + (q/p) g_-(t) \langle f_{CP} | H | \bar{B}^0 \rangle$$

$$= g_+(t) A_{f_{CP}} + (q/p) g_-(t) \bar{A}_{f_{CP}}$$

$$\langle f_{CP} | H | \bar{B}_{phys}^0(t) \rangle = (p/q) g_-(t) \langle f_{CP} | H | B^0 \rangle + g_+(t) \langle f_{CP} | H | \bar{B}^0 \rangle$$

$$= (p/q) g_-(t) A_{f_{CP}} + g_+(t) \bar{A}_{f_{CP}}$$

$$a_{f_{CP}} = \frac{P(\bar{B}^0 \rightarrow f_{CP}, t) - P(B^0 \rightarrow f_{CP}, t)}{P(\bar{B}^0 \rightarrow f_{CP}, t) + P(B^0 \rightarrow f_{CP}, t)} =$$

CP violation: asymmetry
in time evolution of B
and anti-B

$$= \frac{\left| (p/q)g_-(t)A_{f_{CP}} + g_+(t)\bar{A}_{f_{CP}} \right|^2 - \left| g_+(t)A_{f_{CP}} + (q/p)g_-(t)\bar{A}_{f_{CP}} \right|^2}{\left| (p/q)g_-(t)A_{f_{CP}} + g_+(t)\bar{A}_{f_{CP}} \right|^2 + \left| g_+(t)A_{f_{CP}} + (q/p)g_-(t)\bar{A}_{f_{CP}} \right|^2} =$$

$$= \frac{(1 - |\lambda_{f_{CP}}|^2) \cos(\Delta mt) - 2 \operatorname{Im}(\lambda_{f_{CP}}) \sin(\Delta mt)}{1 + |\lambda_{f_{CP}}|^2}$$

$$= C \cos(\Delta mt) + S \sin(\Delta mt)$$

$$\lambda_{f_{CP}} = \frac{q}{p} \frac{\bar{A}_{f_{CP}}}{A_{f_{CP}}}$$

Non-zero effect if $\operatorname{Im}(\lambda) \neq 0$, even if
 $|\lambda| = 1$

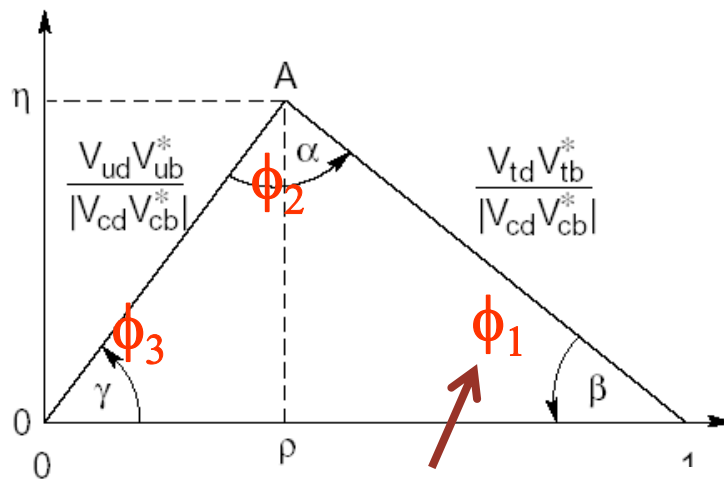
If $|\lambda| = 1 \rightarrow$

$$a_{f_{CP}} = -\operatorname{Im}(\lambda) \sin(\Delta mt)$$

CP violation: related to the angles of the unitarity triangle

$$a_{f_{CP}} = -\text{Im}(\lambda) \sin(\Delta mt)$$

$\text{Im}(\lambda) = \sin 2\phi_1$ in $B \rightarrow J/\psi K_S$ decays!



7-92

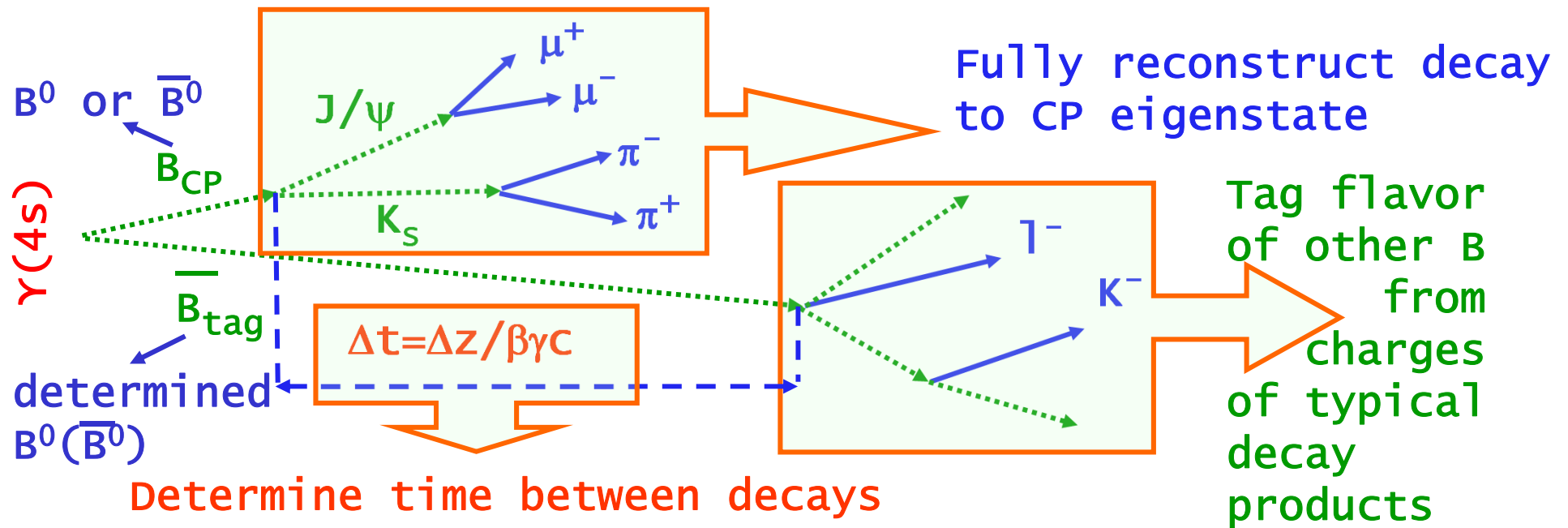
determines CP violation in $B \rightarrow J/\psi K_S$ decays

Unitarity condition:

$$V_{ud} V_{ub}^* + V_{cd} V_{cb}^* + V_{td} V_{tb}^* = 0$$



Typical measurement

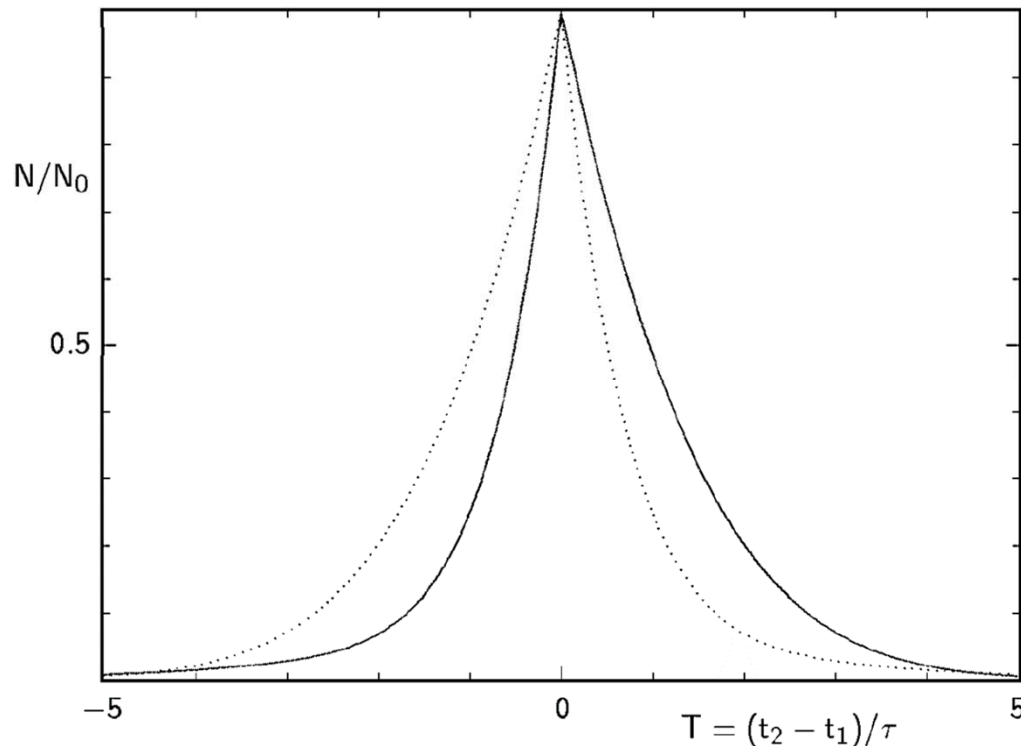


Experimental considerations

What kind of vertex resolution do we need to measure the asymmetry?

$$P(B^0(\bar{B}^0) \rightarrow f_{CP}, t) = e^{-\Gamma t} (1 \pm \sin(2\phi_1) \sin(\Delta m t))$$

↑ We are measuring this parameter



Want to distinguish the decay rate of **B** (dotted) from the decay rate of **anti-B** (full).

-> the two curves should not be smeared too much

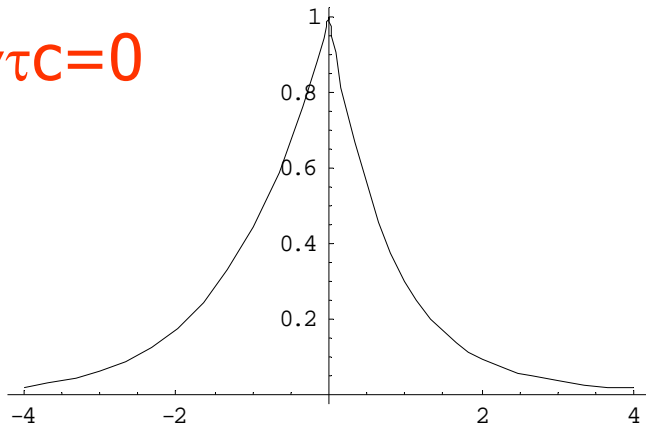
Integrals are equal, time information mandatory!

T = time difference of the two decays

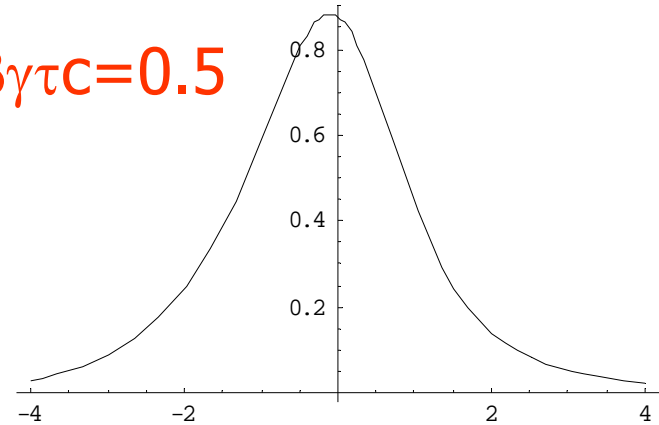
Experimental considerations

B decay rate vs t for different vertex resolutions in units of typical B flight length $\sigma(z)/\beta\gamma\tau c$

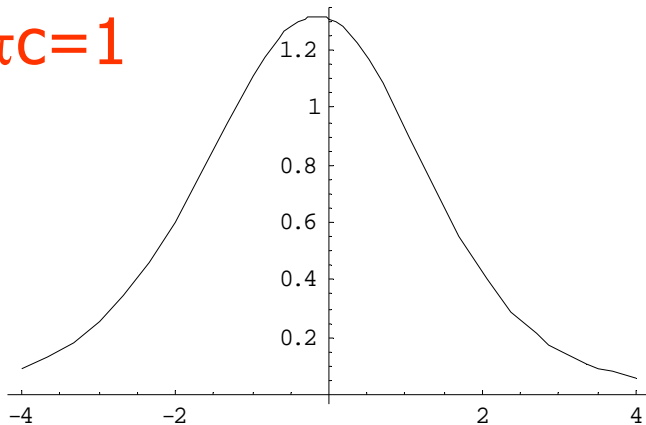
$$\sigma(z)/\beta\gamma\tau c = 0$$



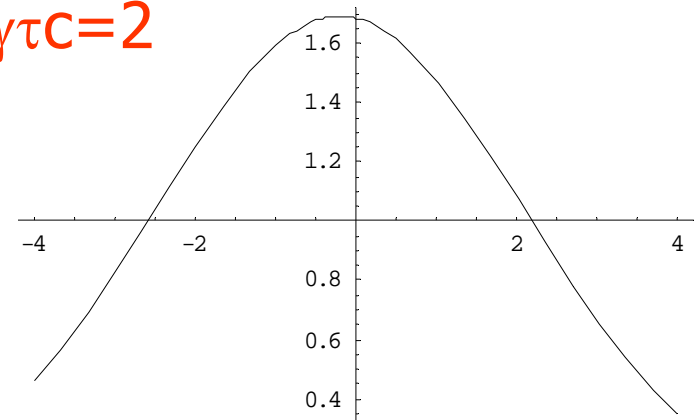
$$\sigma(z)/\beta\gamma\tau c = 0.5$$



$$\sigma(z)/\beta\gamma\tau c = 1$$



$$\sigma(z)/\beta\gamma\tau c = 2$$

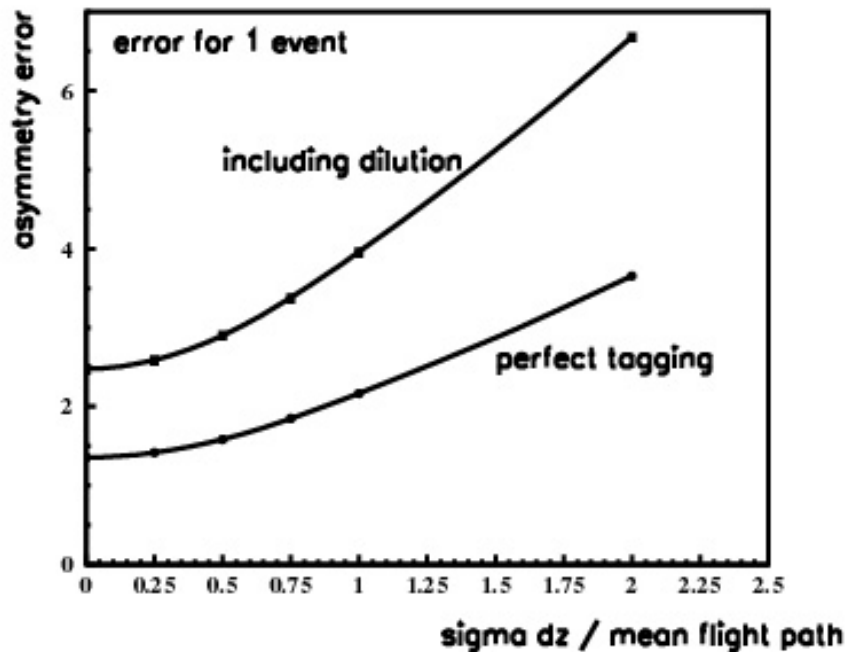


Measured distribution: convolution of $P(t)$ and the resolution function (e.g., a Gaussian with $\sigma = \sigma(z)/\beta\gamma\tau c$)

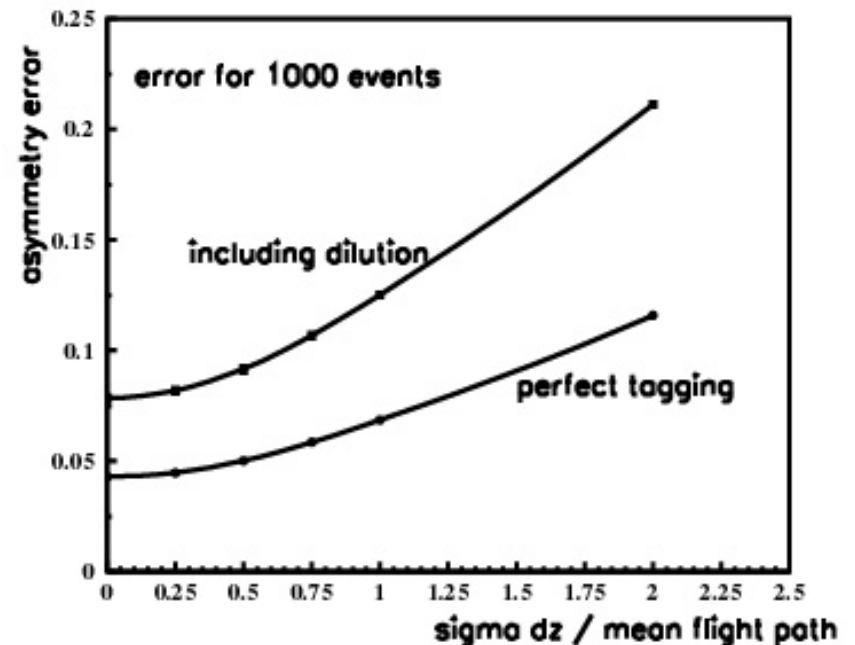
Experimental considerations

Error on $\sin 2\phi_1 = \sin 2\beta$ as a function of the vertex resolution in units of typical B flight length $\sigma(z)/\beta\gamma\tau c$

For 1 event



for 1000 events



Experimental considerations

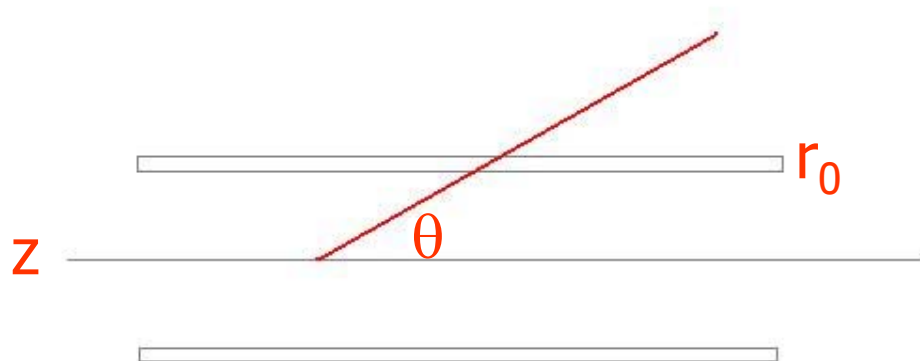
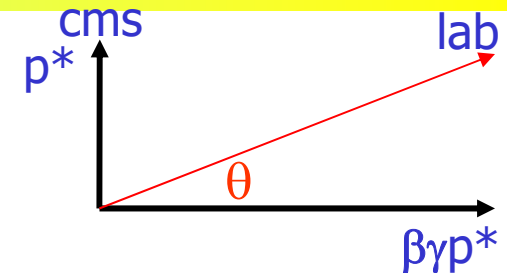
Choice of boost $\beta\gamma$:

Vertex resolution vs. path length

Typical B flight length: $z_B = \beta\gamma\tau c$

Typical two-body topology: decay products at 90° in cms; at $\theta = \text{atan}(1/\beta\gamma)$ in the lab

Assume: vertex resolution determined by multiple scattering in the first detector layer and beam pipe wall at r_0



$$\sigma_\theta = 15 \text{ MeV}/p \sqrt{d/\sin\theta X_0}$$

$$\sigma(z) = \sigma_\theta (dz/d\theta) = r_0 \sigma_\theta / \sin^2\theta$$

➔ $\sigma(z) \propto r_0 / \sin^{5/2}\theta$

Experimental considerations

Choice of boost $\beta\gamma$:

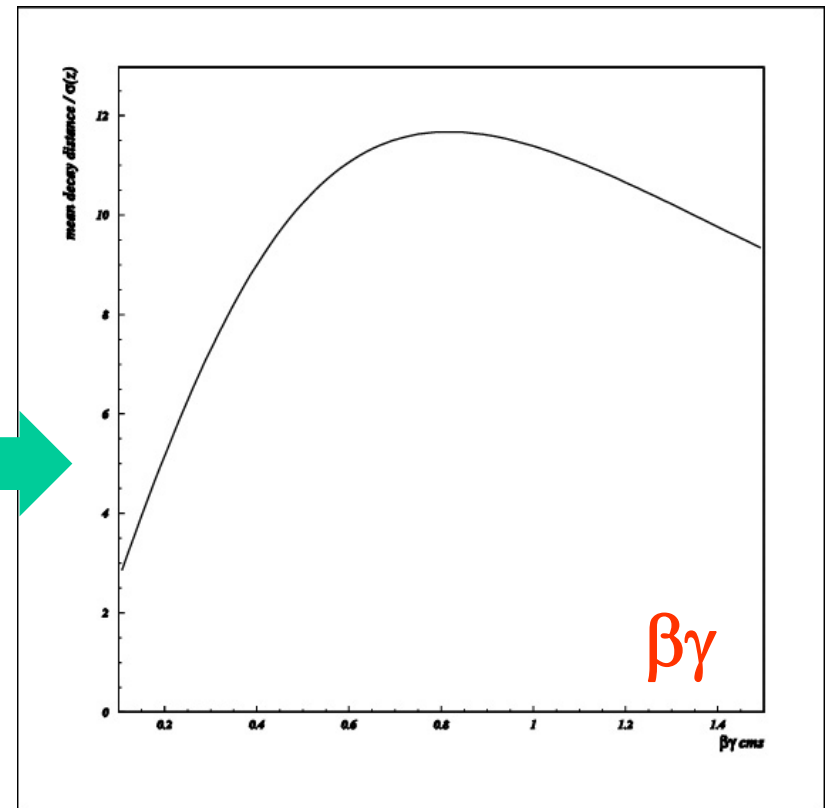
Maximize the ratio between the average flight path $\beta\gamma\tau c$ and the vertex resolution $\sigma(z)$

$\sigma(z) \propto r_0/\sin^{5/2}\theta$ with
 $\theta = \text{atan}(1/\beta\gamma)$

$\beta\gamma\tau c/\sigma(z) \propto (1/r_0) \beta\gamma\tau c \sin^{5/2}\theta =$
 $= (1/r_0) \beta\gamma\tau c \sin^{5/2}(\text{atan}(1/\beta\gamma))$

Boost around $\beta\gamma=0.8$ seems optimal

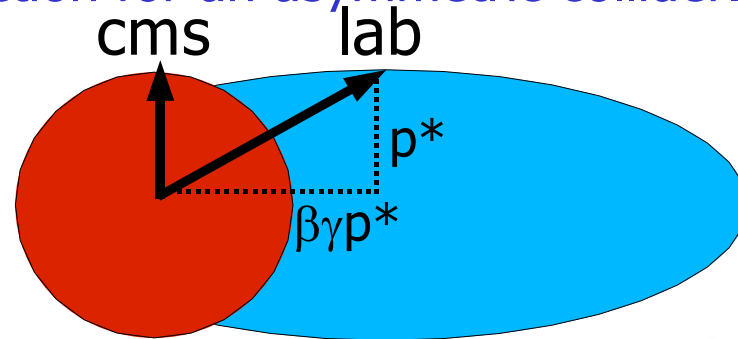
$\beta\gamma\tau c/\sigma(z)$



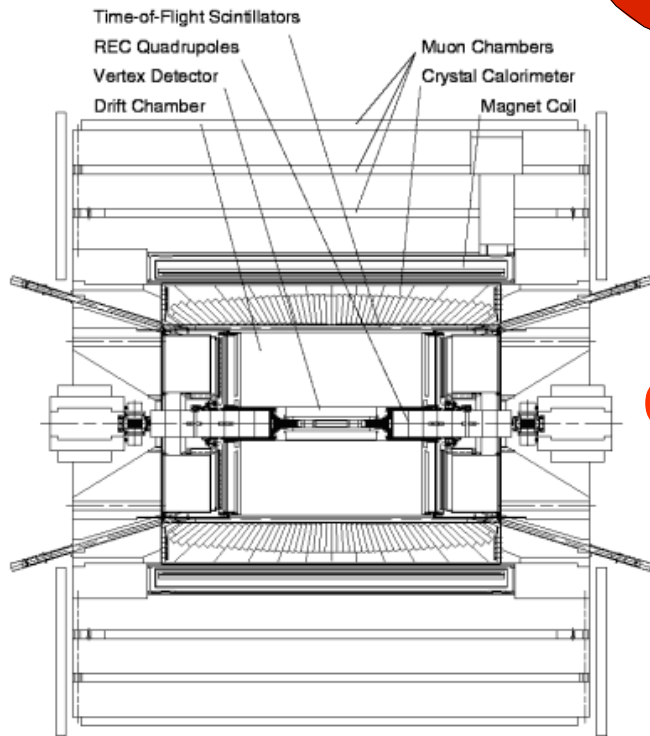
Not the whole story....

Experimental considerations

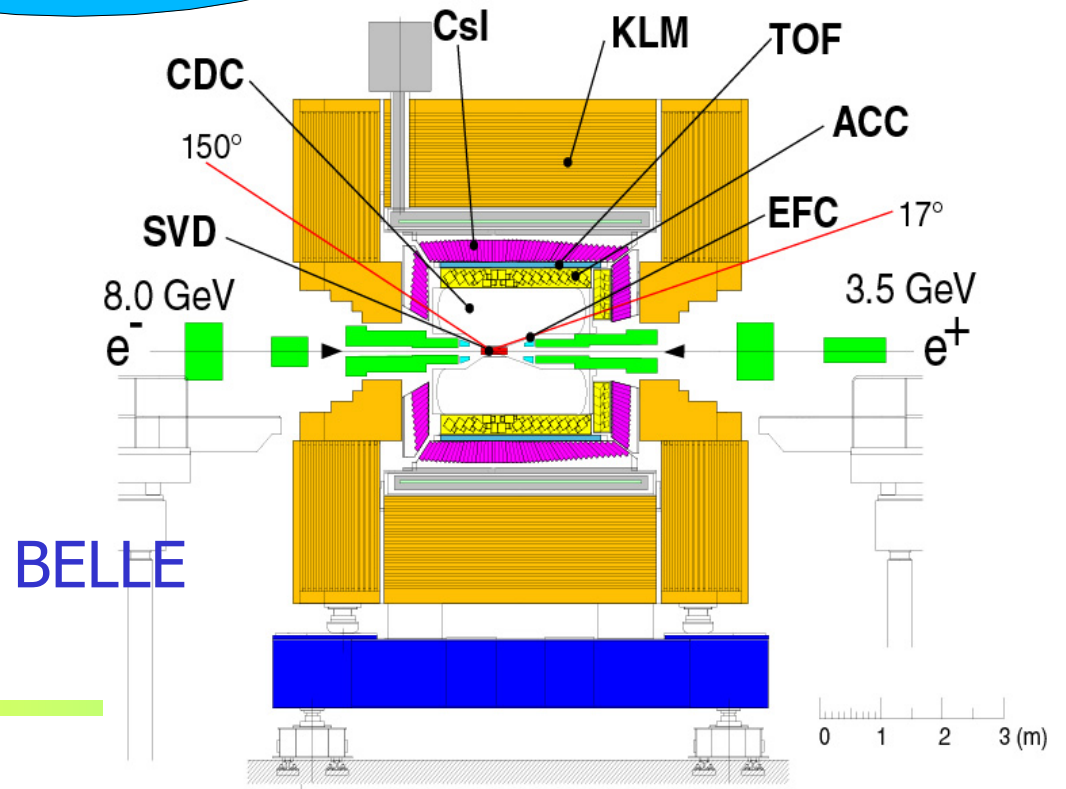
Detector form: symmetric for symmetric energy beams; extended in the boost direction for an asymmetric collider.



Exaggerated plot: in reality $\beta\gamma=0.5$



CLEO



BELLE

Experimental considerations

Which boost...

Arguments for a smaller boost:

- Larger boost -> smaller acceptance
(particles escape in the boosted direction) ->
- Larger boost -> it becomes hard to damp the betatron oscillations of the low energy beam: less synchrotron radiation at fixed ring radius (same as the high energy beam)

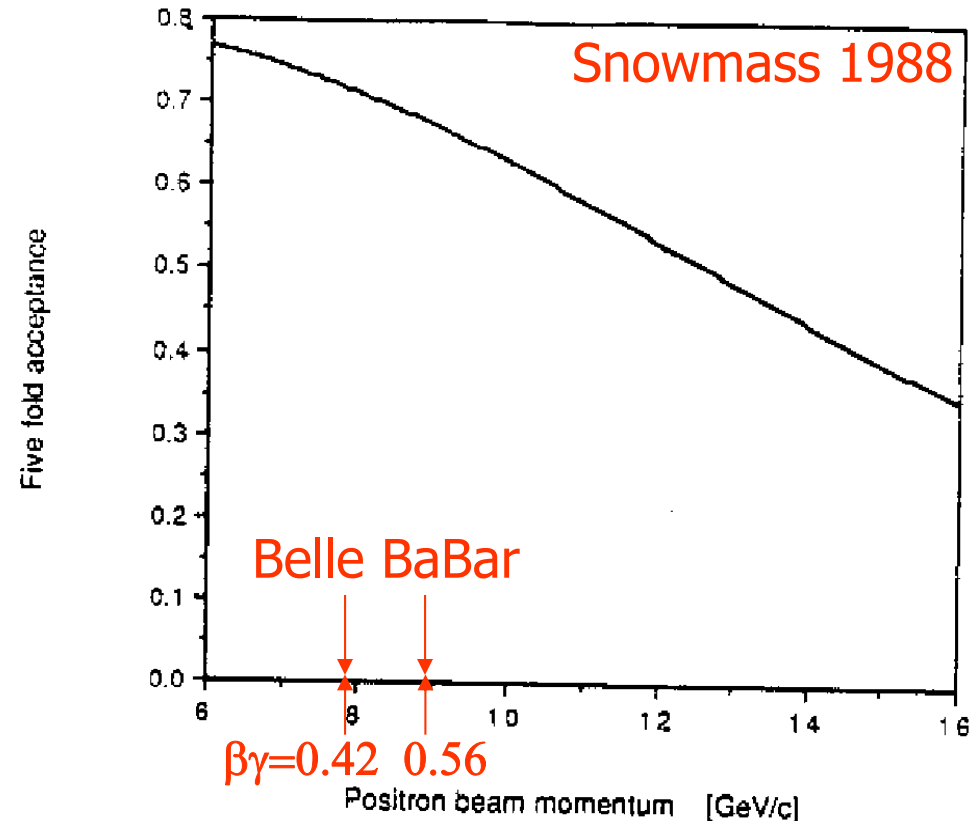
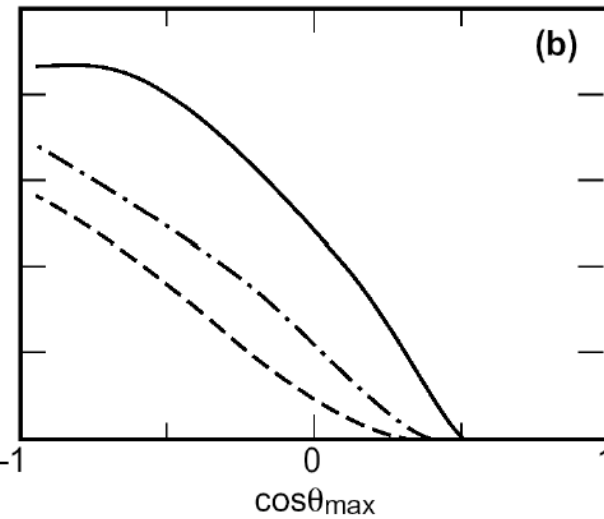
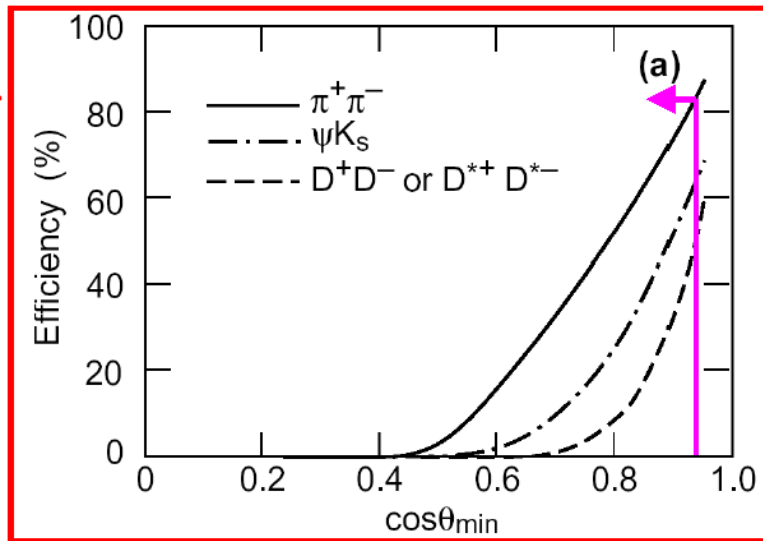
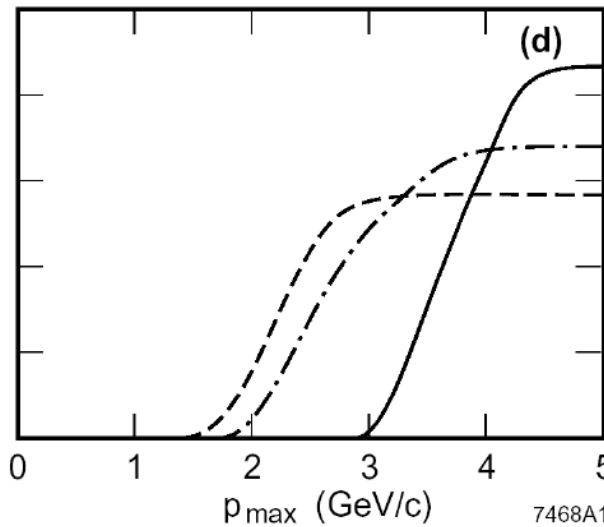
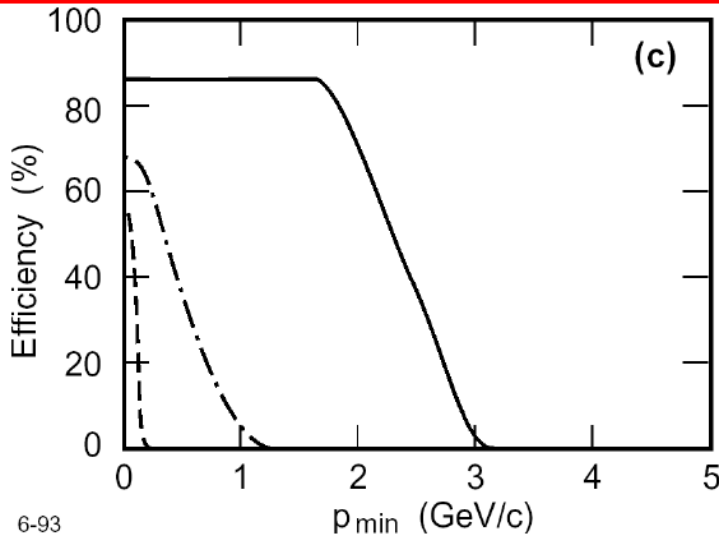


Figure 4. The acceptance of a detector covering $|\cos \theta_{lab}| < 0.95$ for five uncorrelated particles as a function of the energy of the more energetic beam in an asymmetric collider at the $\Upsilon(4S)$.

Requirements: Geometric Acceptance



Angular coverage



Momentum coverage

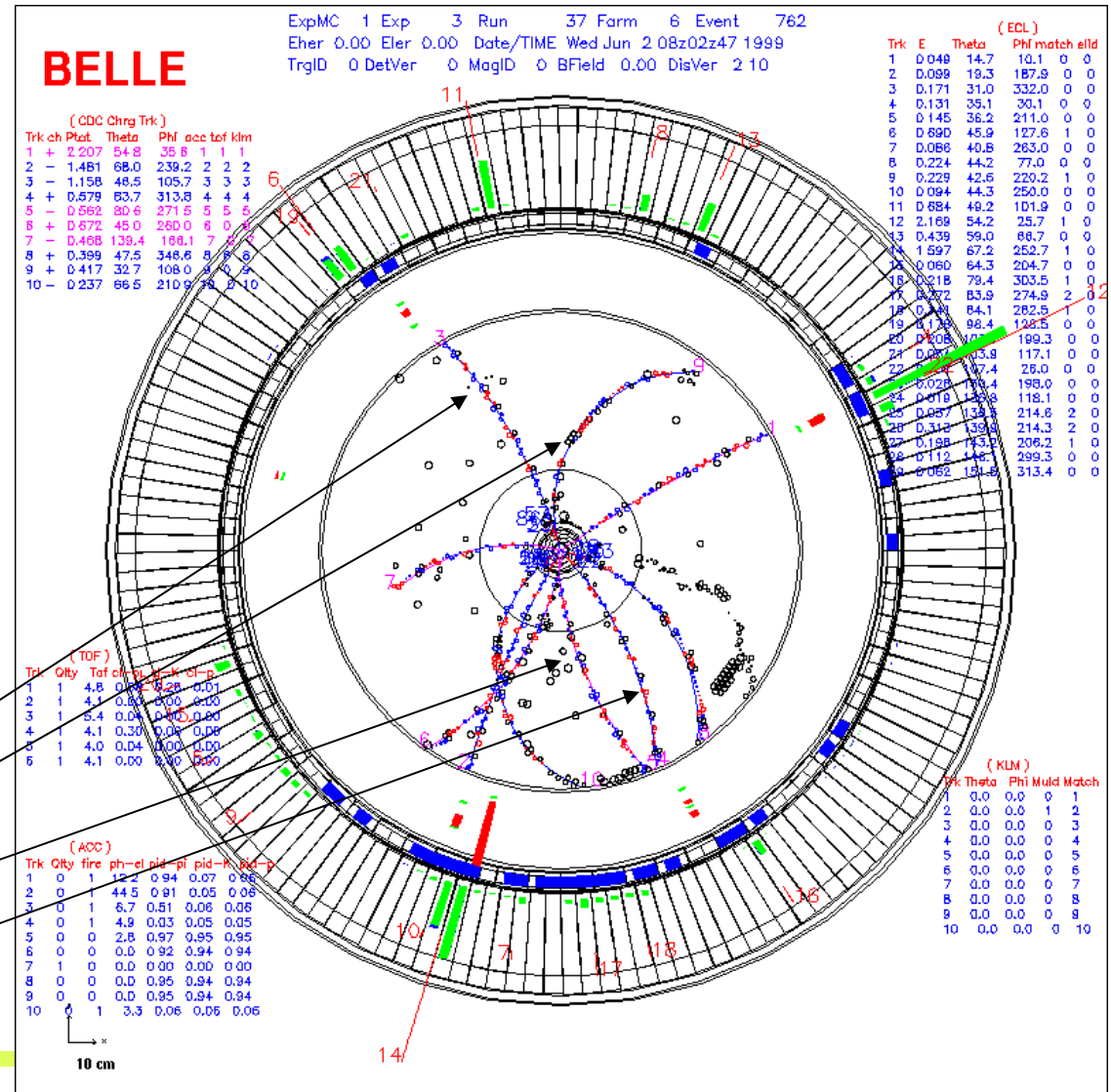
How to understand what happened in a collision?

Illustration on an example:

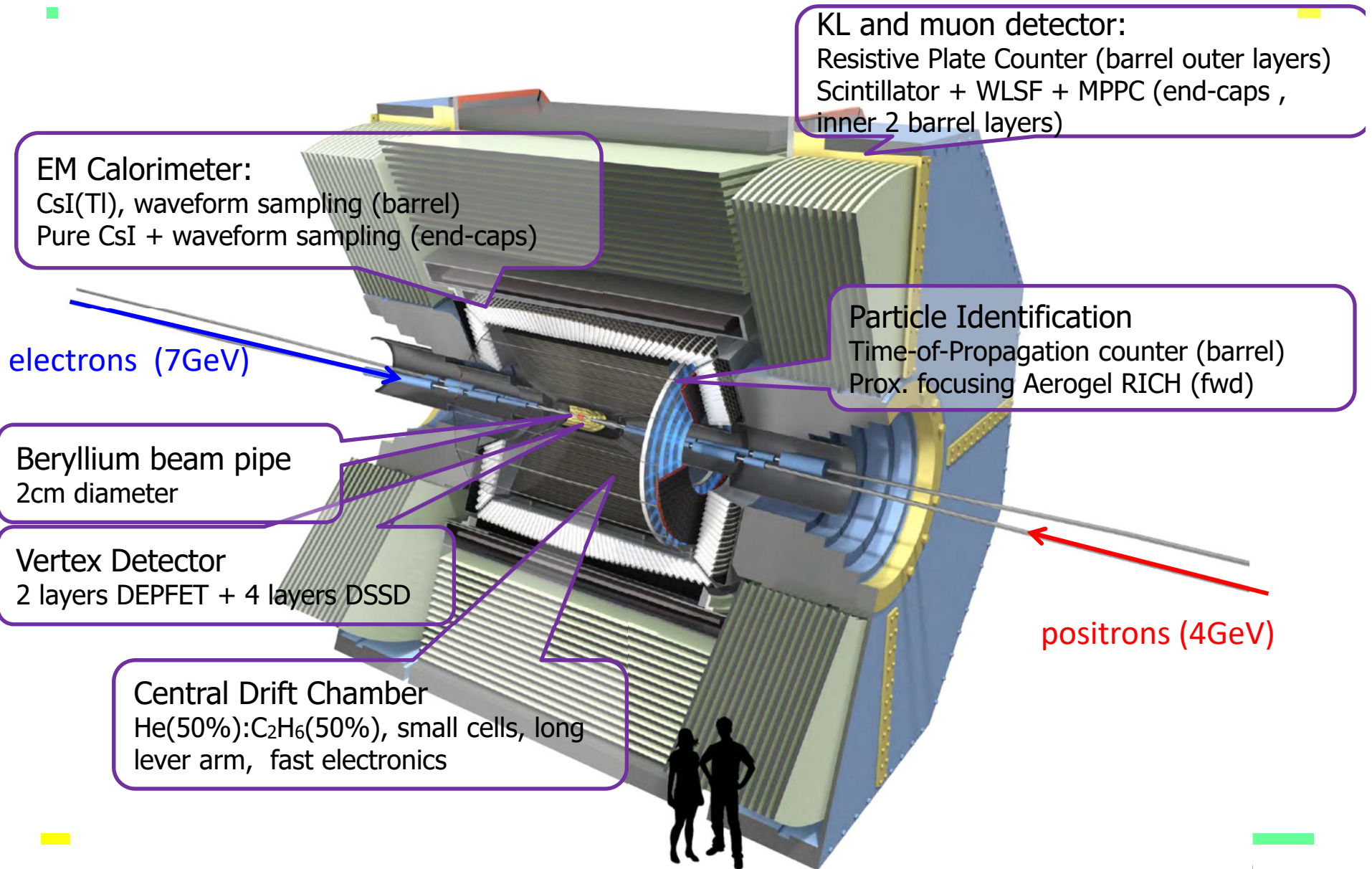
$$B^0 \rightarrow K_S^0 J/\psi$$

$$K_S^0 \rightarrow \pi^- \pi^+$$

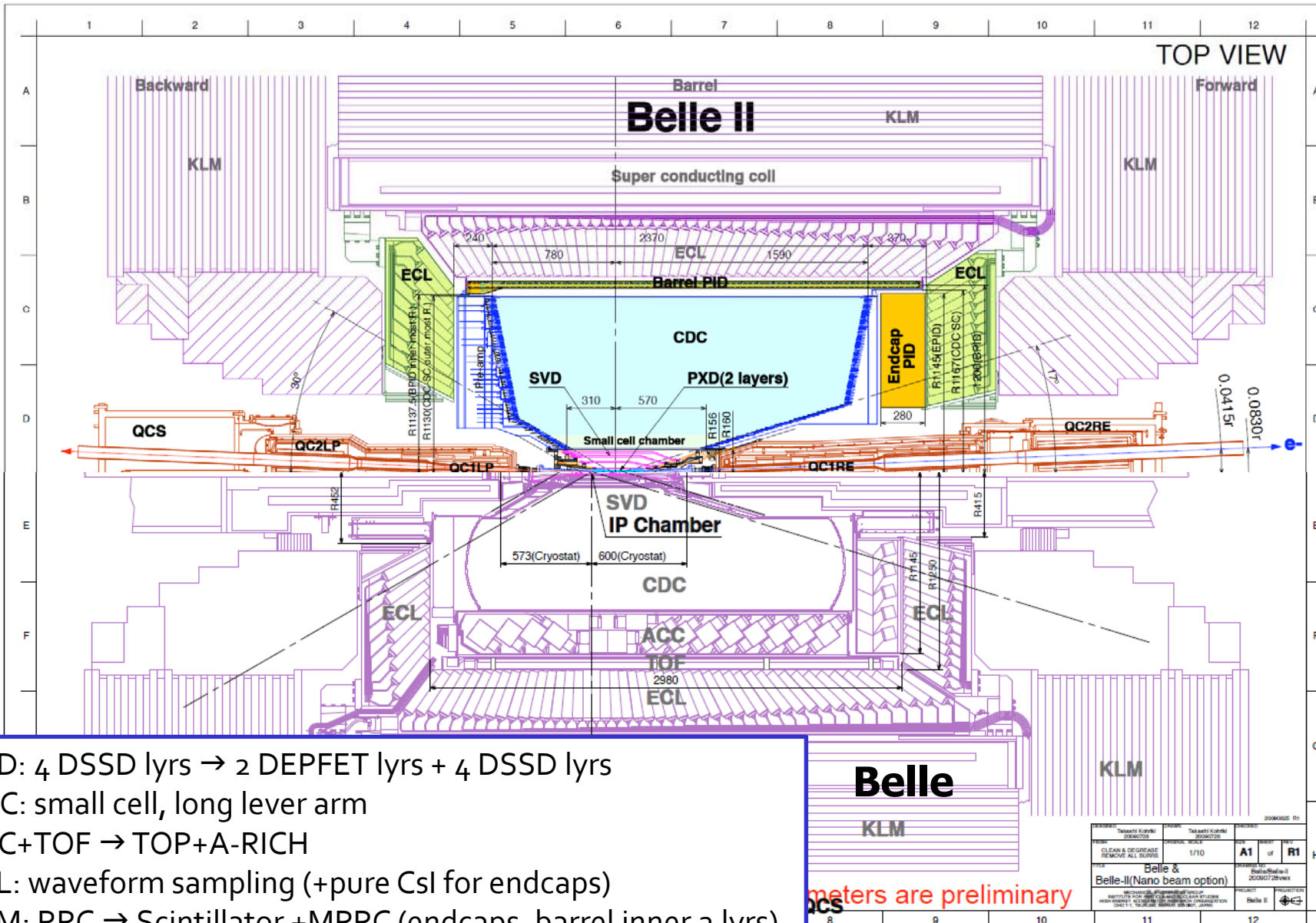
$$J/\psi \rightarrow \mu^- \mu^+$$



Belle II Detector



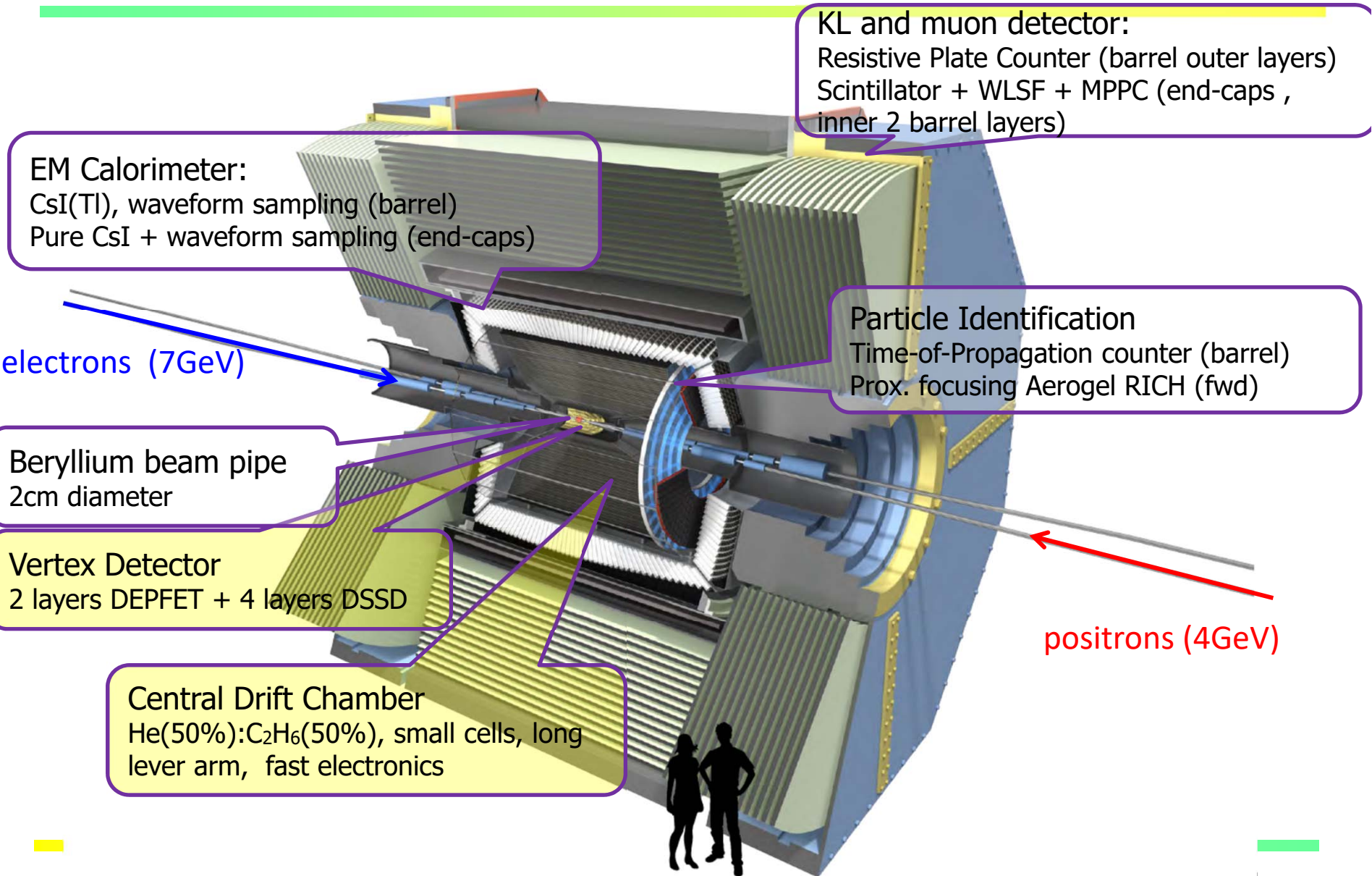
Belle II Detector (in comparison with Belle)



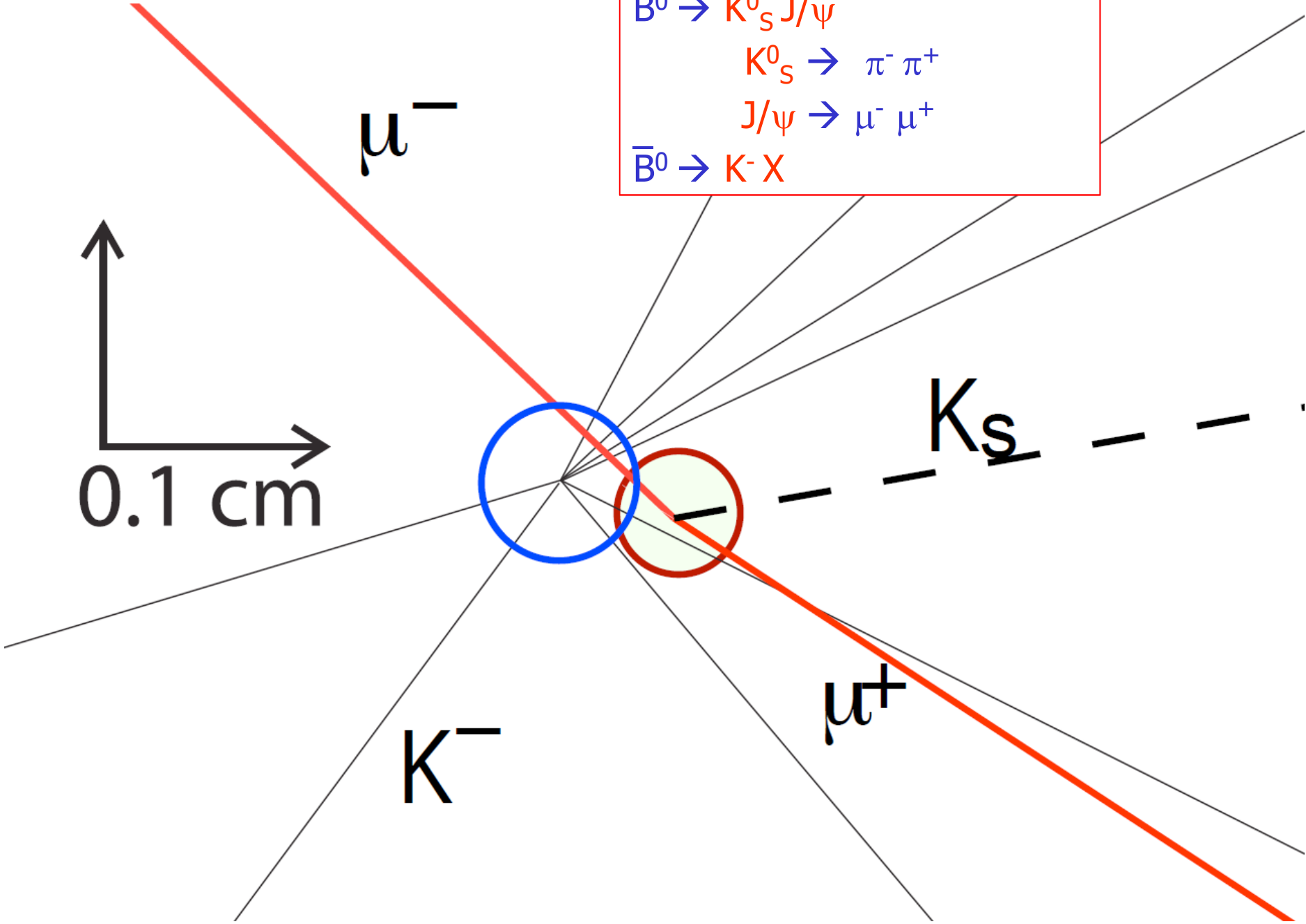
SVD: 4 DSSD lyrs → 2 DEPFET lyrs + 4 DSSD lyrs
 CDC: small cell, long lever arm
 ACC+TOF → TOP+A-RICH
 ECL: waveform sampling (+pure CsI for endcaps)
 KLM: RPC → Scintillator +MPPC (endcaps, barrel inner 2 lyrs)

meters are preliminary

Tracking and vertex systems in Belle II

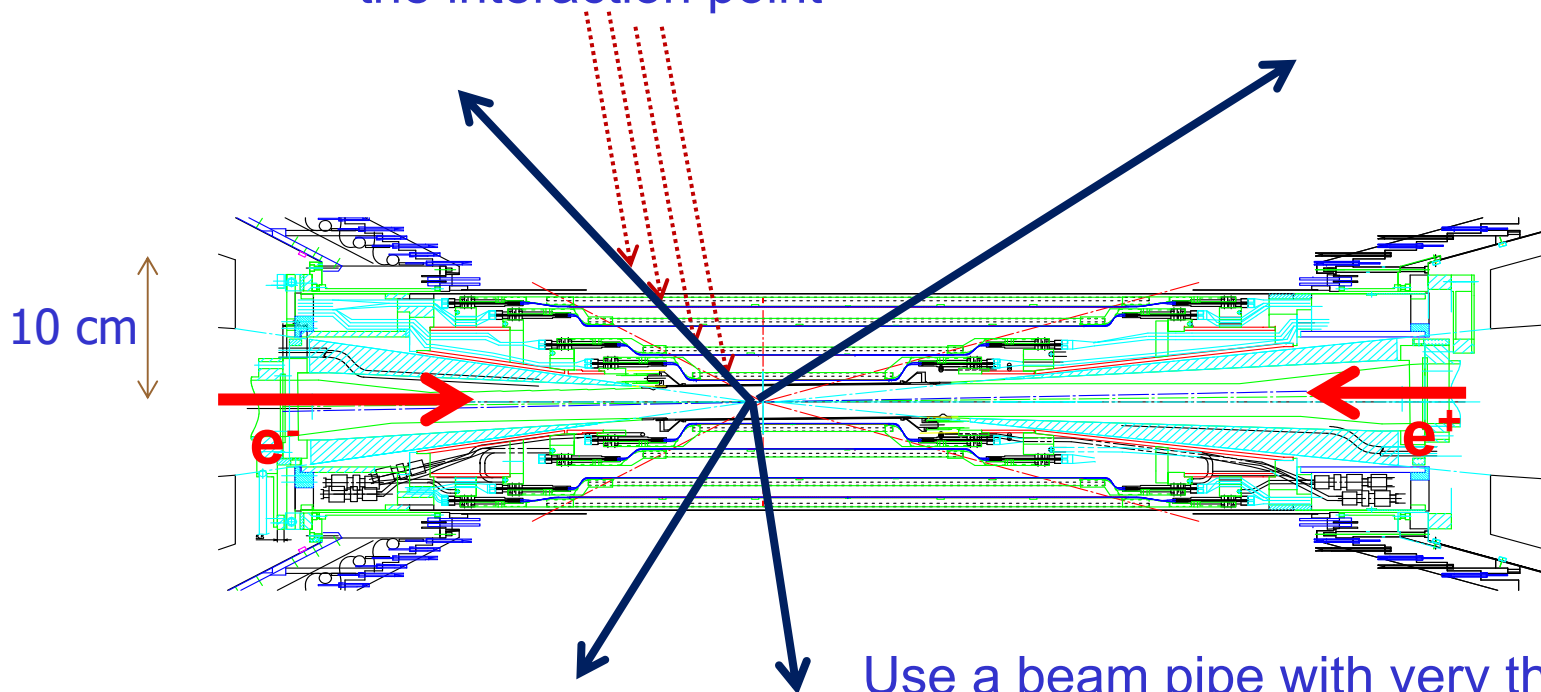


Vertexing, example:
 $B^0 \rightarrow K_S^0 J/\psi$
 $K_S^0 \rightarrow \pi^- \pi^+$
 $J/\psi \rightarrow \mu^- \mu^+$
 $\bar{B}^0 \rightarrow K^- X$



Vertexing

Measure very accurately
points on the track close to
the interaction point



Use a beam pipe with very thin walls
(and light material – long X_0) to
reduce multiple scattering

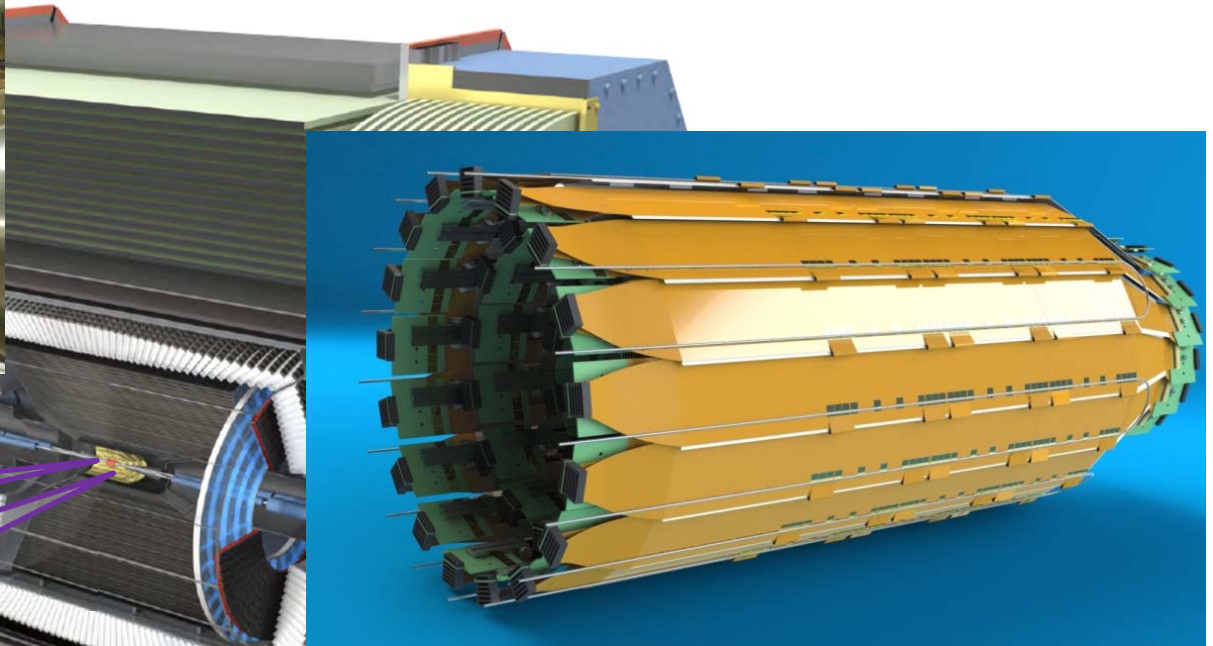
6. ATOMIC AND NUCLEAR PROPERTIES OF MATERIALS

Table 6.1 Abridged from pdg.lbl.gov/AtomicNuclearProperties by D. E. Groom (2007). See web pages for more detail about entries in this table including chemical formulae, and for several hundred other entries. Quantities in parentheses are for NTP (20° C and 1 atm), and square brackets indicate quantities evaluated at STP. Boiling points are at 1 atm. Refractive indices n are evaluated at the sodium D line blend (589.2 nm); values $\gg 1$ in brackets are for $(n - 1) \times 10^6$ (gases).

Material	Z	A	$\langle Z/A \rangle$	Nucl.coll. length λ_T {g cm ⁻² }	Nucl.inter. length λ_I {g cm ⁻² }	Rad.len. X_0 {g cm ⁻² }	$dE/dx _{\min}$ { MeV g ⁻¹ cm ² }	Density {g cm ⁻³ } ({gℓ ⁻¹ })	Melting point (K)	Boiling point (K)	Refract. index (@ Na D)
H ₂	1	1.00794(7)	0.99212	42.8	52.0	63.04	(4.103)	0.071(0.084)	13.81	20.28	1.11[132.]
D ₂	1	2.01410177803(8)	0.49650	51.3	71.8	125.97	(2.053)	0.169(0.168)	18.7	23.65	1.11[138.]
He	2	4.002602(2)	0.49967	51.8	71.0	94.32	(1.937)	0.125(0.166)		4.220	1.02[35.0]
Li	3	6.941(2)	0.43221	52.2	71.3	82.78	1.639	0.534	453.6	1615.	
Be	4	9.012182(3)	0.44384	55.3	77.8	65.19	1.595	1.848	1560.	2744.	
C diamond	6	12.0107(8)	0.49955	59.2	85.8	42.70	1.725	3.520			2.42
C graphite	6	12.0107(8)	0.49955	59.2	85.8	42.70	1.742	2.210			
N ₂	7	14.0067(2)	0.49976	61.1	89.7	37.99	(1.825)	0.807(1.165)	63.15	77.29	1.20[298.]
O ₂	8	15.9994(3)	0.50002	61.3	90.2	34.24	(1.801)	1.141(1.332)	54.36	90.20	1.22[271.]
F ₂	9	18.9984032(5)	0.47372	65.0	97.4	32.93	(1.676)	1.507(1.580)	53.53	85.03	[195.]
Ne	10	20.1797(6)	0.49555	65.7	99.0	28.93	(1.724)	1.204(0.839)	24.56	27.07	1.09[67.1]
Al	13	26.9815386(8)	0.48181	69.7	107.2	24.01	1.615	2.699	933.5	2792.	
Si	14	28.0855(3)	0.49848	70.2	108.4	21.82	1.664	2.329	1687.	3538.	3.95
Cl ₂	17	35.453(2)	0.47951	73.8	115.7	19.28	(1.630)	1.574(2.980)	171.6	239.1	[773.]
Ar	18	39.948(1)	0.45059	75.7	119.7	19.55	(1.519)	1.396(1.662)	83.81	87.26	1.23[281.]
Ti	22	47.867(1)	0.45961	78.8	126.2	16.16	1.477	4.540	1941.	3560.	
Fe	26	55.845(2)	0.46557	81.7	132.1	13.84	1.451	7.874	1811.	3134.	
Cu	29	63.546(3)	0.45636	84.2	137.3	12.86	1.403	8.960	1358.	2835.	
Ge	32	72.64(1)	0.44053	86.9	143.0	12.25	1.370	5.323	1211.	3106.	
Sn	50	118.710(7)	0.42119	98.2	166.7	8.82	1.263	7.310	505.1	2875.	
Xe	54	131.293(6)	0.41129	100.8	172.1	8.48	(1.255)	2.953(5.483)	161.4	165.1	1.39[701.]
W	74	183.84(1)	0.40252	110.4	191.9	6.76	1.145	19.300	3695.	5828.	
Pt	78	195.084(9)	0.39983	112.2	195.7	6.54	1.128	21.450	2042.	4098.	
Au	79	196.966569(4)	0.40108	112.5	196.3	6.46	1.134	19.320	1337.	3129.	
Pb	82	207.2(1)	0.39575	114.1	199.6	6.37	1.122	11.350	600.6	2022.	
U	92	[238.02891(3)]	0.38651	118.6	209.0	6.00	1.081	18.950	1408.	4404.	
Air (dry, 1 atm)			0.49919	61.3	90.1	36.62	(1.815)	(1.205)		78.80	
Shielding concrete			0.50274	65.1	97.5	26.57	1.711	2.300			
Borosilicate glass (Pyrex)			0.49707	64.6	96.5	28.17	1.696	2.230			

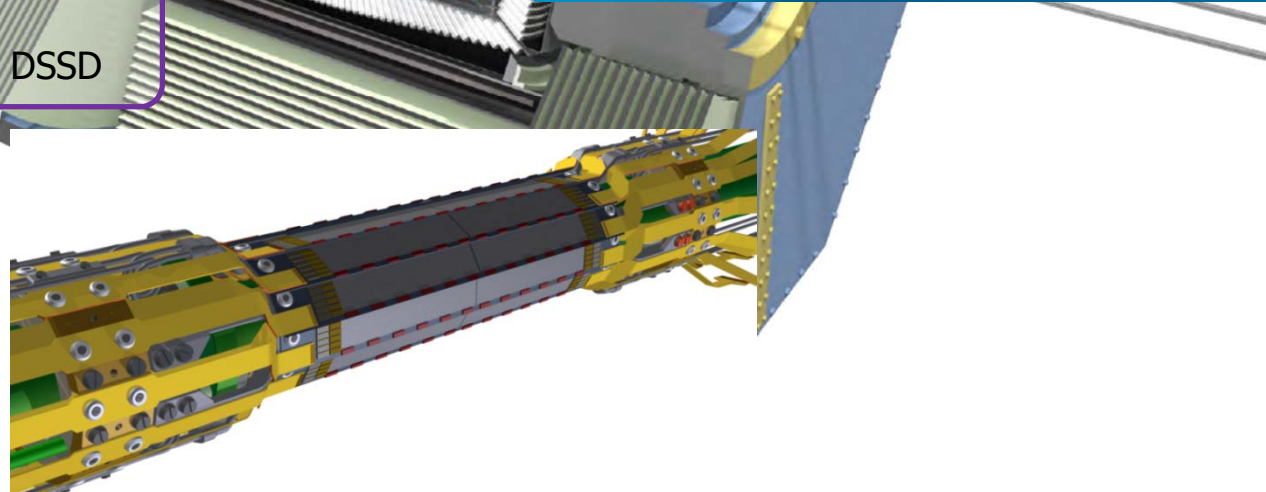
W	74	183.84(1)	0.40252	110.4	191.9	6.76	1.145	19.300	3695.	5828.
Pt	78	195.084(9)	0.39983	112.2	195.7	6.54	1.128	21.450	2042.	4098.
Au	79	196.966569(4)	0.40108	112.5	196.3	6.46	1.134	19.320	1337.	3129.
Pb	82	207.2(1)	0.39575	114.1	199.6	6.37	1.122	11.350	600.6	2022.
U	92	[238.02891(3)]	0.38651	118.6	209.0	6.00	1.081	18.950	1408.	4404.
Air (dry, 1 atm)			0.49919	61.3	90.1	36.62	(1.815)	(1.205)		78.80
Shielding concrete			0.50274	65.1	97.5	26.57	1.711	2.300		
Borosilicate glass (Pyrex)			0.49707	64.6	96.5	28.17	1.696	2.230		
Lead glass			0.42101	95.9	158.0	7.87	1.255	6.220		
Standard rock			0.50000	66.8	101.3	26.54	1.688	2.650		
Methane (CH ₄)			0.62334	54.0	73.8	46.47	(2.417)	(0.667)	90.68	111.7 [444.]
Ethane (C ₂ H ₆)			0.59861	55.0	75.9	45.66	(2.304)	(1.263)	90.36	184.5
Propane (C ₃ H ₈)			0.58962	55.3	76.7	45.37	(2.262)	0.493(1.868)	85.52	231.0
Butane (C ₄ H ₁₀)			0.59497	55.5	77.1	45.23	(2.278)	(2.489)	134.9	272.6
Octane (C ₈ H ₁₈)			0.57778	55.8	77.8	45.00	2.123	0.703	214.4	398.8
Paraffin (CH ₃ (CH ₂) _n ≈23CH ₃)			0.57275	56.0	78.3	44.85	2.088	0.930		
Nylon (type 6, 6/6)			0.54790	57.5	81.6	41.92	1.973	1.18		
Polycarbonate (Lexan)			0.52697	58.3	83.6	41.50	1.886	1.20		
Polyethylene ([CH ₂ CH ₂] _n)			0.57034	56.1	78.5	44.77	2.079	0.89		
Polyethylene terephthalate (Mylar)			0.52037	58.9	84.9	39.95	1.848	1.40		
Polyimide film (Kapton)			0.51264	59.2	85.5	40.58	1.820	1.42		
Polymethylmethacrylate (acrylic)			0.53937	58.1	82.8	40.55	1.929	1.19		1.49
Polypropylene			0.55998	56.1	78.5	44.77	2.041	0.90		
Polystyrene ([C ₆ H ₅ CHCH ₂] _n)			0.53768	57.5	81.7	43.79	1.936	1.06		1.59
Polytetrafluoroethylene (Teflon)			0.47992	63.5	94.4	34.84	1.671	2.20		
Polyvinyltoluene			0.54141	57.3	81.3	43.90	1.956	1.03		1.58
Aluminum oxide (sapphire)			0.49038	65.5	98.4	27.94	1.647	3.970	2327.	3273. 1.77
Barium fluoride (BaF ₂)			0.42207	90.8	149.0	9.91	1.303	4.893	1641.	2533. 1.47
Bismuth germanate (BGO)			0.42065	96.2	159.1	7.97	1.251	7.130	1317.	2.15
Carbon dioxide gas (CO ₂)			0.49989	60.7	88.9	36.20	1.819	(1.842)		[449.]
Solid carbon dioxide (dry ice)			0.49989	60.7	88.9	36.20	1.787	1.563	Sublimes at 194.7 K	
Cesium iodide (CsI)			0.41569	100.6	171.5	8.39	1.243	4.510	894.2	1553. 1.79
Lithium fluoride (LiF)			0.46262	61.0	88.7	39.26	1.614	2.635	1121.	1946. 1.39
Lithium hydride (LiH)			0.50321	50.8	68.1	79.62	1.897	0.820	965.	
Lead tungstate (PbWO ₄)			0.41315	100.6	168.3	7.39	1.229	8.300	1403.	2.20
Silicon dioxide (SiO ₂ , fused quartz)			0.49930	65.2	97.8	27.05	1.699	2.200	1986.	3223. 1.46
Sodium chloride (NaCl)			0.55509	71.2	110.1	21.91	1.847	2.170	1075.	1738. 1.54
Sodium iodide (NaI)			0.42697	93.1	154.6	9.49	1.305	3.667	933.2	1577. 1.77
Water (H ₂ O)			0.55509	58.5	83.3	36.08	1.992	1.000(0.756)	273.1	373.1 1.33
Silica aerogel			0.50093	65.0	97.3	27.25	1.740	0.200	(0.03 H ₂ O, 0.97 SiO ₂)	

Belle II Detector – vertex region

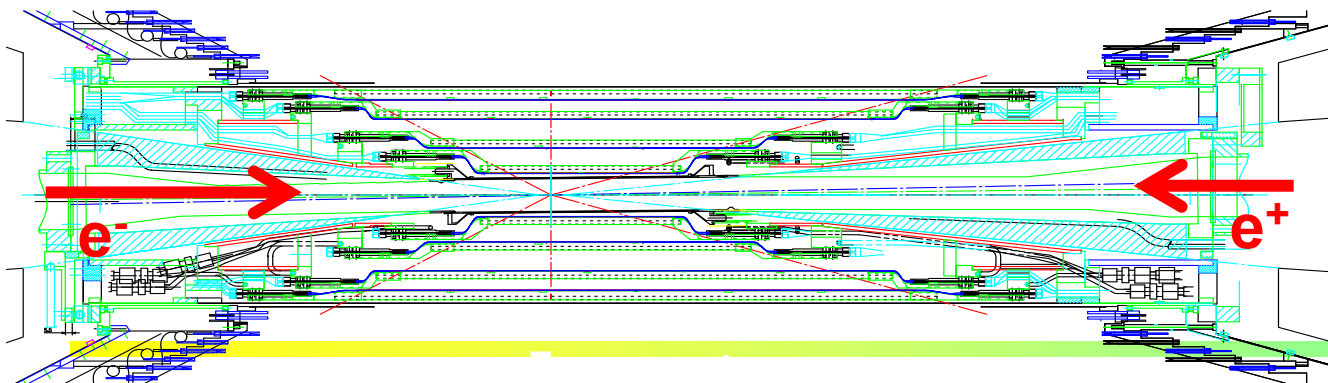
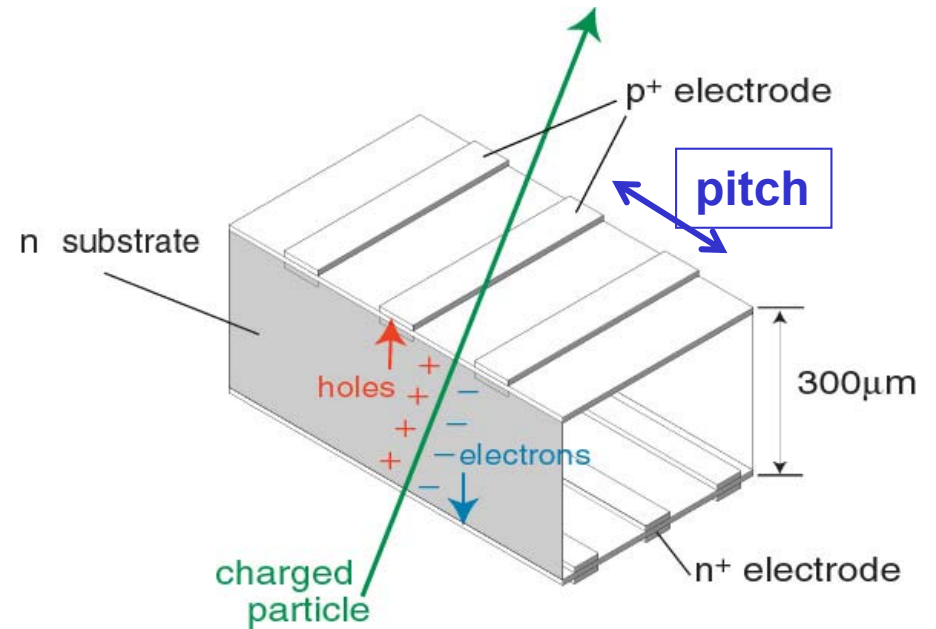
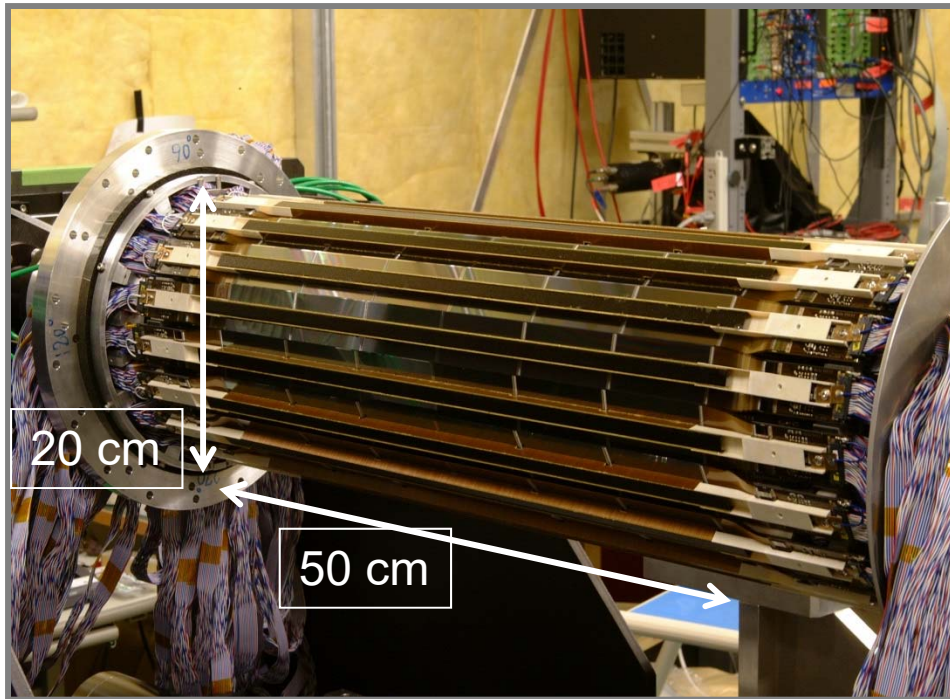


Beryllium beam pipe
2cm diameter

Vertex Detector
2 layers DEPFET + 4 layers DSSD



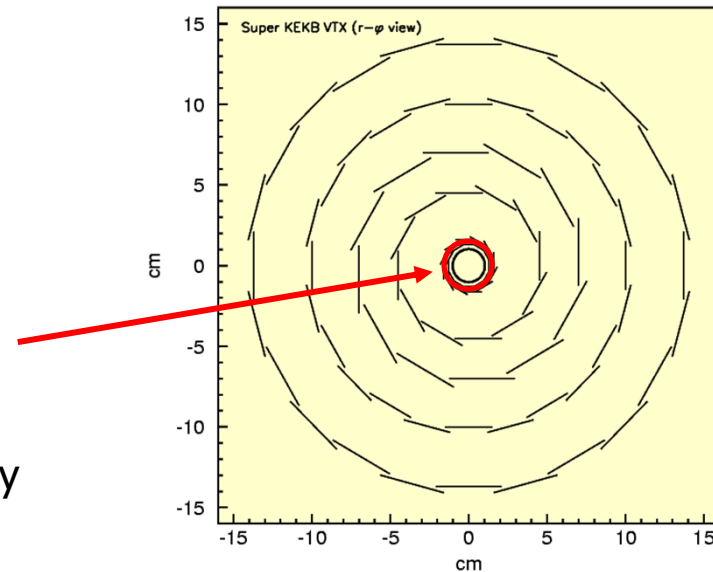
Silicon vertex detector (SVD)



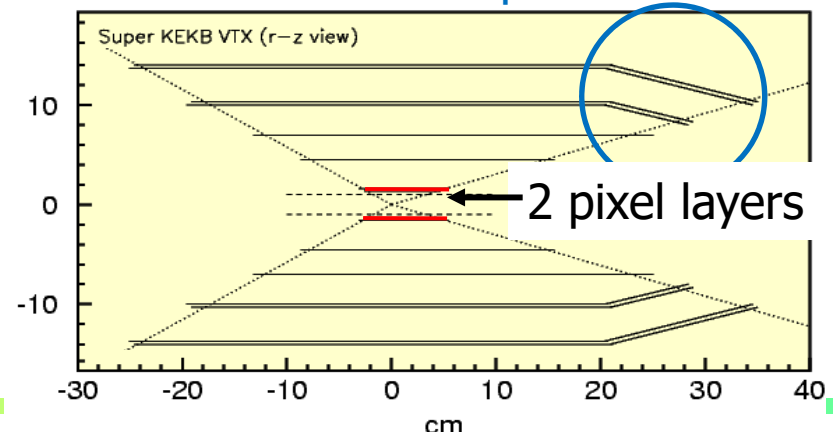
Two coordinates measured at the same time;
strip pitch: 50µm (75µm);
resolution 15µm (20µm).

Belle II Vertex detector SVD+PXD

- Sensors of the innermost layers:
Normal double sided Si detector (DSSD) → DEPFET Pixel sensors
- Configuration: 4 layers → 6 layers
(outer radius = 8cm → 14cm)
 - More robust tracking
 - Higher Ks vertex reconstruction efficiency
- Inner radius: 1.5cm → 1.3cm
 - Better vertex resolution



Slant layer to keep the acceptance



Pixel vertex detector PXD principle: DEPFET

p-channel FET on a completely depleted bulk

A deep n-implant creates a potential minimum for electrons under the gate ("internal gate")

Signal electrons accumulate in the internal gate and modulate the transistor current ($g_q \sim 400 \text{ pA/e}^-$)

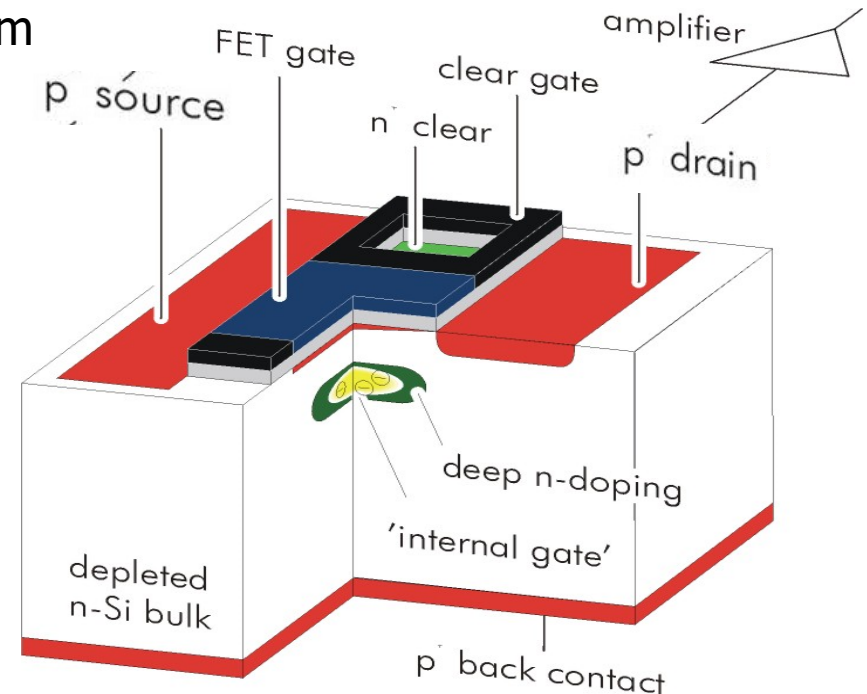
Accumulated charge can be removed by a clear contact ("reset")

Fully depleted:

→ large signal, fast signal collection

Low capacitance, internal amplification → low noise

Depleted p-channel FET

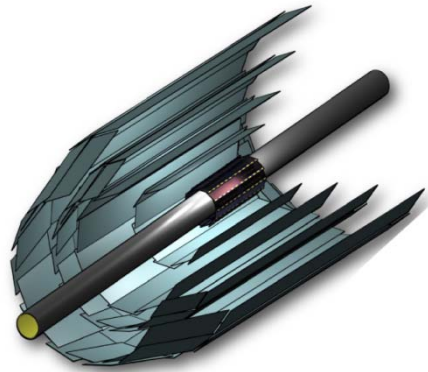


Transistor on only during readout:
low power

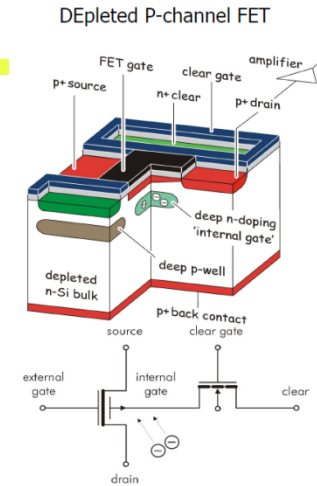
Complete clear → no reset noise

Vertex Detector

DEPFET:
<http://aldebaran.hll.mpg.de/twiki/bin/view/DEPFET/WebHome>



Beam Pipe	r = 10mm
DEPFET	
Layer 1	r = 14mm
Layer 2	r = 22mm
DSSD	
Layer 3	r = 38mm
Layer 4	r = 80mm
Layer 5	r = 115mm
Layer 6	r = 140mm



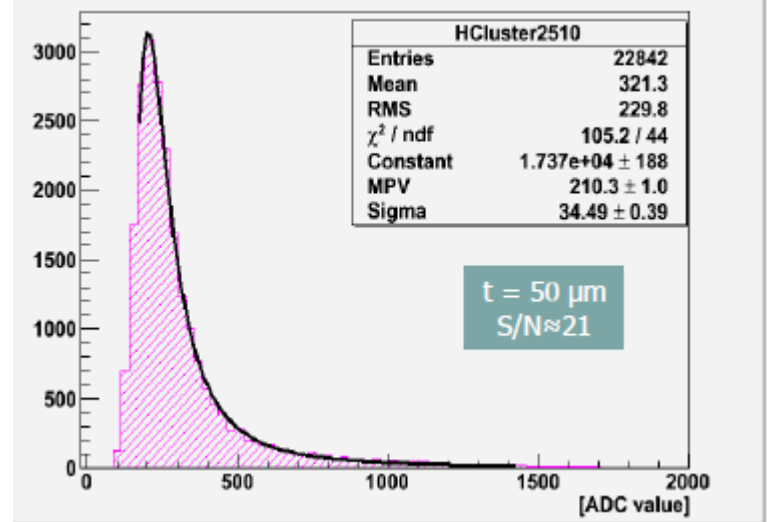
Mechanical mockup of pixel detector



DEPFET pixel sensor



Cluster 5x5 (Mod10)(RunNo6615)



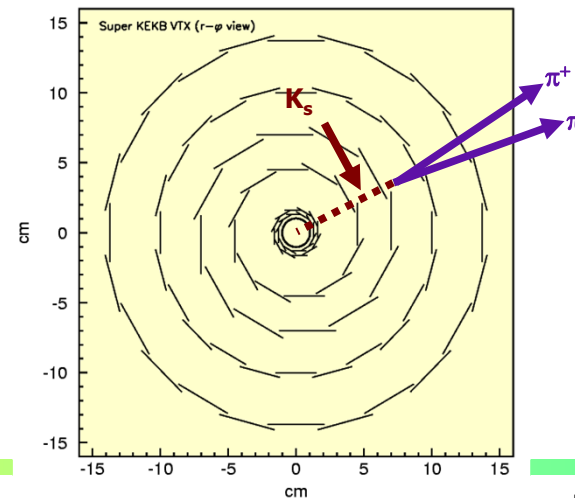
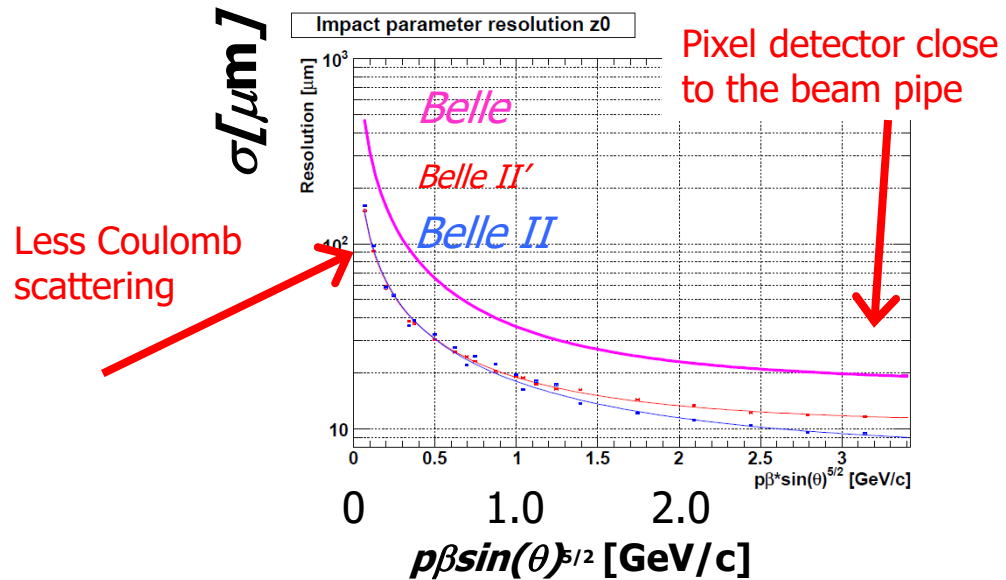
DEPFET sensor: very good S/N

Expected performance

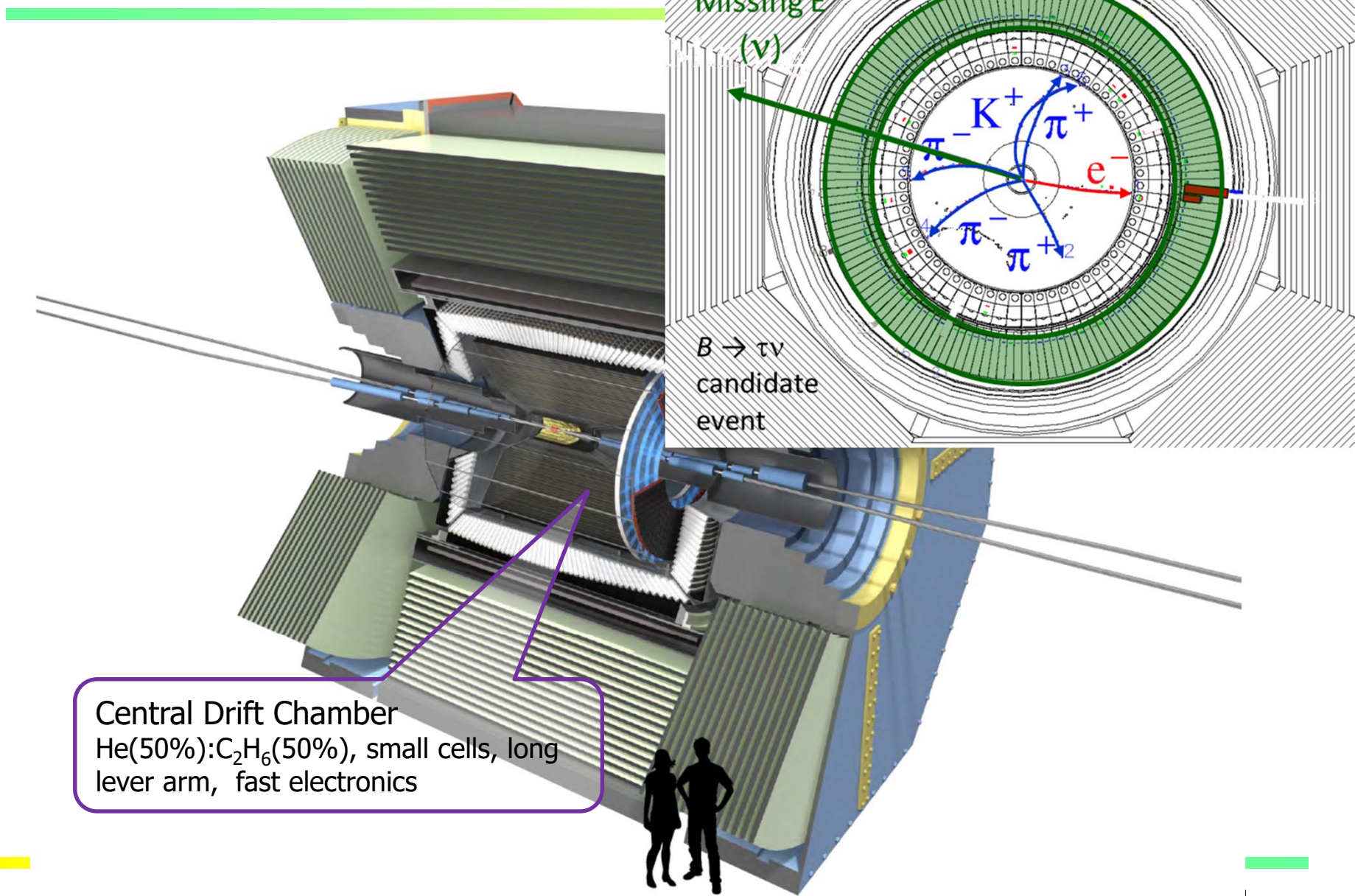
$$\sigma = a + \frac{b}{p\beta \sin^v \theta}$$

4 layers of silicons strip detectors → 2 layers of pixel detectors + 4 layers of silicons strip detectors: significant improvement in vertex resolution!

Larger detector volume → significant improvement in K_s reconstruction efficiency



Main tracking device: small cell drift chamber



Central Drift Chamber
He(50%):C₂H₆(50%), small cells, long lever arm, fast electronics

Search for unstable particles which decayed close to the production point

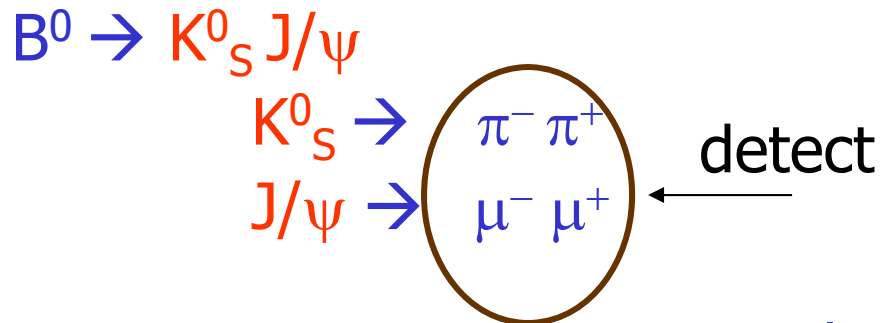
How do we reconstruct final states that decayed to two stable particles?

From the measured tracks calculate the invariant mass of the system ($i= 1,2$):

$$Mc^2 = \sqrt{(\sum E_i)^2 - (\sum p_i)^2 c^2}$$

The candidates for the $X \rightarrow 12$ decay show up as a peak in the distribution on (mostly combinatorial) background.

How do we know it was precisely this reaction?



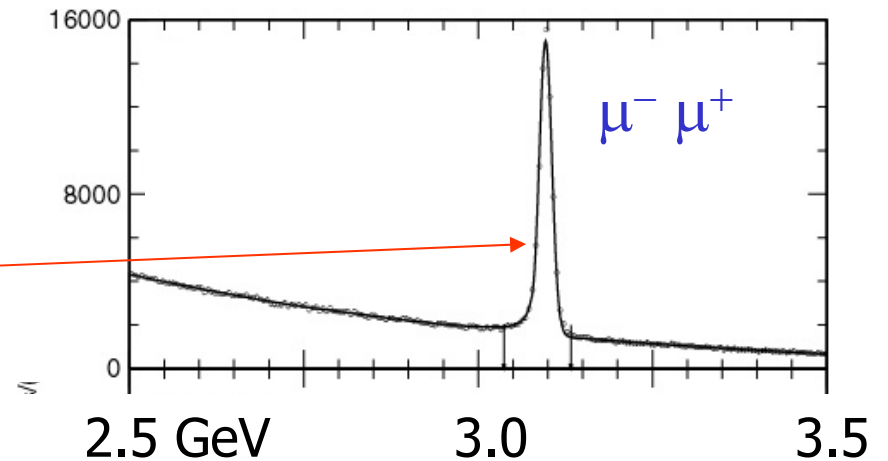
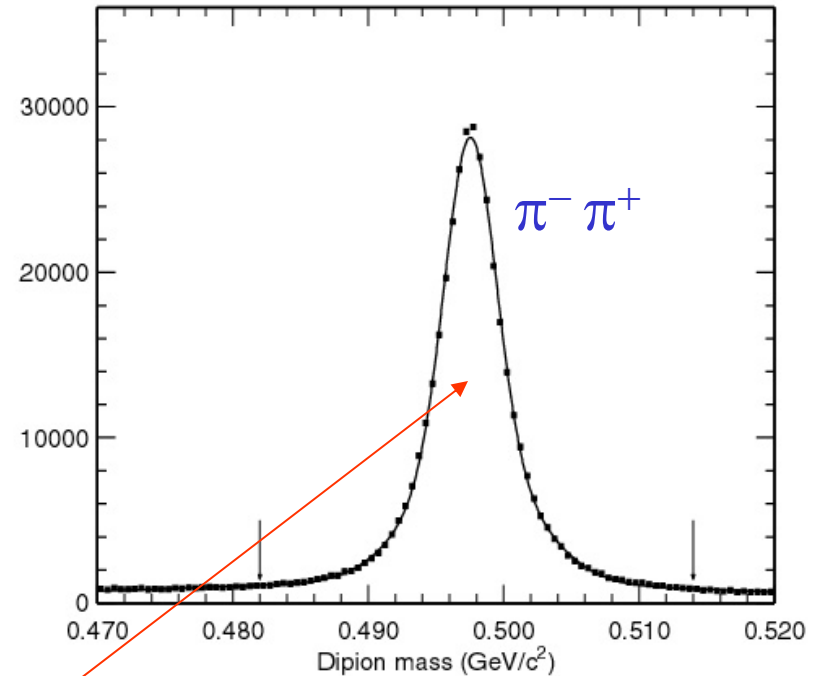
For $\pi^- \pi^+$ in $\mu^- \mu^+$ pairs we calculate the invariant mass:

$$M^2 c^4 = (E_1 + E_2)^2 - (\mathbf{p}_1 + \mathbf{p}_2)^2$$

$M c^2$ must be for K_S^0 close to **0.5 GeV**,

for J/ψ close to **3.1 GeV**.

Rest in the histogram: random coincidences ('combinatorial background')



Invariant mass resolution – momentum resolution

The name of the game: have as little background under the peak as possible without losing the events in the peak (=reduce background and have a **narrow peak**).

$$Mc^2 = \sqrt{(\sum E_i)^2 - (\sum \vec{p}_i)^2} c^2$$

To understand the impact of momentum resolution, simplify the expression for the case where final state particles have a small mass compared to their momenta.

Example $J/\psi \rightarrow \mu^- \mu^+$

$$M^2c^4 = (E_1 + E_2)^2 - (p_1 + p_2)^2 \rightarrow M^2c^4 = 2 p_1 p_2 (1 - \cos\Theta_{12})$$

Resolution in invariant mass

$$B^0 \rightarrow K_S^0 J/\psi, K_S^0 \rightarrow \pi^- \pi^+, J/\psi \rightarrow \mu^- \mu^+$$

$$M^2 c^4 = (E_1 + E_2)^2 - (p_1 + p_2)^2 c^2 \rightarrow M^2 c^4 = 2 p_1 p_2 c^2 (1 - \cos\Theta_{12})$$

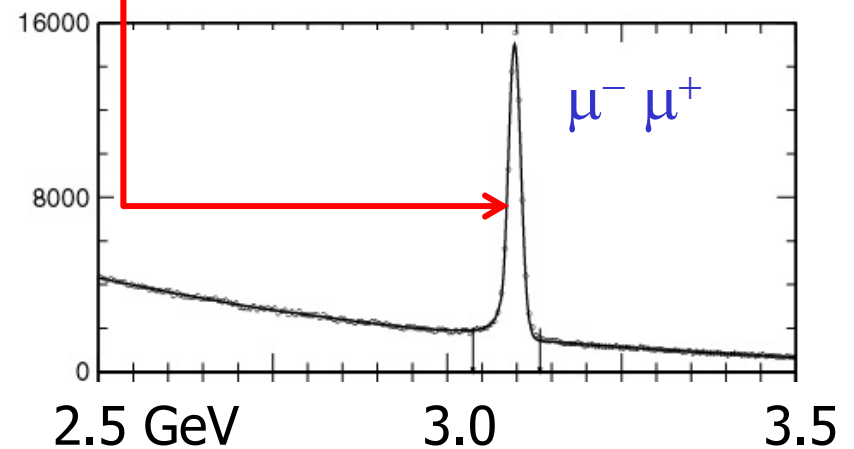
The J/ψ peak should be narrow to minimize the contribution of random coincidences ('combinatorial background')

The required resolution in Mc^2 : about **10 MeV**.

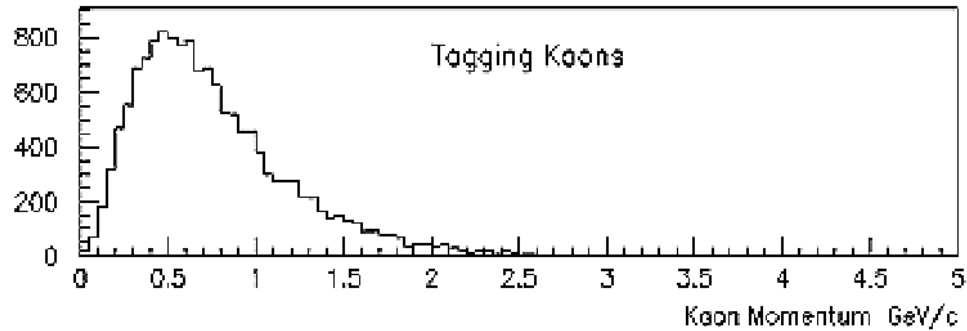
What is the corresponding momentum resolution?

For simplicity assume J/ψ is at rest \rightarrow
 $\Theta_{12} = 180^\circ$, $p_1 = p_2 = p = 1.5 \text{ GeV}/c$, $Mc^2 = 2pc$
 $\rightarrow \sigma(Mc^2) = 2 \sigma(pc)$ at $p = 1.5 \text{ GeV}/c$

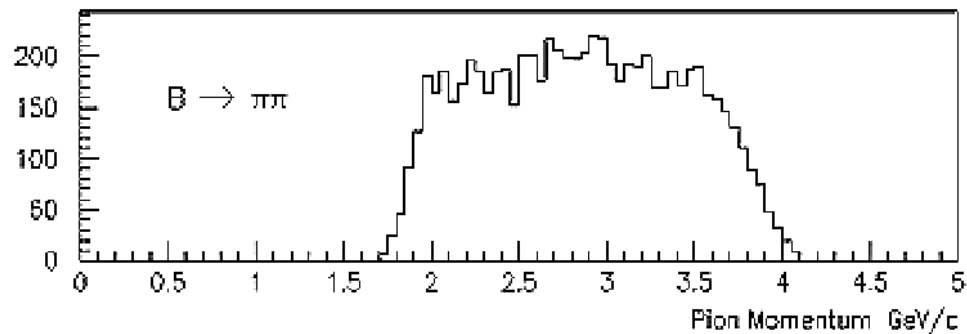
$\rightarrow \sigma(p)/p = 10 \text{ MeV}/2/1.5 \text{ GeV} = 0.3\%$



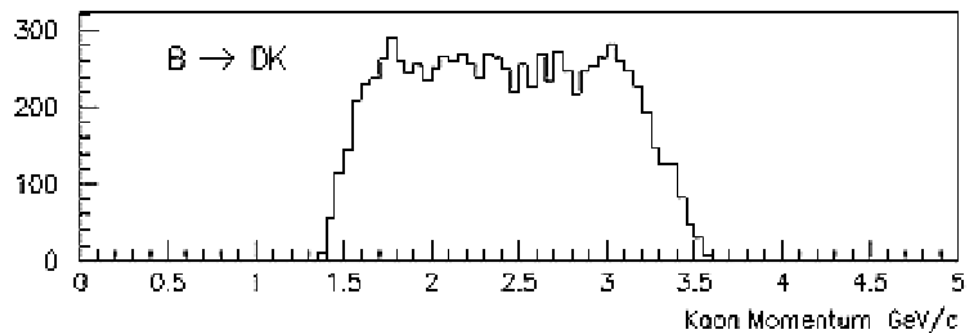
Requirements: momentum spectrum



Tagging Kaons



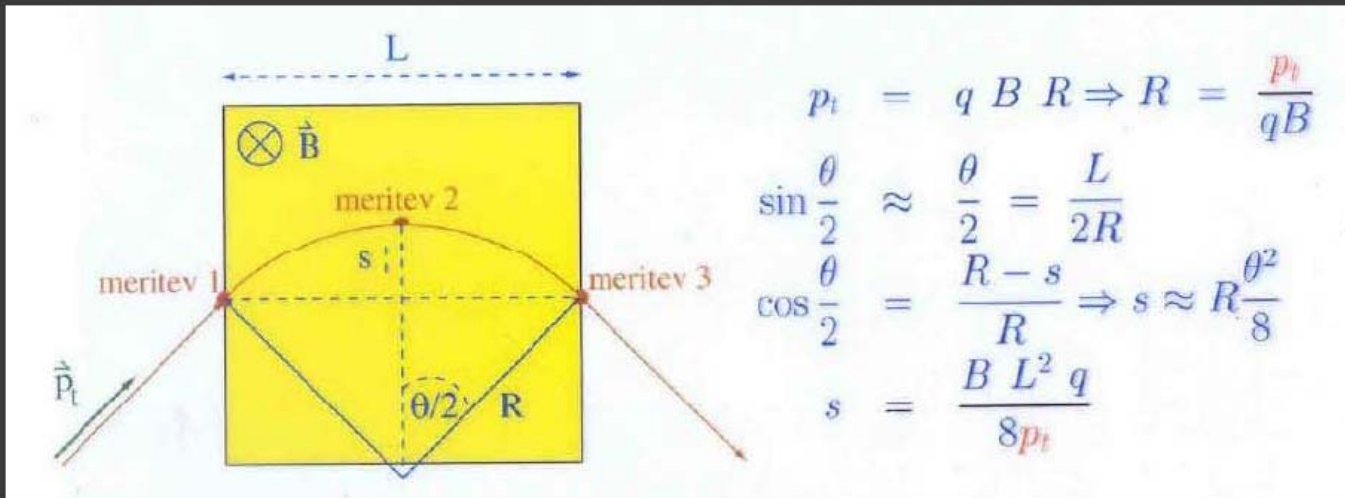
$B \rightarrow \pi\pi$



$B \rightarrow DK$

From raw data to summary data momentum measurement

Example of momentum determination:



if s determined by
3 measurement points:

$$s = x_2 - \frac{x_1 + x_3}{2}$$

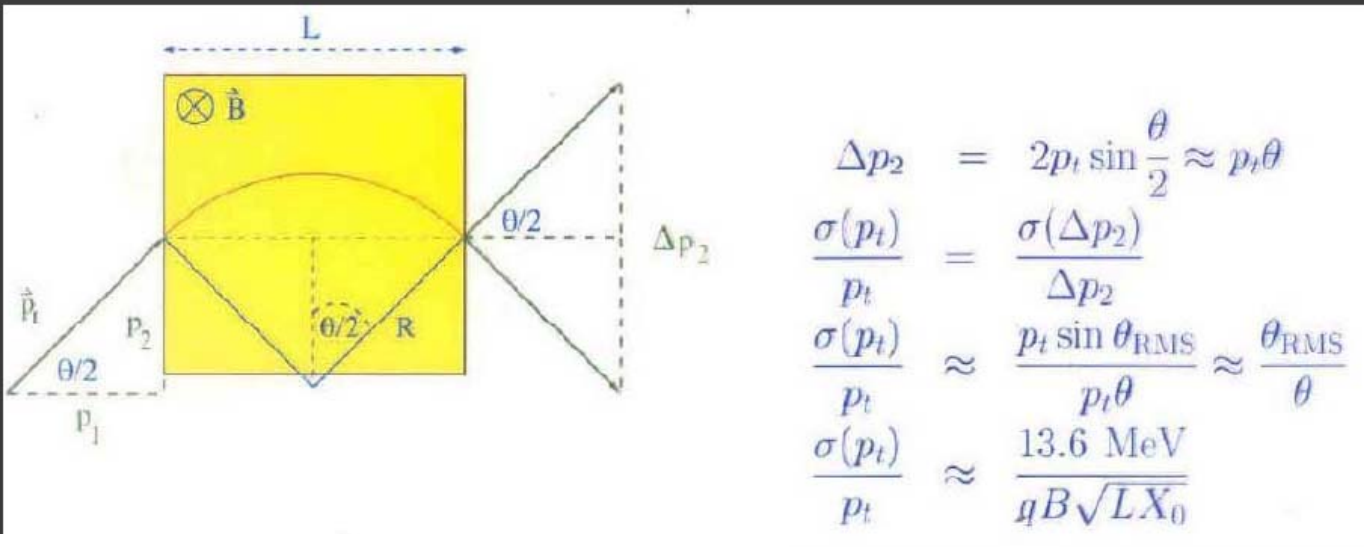
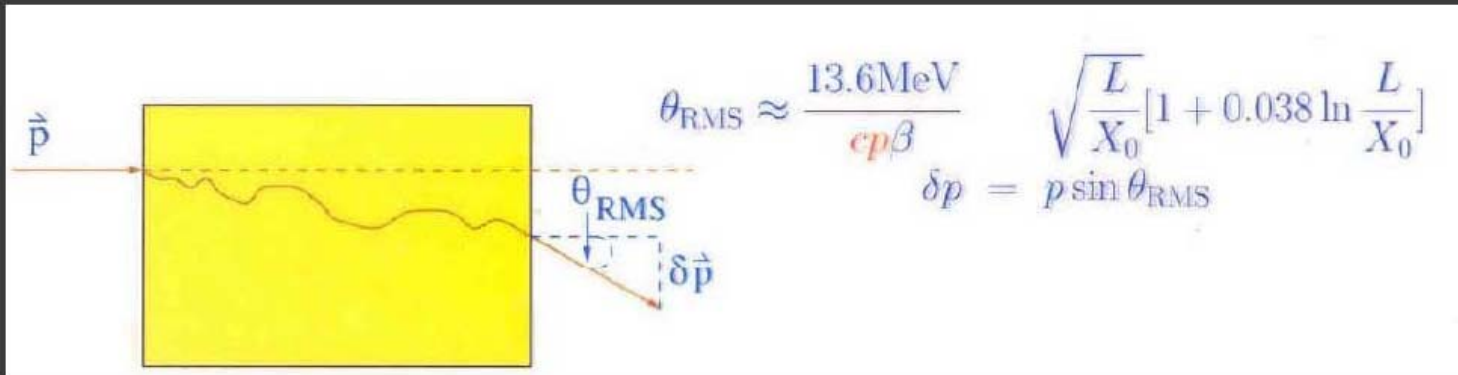
$$\frac{\sigma(p_t)}{p_t} = \frac{\sigma(s)}{s} = \frac{\sqrt{\frac{3}{2}} \sigma(x) 8 p_t}{B L^2 q}$$

for N measurement points:

$$\frac{\sigma_{p_T}}{p_T} = \frac{\sigma_x p_T}{e B L^2} \sqrt{\frac{720}{N+4}}$$

From raw data to summary data momentum measurement

Multiple scattering:



Momentum resolution

Tracking system
uncertainty

$$\frac{\sigma_{p_T}}{p_T} = \frac{\sigma_x p_T}{eBL^2} \sqrt{\frac{720}{N+4}}$$

$$eB = 0.3 \text{ (B/T) (1/m) GeV/c}$$

$$\frac{\sigma_{p_T}}{p_T} = p_T \frac{0.1 \times 10^{-3} \text{ m}}{0.3(\text{GeV/m}) \times 1.5 \times 1 \text{ m}^2} \sqrt{\frac{720}{54}} = \frac{p_T \times 0.0008}{\text{GeV}}$$

For $B=1.5\text{T}$, $L = 1\text{m}$, $\sigma_x = 0.1 \text{ mm}$

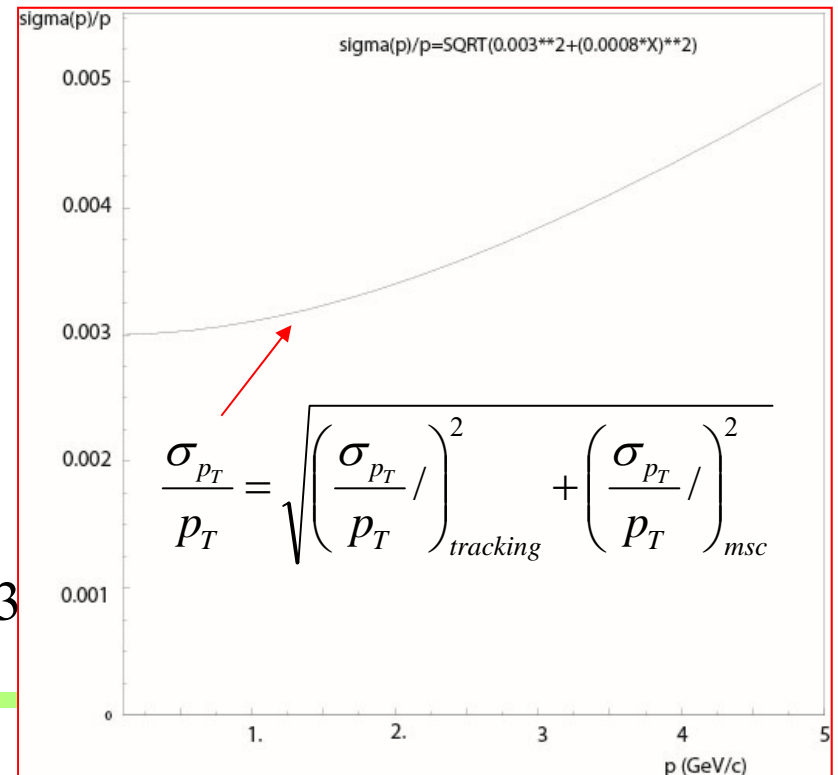
For $p_T = 1 \text{ GeV}$: $\sigma_{p_T} / p_T = 0.08\%$

For $p_T = 2 \text{ GeV}$: $\sigma_{p_T} / p_T = 0.16\%$

Uncertainty from multiple
scattering

$$\frac{\sigma_{p_T}}{p_T} = \frac{13.6 \text{ MeV}}{eB \sqrt{LX_0}}$$

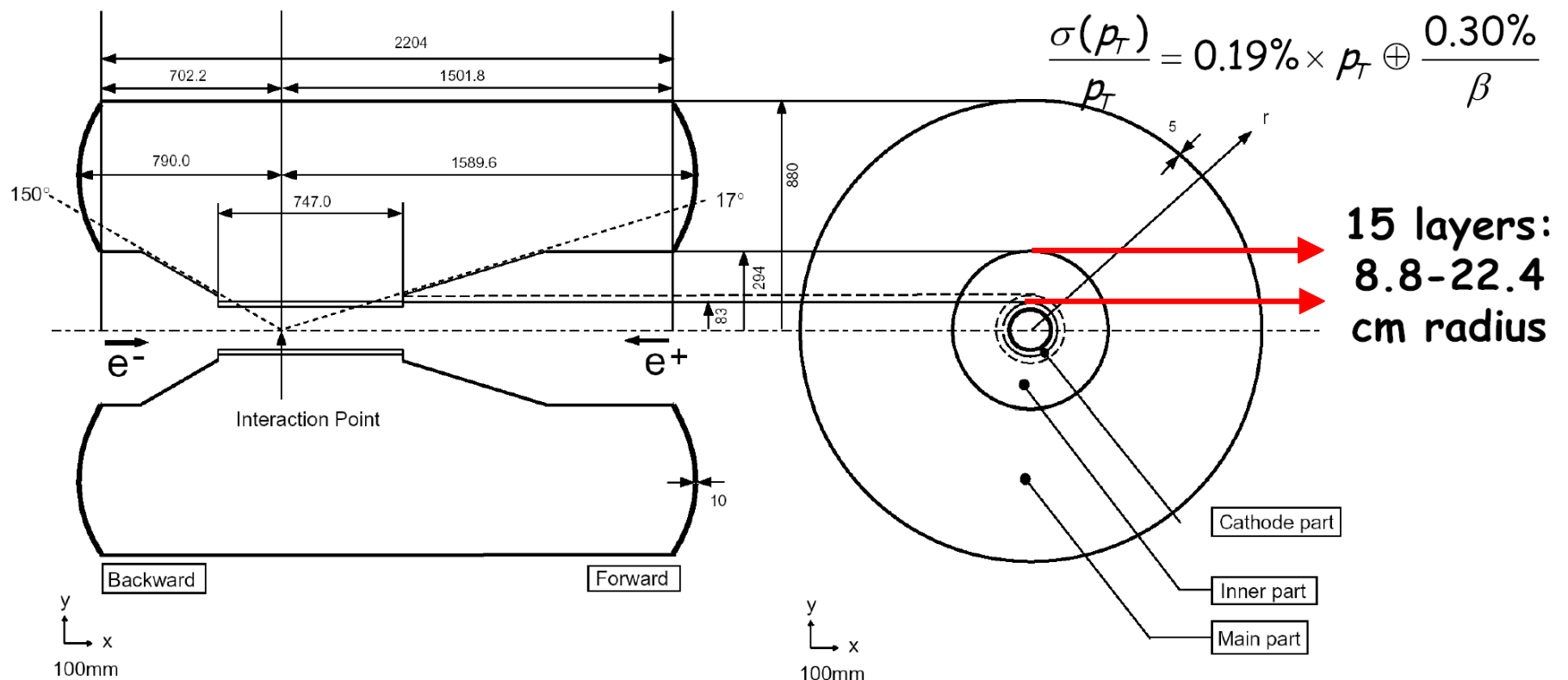
$$\frac{\sigma_{p_T}}{p_T} = \frac{13.6 \text{ MeV}}{0.3(\text{GeV/m}) \times 1.5 \sqrt{1 \text{ m} \times 100 \text{ m}}} = 0.003$$



Tracking: Belle central drift chamber



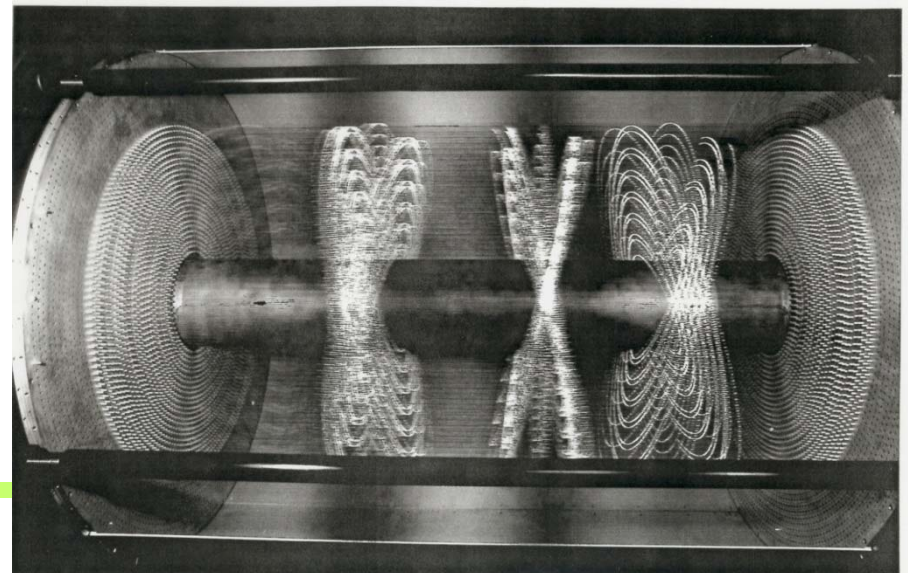
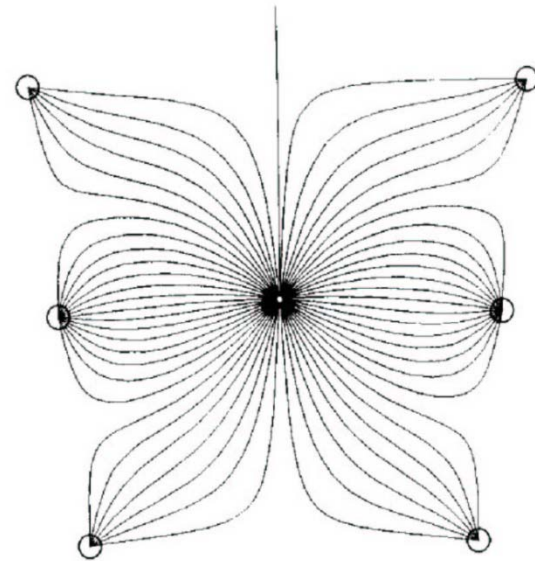
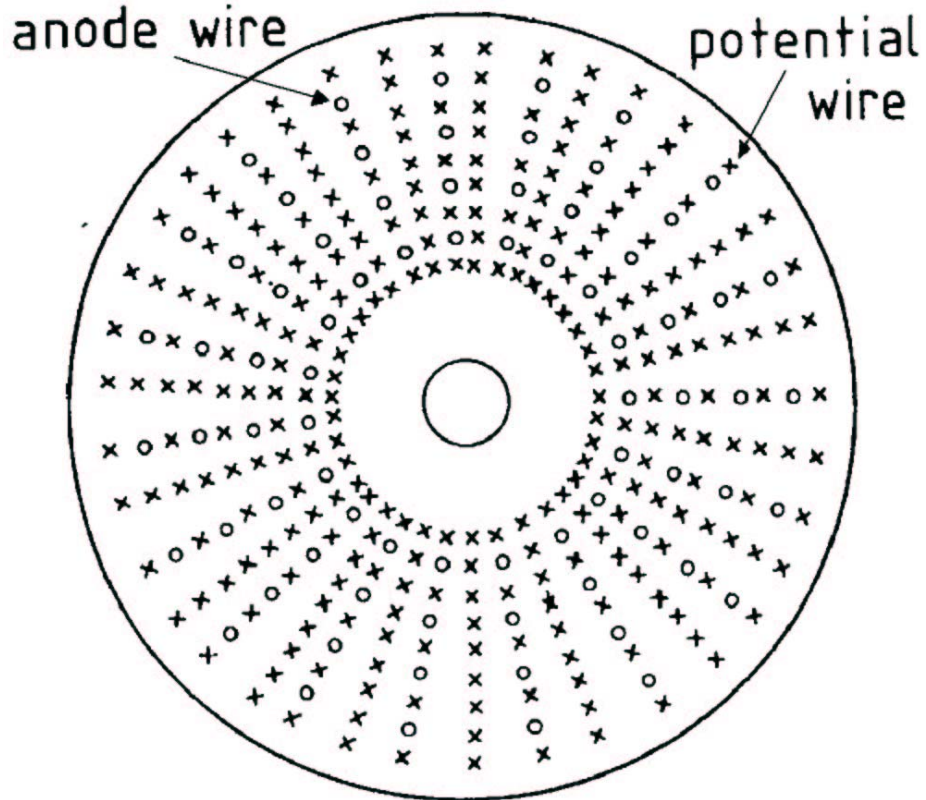
- 50 layers of wires (8400 cells) in 1.5 Tesla magnetic field
- Helium:Ethane 50:50 gas, W anode wires, Al field wires, CF inner wall with cathodes, and preamp only on endplates
- Particle identification from ionization loss (5.6-7% resolution)



15 layers:
8.8-22.4
cm radius

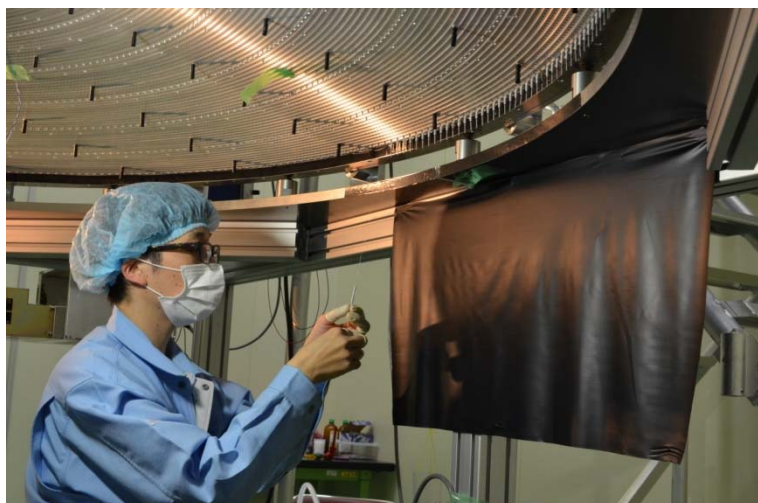
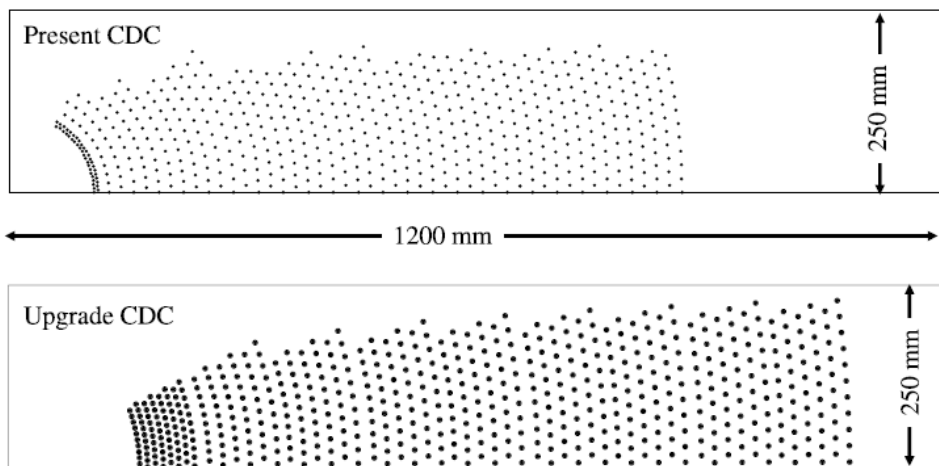
Drift chamber with small cells

One big gas volume, small cells defined by the anode and field shaping (potential) wires



Belle II CDC

Wire Configuration

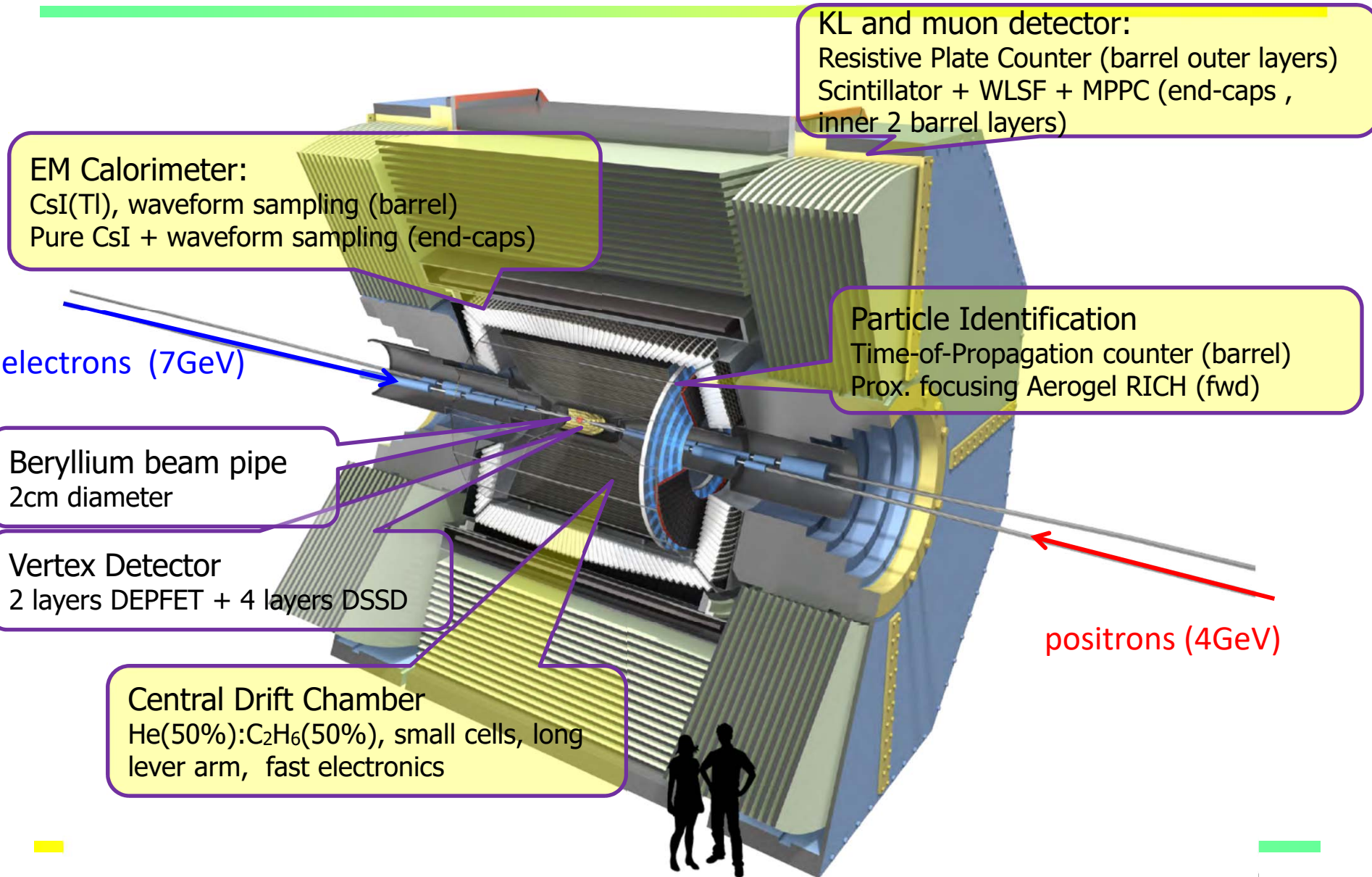


Wire stringing in a clean room

- thousands of wires,
- 1 year of work...



Particle identification systems in Belle II



Identification of charged particles

Particles are identified by their **mass** or by the **way they interact**.

Determination of mass: from the relation between momentum and velocity, $p = \gamma m v$.

Momentum known (radius of curvature in magnetic field)

→ Measure velocity:

time of flight

ionisation losses dE/dx

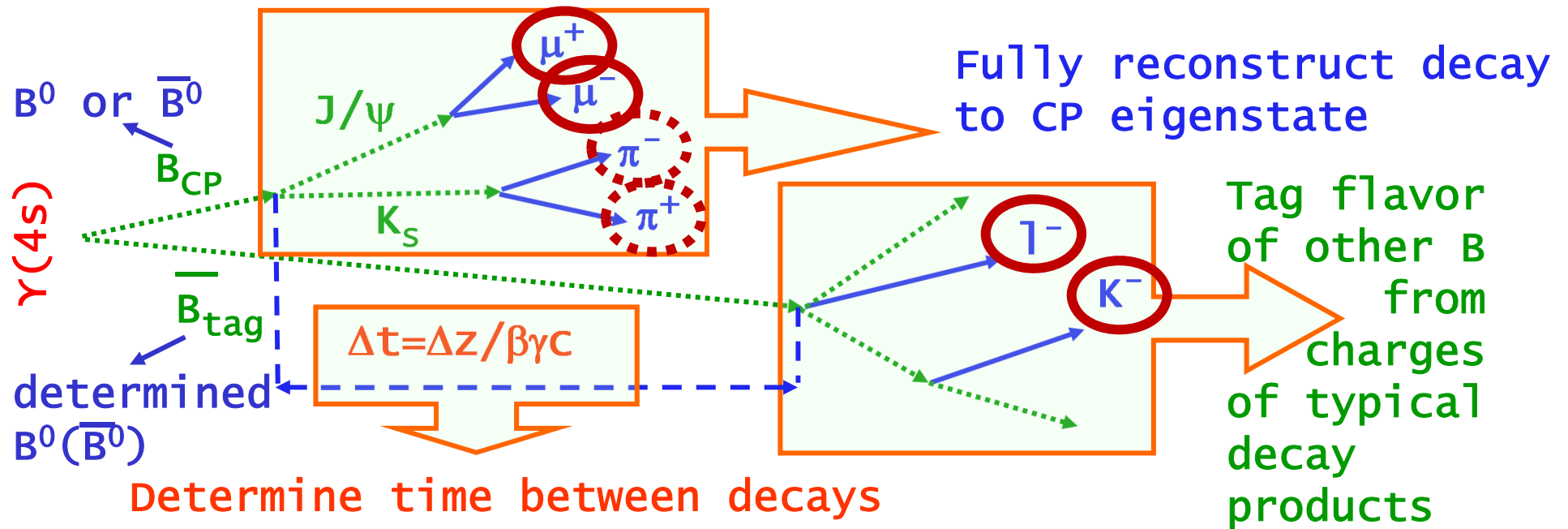
Cherenkov angle

transition radiation

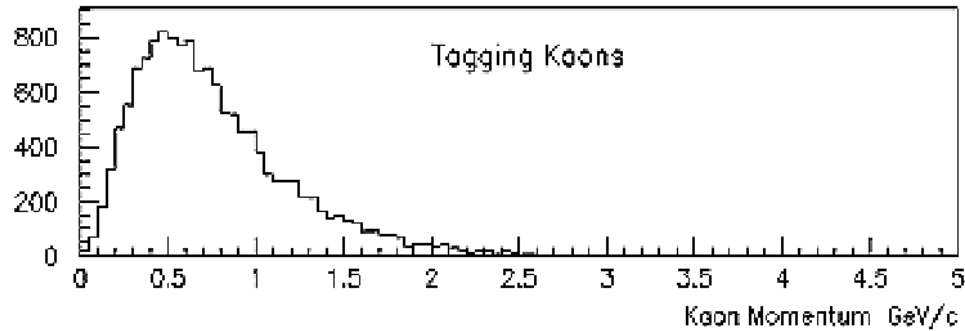
Mainly used for the identification of hadrons.

Identification through interaction: electrons and muons

Reminder: where do we need identification?

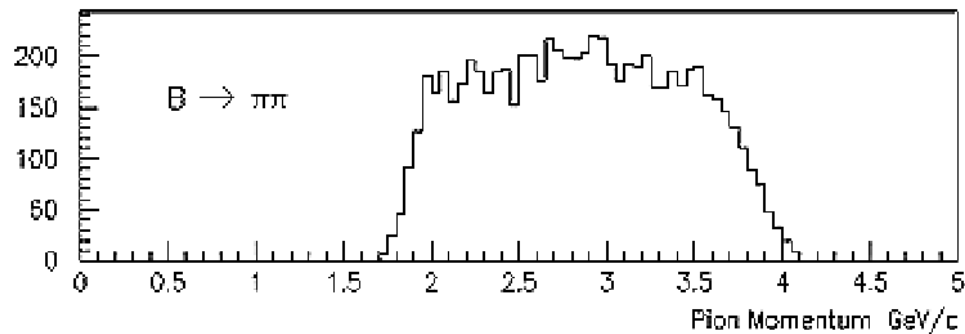


Requirements: Particle Identification



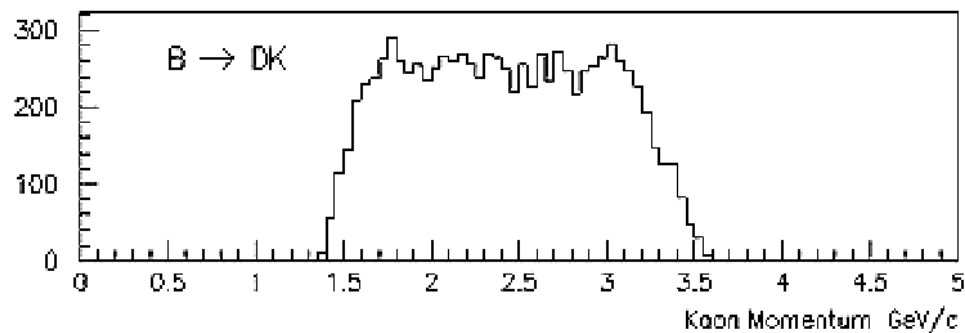
Tagging Kaons

Relatively soft,
ms dominated
for tracking



$B \rightarrow \pi\pi$

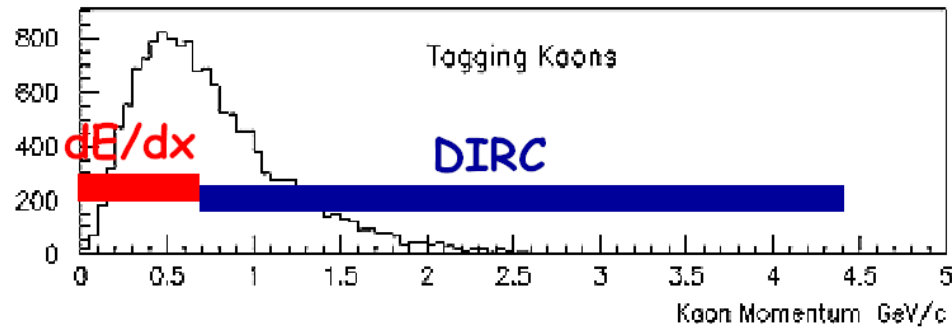
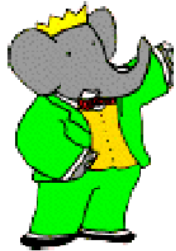
Requires
dedicated PID



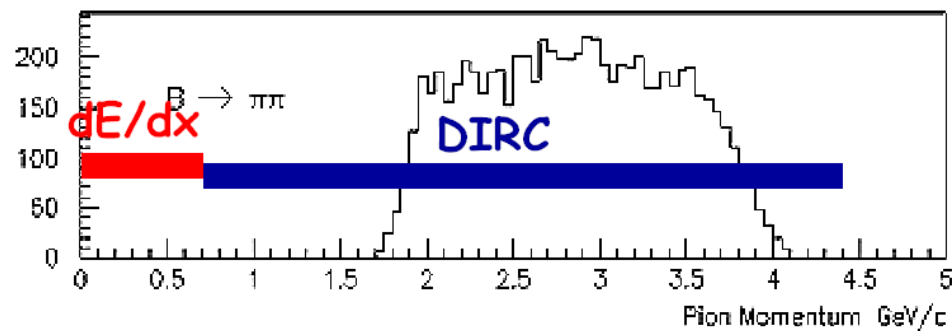
$B \rightarrow DK$

Requires
dedicated PID

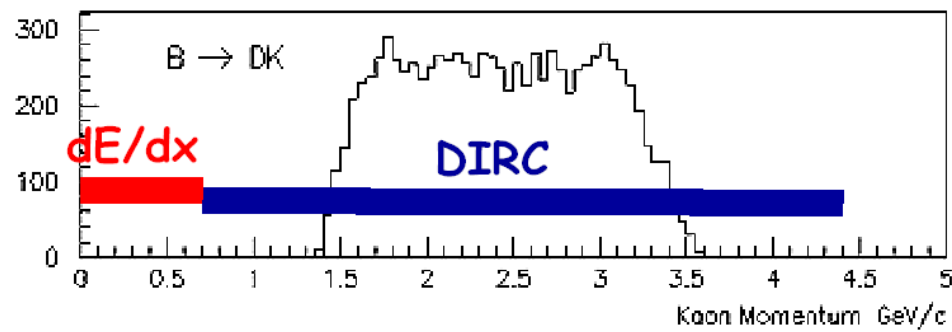
PID coverage of kaon/pion spectra



Tagging Kaons

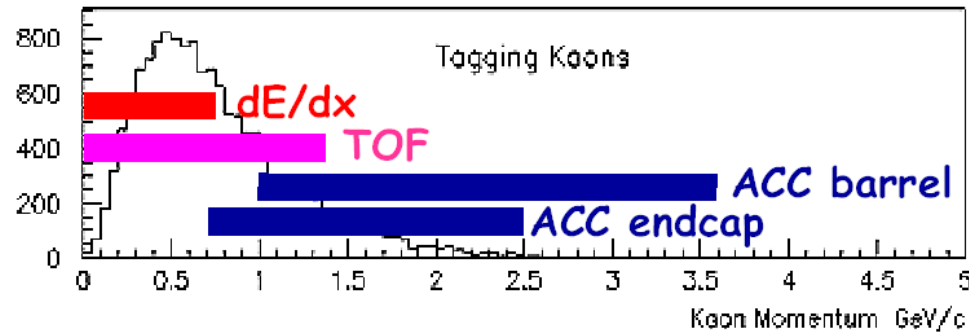


$B \rightarrow \pi\pi$

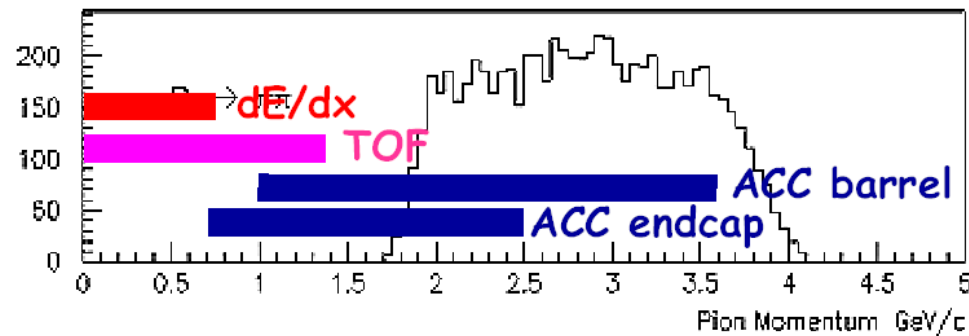


$B \rightarrow DK$

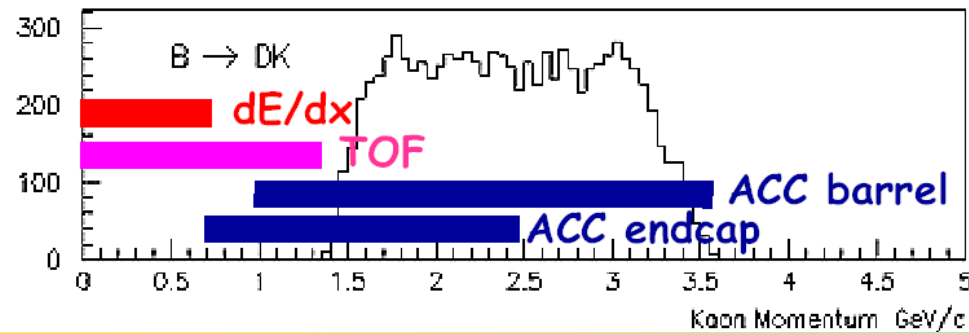
PID coverage of kaon/pion spectra



Tagging Kaons

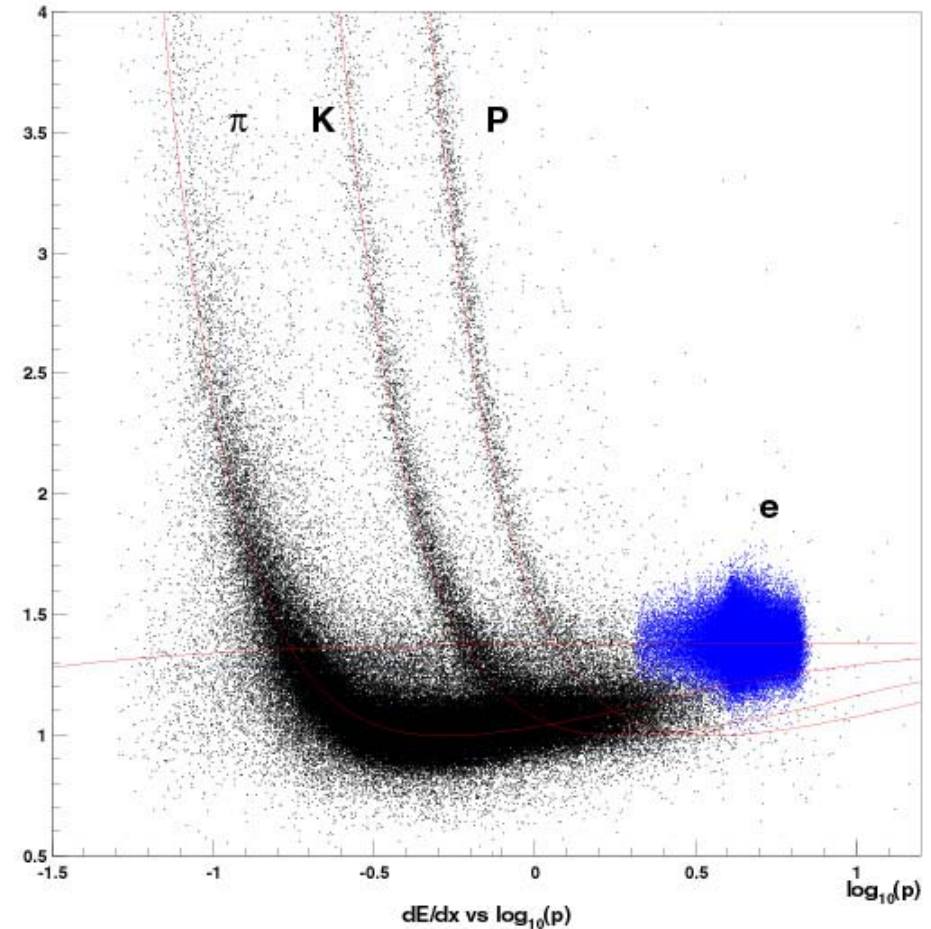
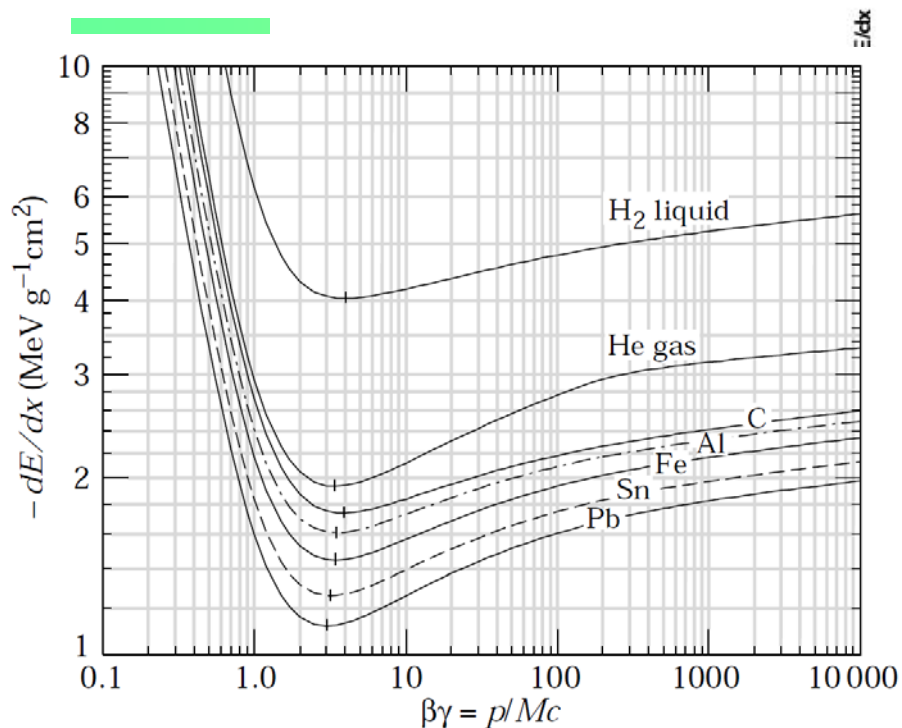


$B \rightarrow \pi\pi$



$B \rightarrow DK$

Identification with the dE/dx measurement

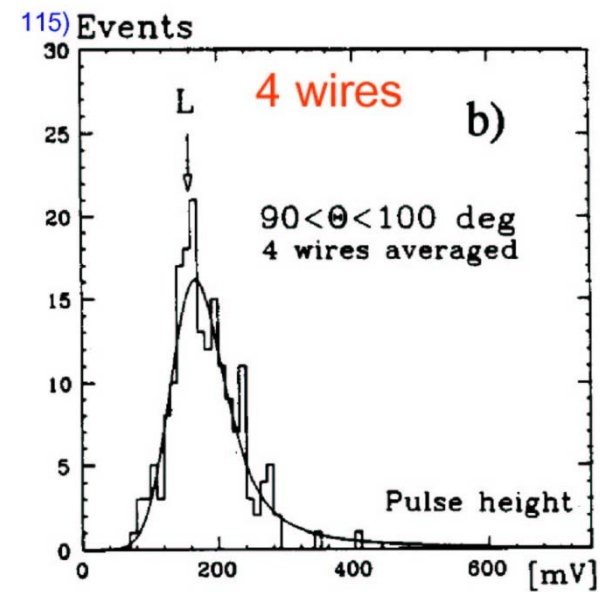
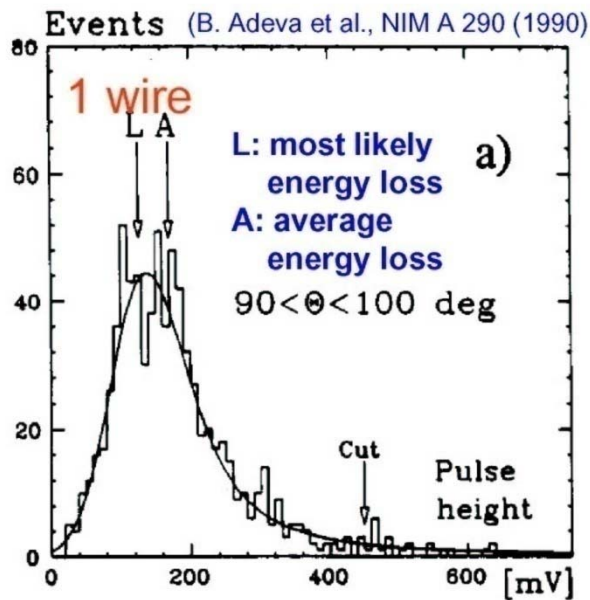
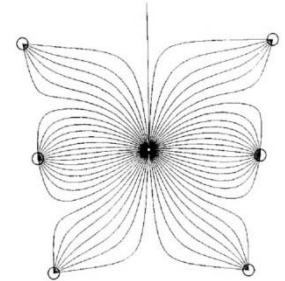


dE/dx is a function of velocity β
For particles with different mass the
Bethe-Bloch curve gets displaced
if plotted as a function of p

For good separation: resolution should be $\sim 5\%$

Identification with dE/dx measurement

Problem: long tails (Landau distribution, not Gaussian) of a single measurement (one drift chamber cell)



Measure in each of the 50 drift chamber layers – use truncated mean (discard 30% largest values – from the tail).

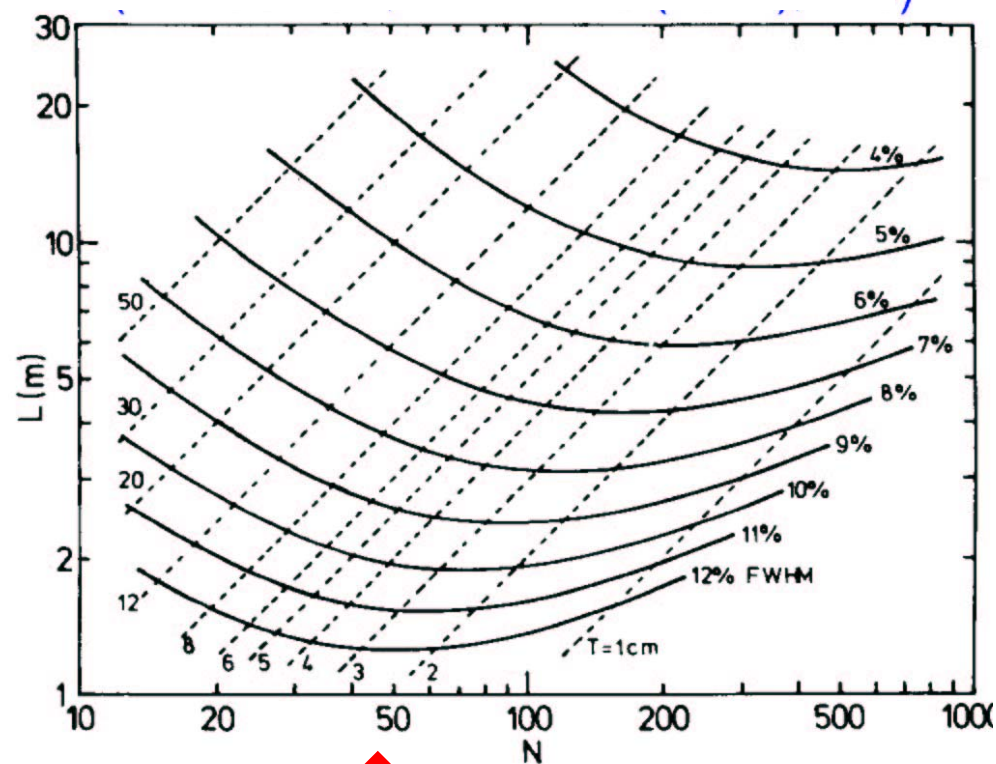
Identification with dE/dx measurement

Optimisation of the counter: length L , number of samples N , resolution (FWHM)

If the distribution of individual measurements were Gaussian, only the total detector length L would be relevant.

Tails: eliminate the largest 30% values \rightarrow the optimum depends also on the number of samples.

At about 1m path length: optimal number of samples: **50**

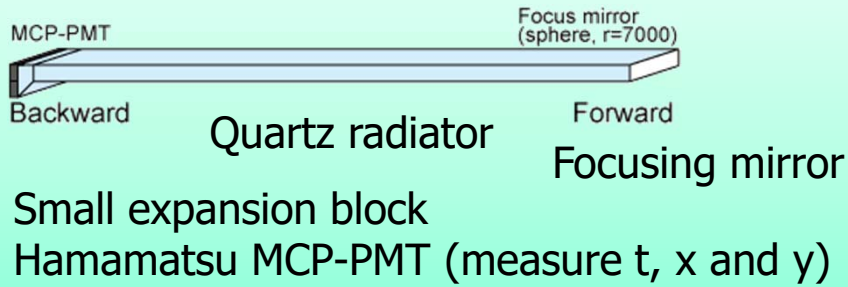


FWHM: full width at half maximum = 2.35 sigma for a Gaussian distribution

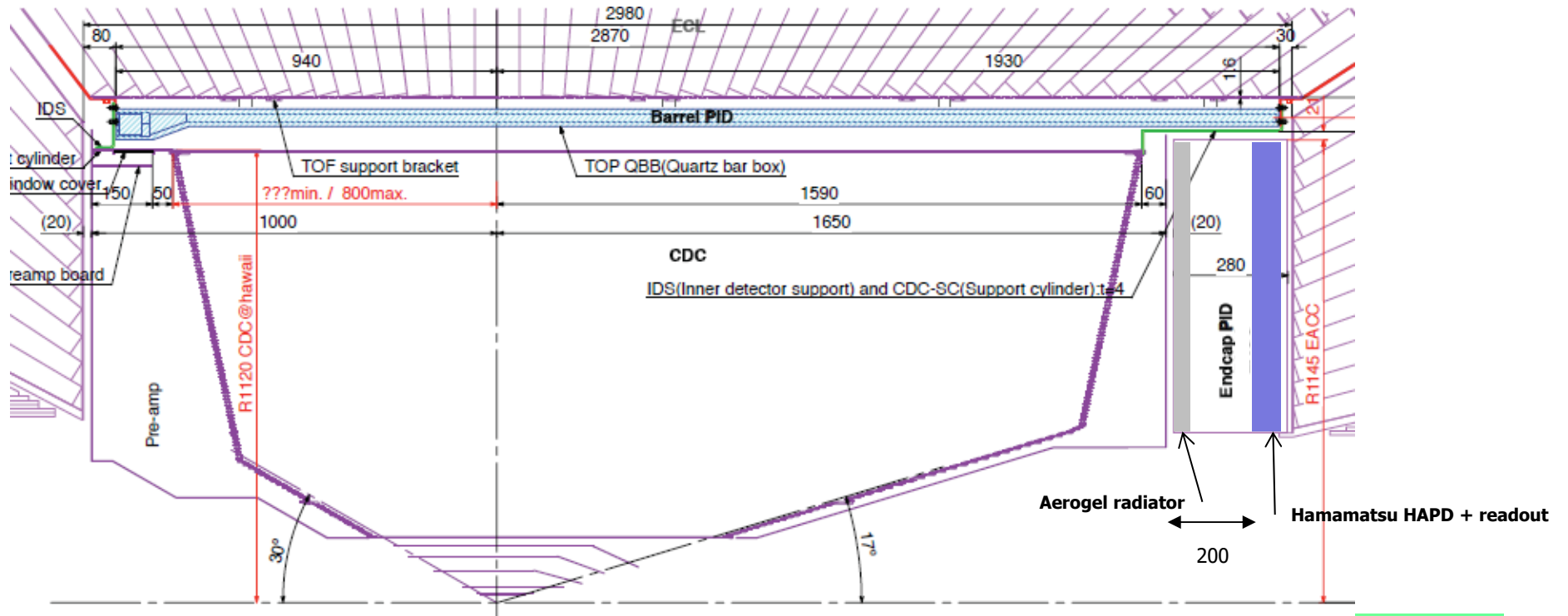
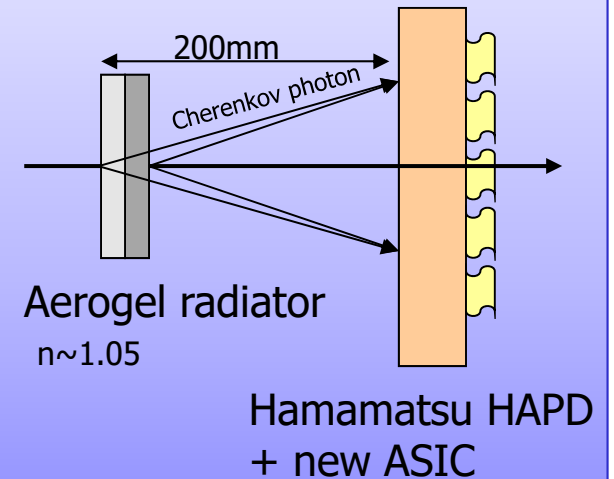


Cherenkov detectors

Barrel PID: Time of Propagation Counter (TOP)



Endcap PID: Aerogel RICH (ARICH)



Cherenkov radiation

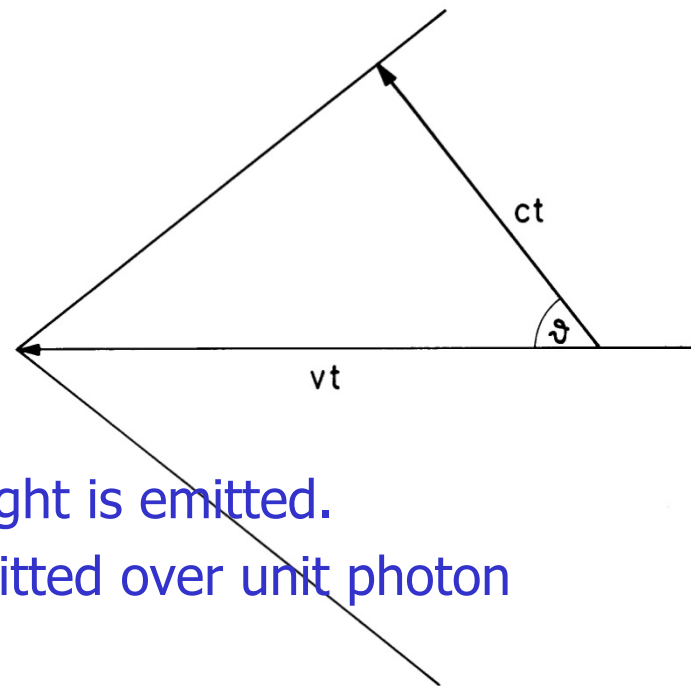
A charged track with velocity $v = \beta c$ exceeding the speed of light c/n in a medium with refractive index n emits **polarized light** at a characteristic (Cherenkov) angle,

$$\cos\theta = c/nv = 1/\beta n$$

Two cases:

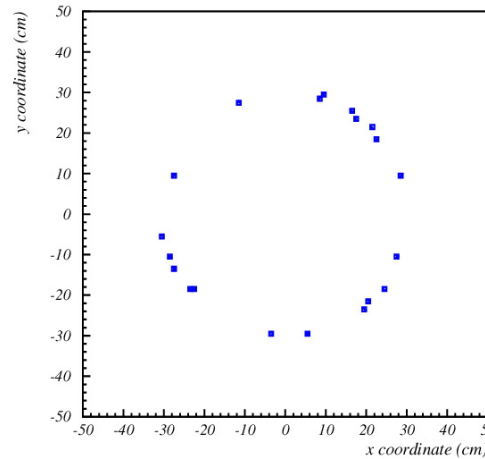
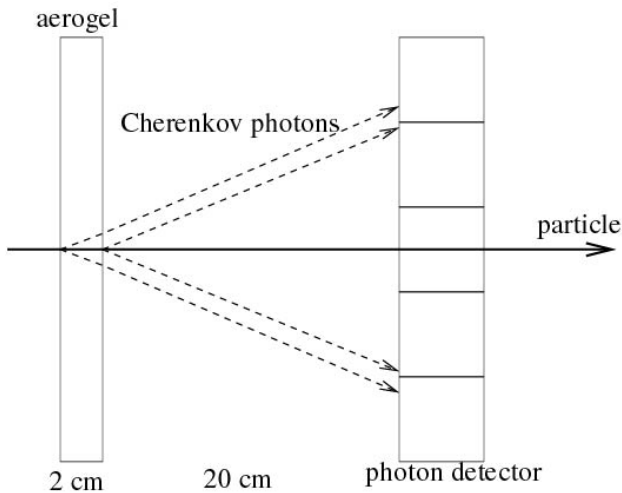
- $\beta < \beta_t = 1/n$: below threshold **no** Cherenkov light is emitted.
- $\beta > \beta_t$: the number of Cherenkov photons emitted over unit photon energy $E = h\nu$ in a radiator of length L :

$$\frac{dN}{dE} = \frac{\alpha}{\eta c} L \sin^2 \theta = 370(\text{cm})^{-1} (\text{eV})^{-1} L \sin^2 \theta$$



→ Few detected photons

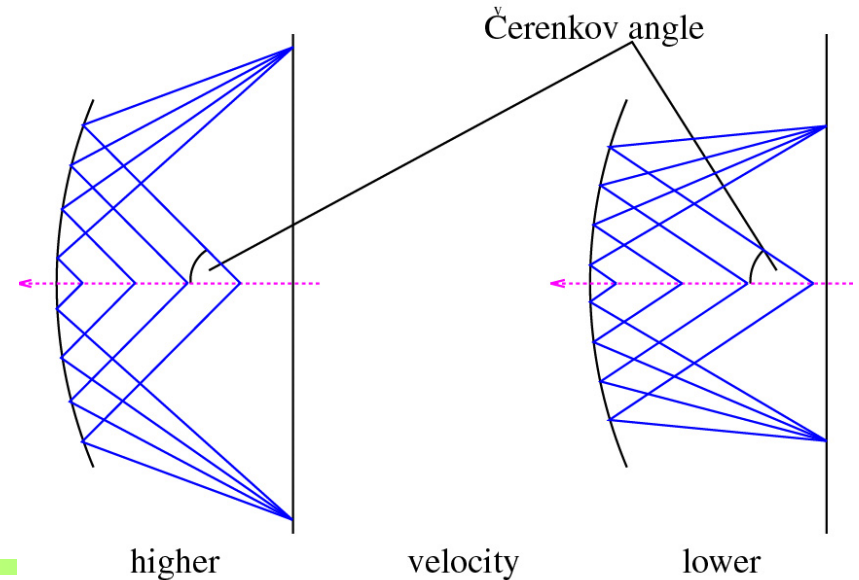
Measuring the Cherenkov angle



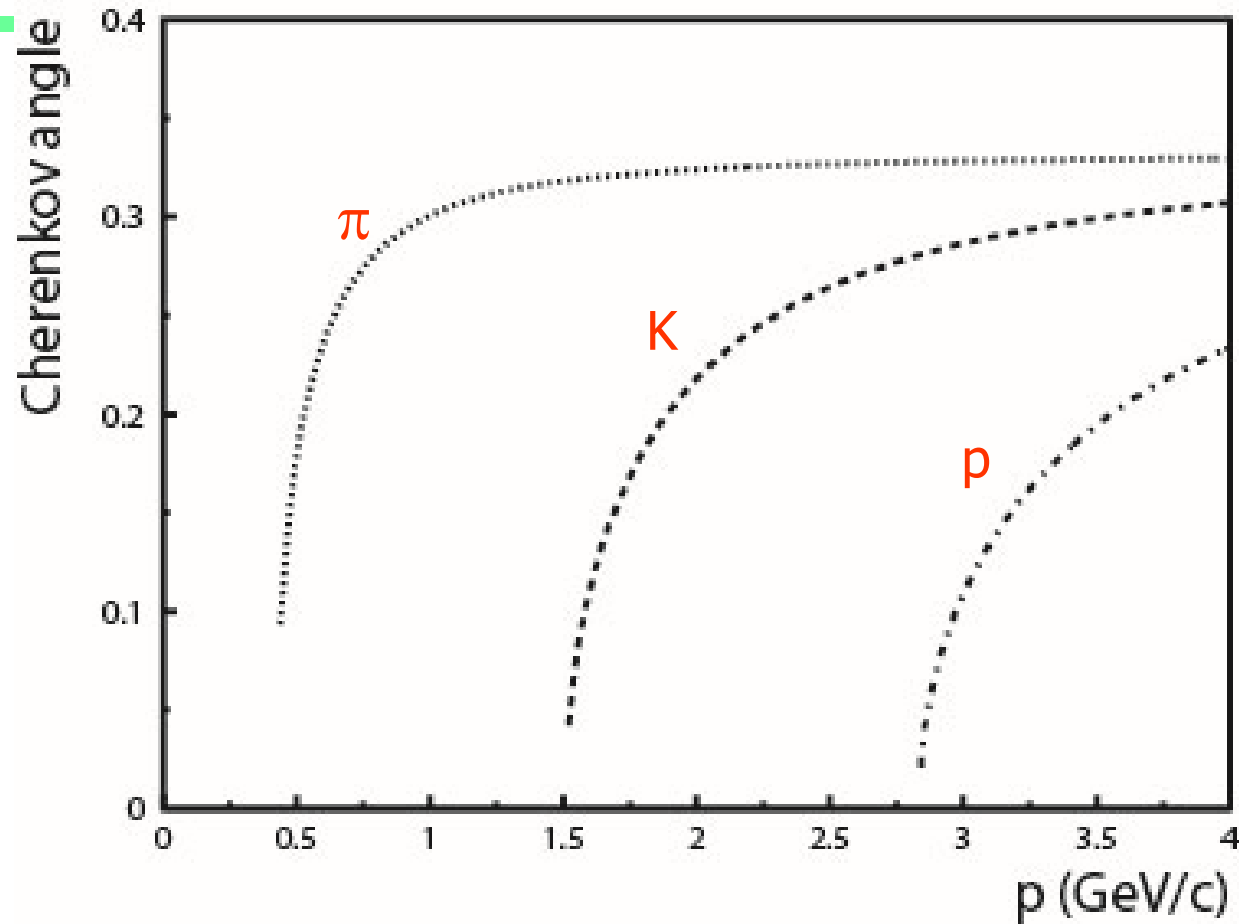
Idea: transform the **direction** into a **coordinate** → ring on the detection plane → **Ring Imaging Cherenkov (RICH) counter**

Proximity focusing RICH

RICH with a focusing mirror



Measuring Cherenkov angle



Radiator:
aerogel, $n=1.06$

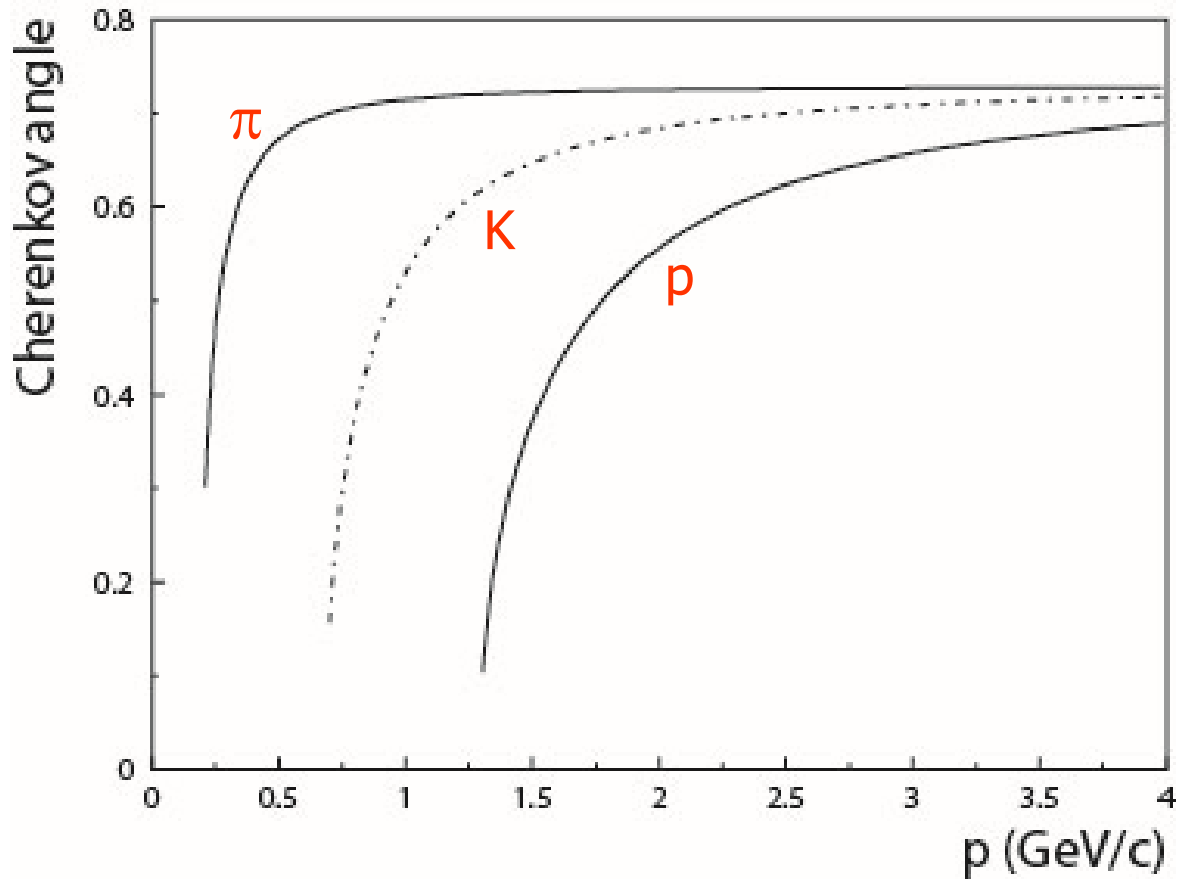
\uparrow
 π

\uparrow
K

\uparrow
p

thresholds

Measuring Cherenkov angle



Radiator:
quartz, $n=1.46$

π K p

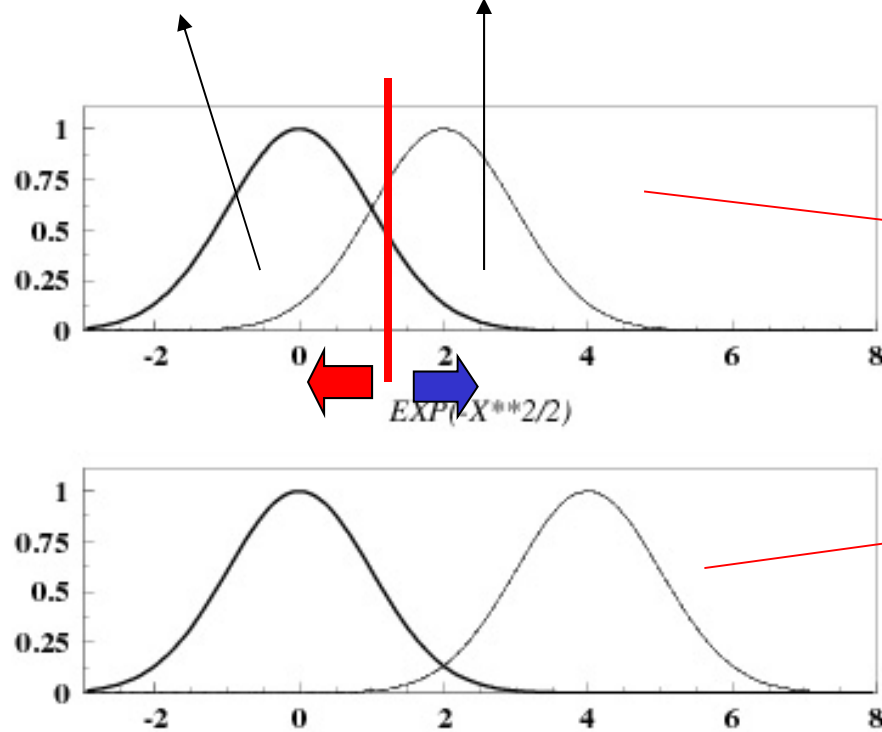
thresholds

Efficiency and purity in particle identification

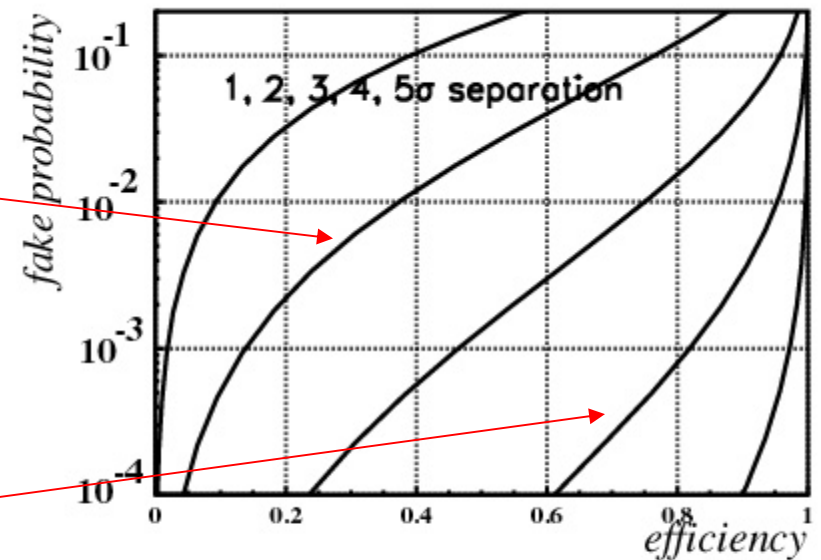
Efficiency and purity are tightly coupled!

Two examples:

particle type 1 type 2

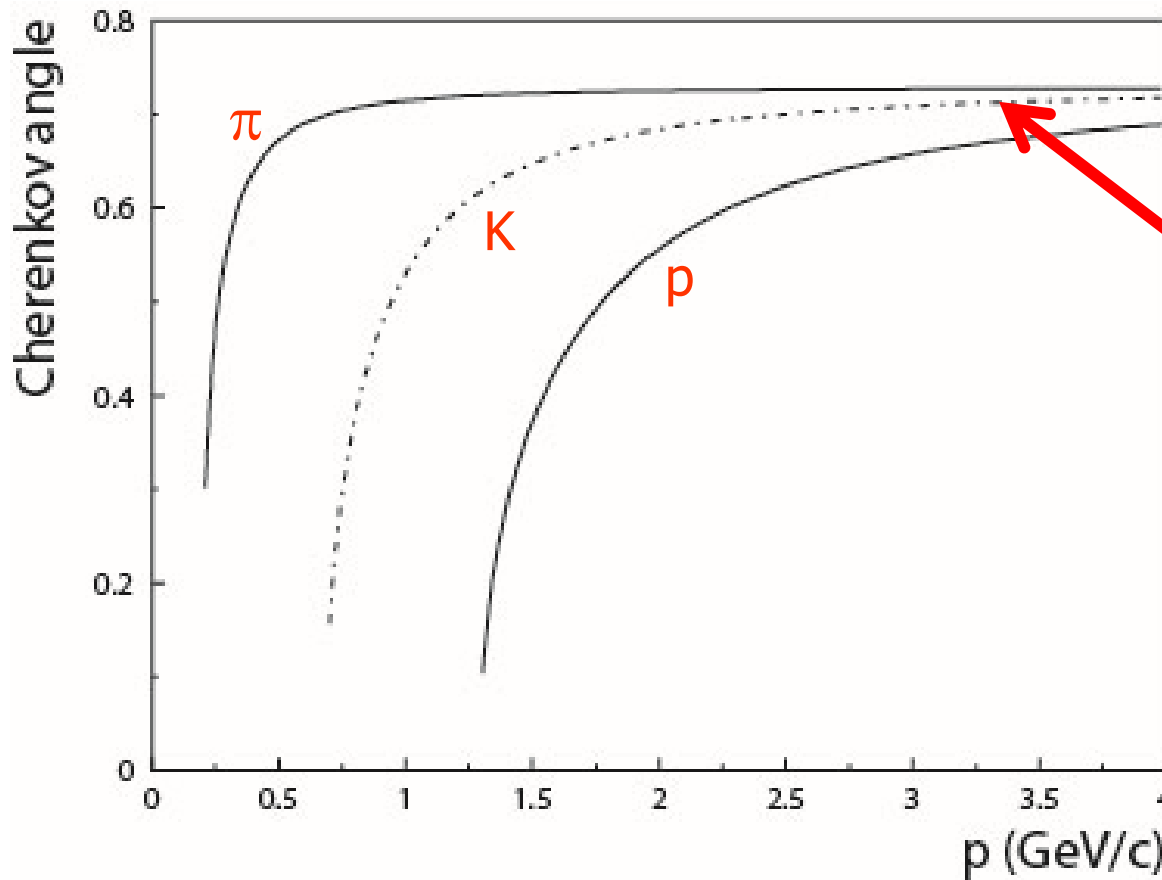


eff. vs fake probability



any discriminating variable, e.g.
Cherenkov angle

Measuring Cherenkov angle



Radiator:
quartz, $n=1.06$

K/ π overlap



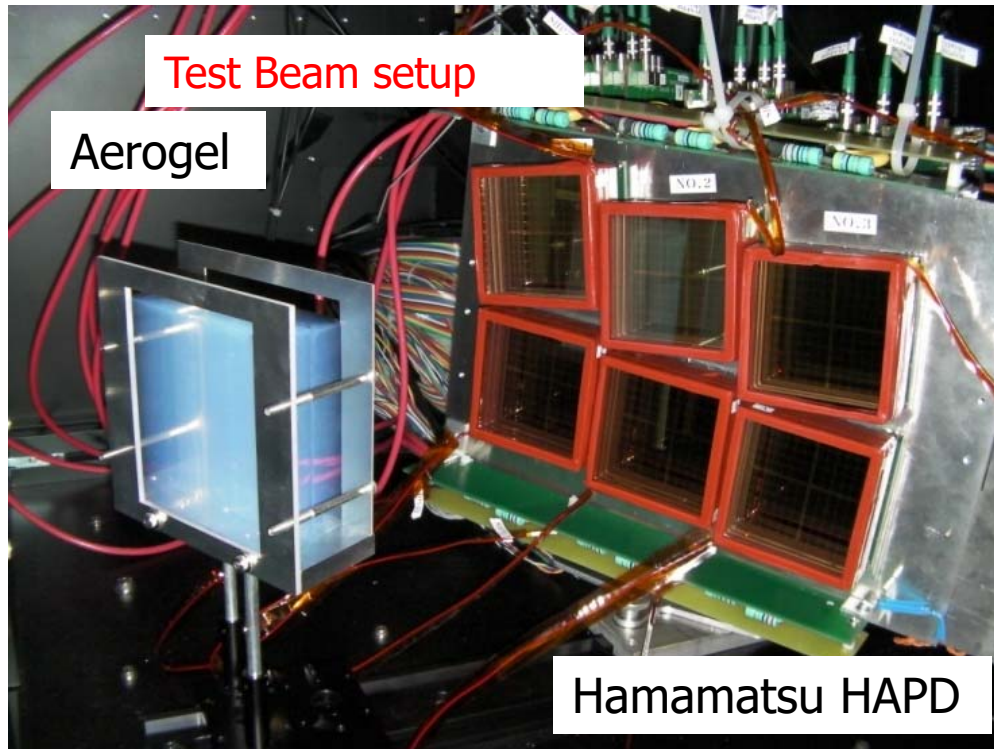
P_{\min} for K/ π separation



P_{\max} for K/ π separation



Aerogel RICH (endcap PID): larger particle momenta



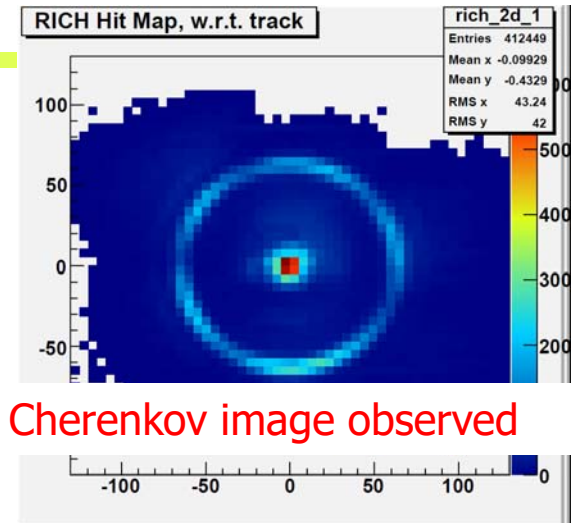
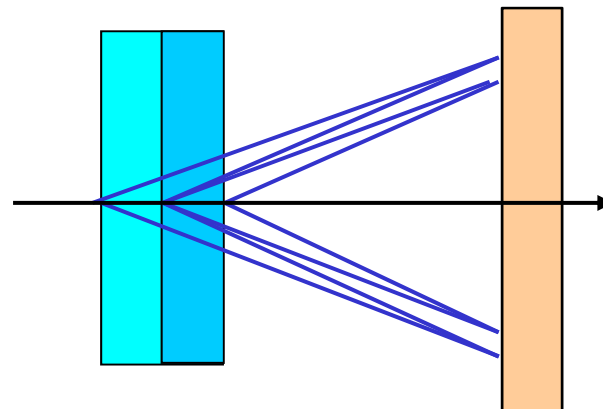
Test Beam setup

Aerogel

Hamamatsu HAPD

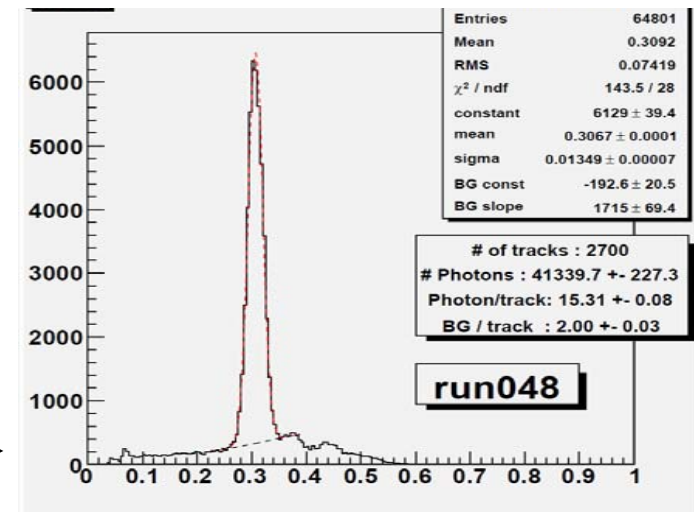
RICH with a novel "focusing" radiator – a two layer radiator

Employ multiple layers with different refractive indices → Cherenkov images from individual layers overlap on the photon detector.



Clear Cherenkov image observed

Cherenkov angle distribution



6.6 σ π/K at 4GeV/c !

Peter Križan, Ljubljana

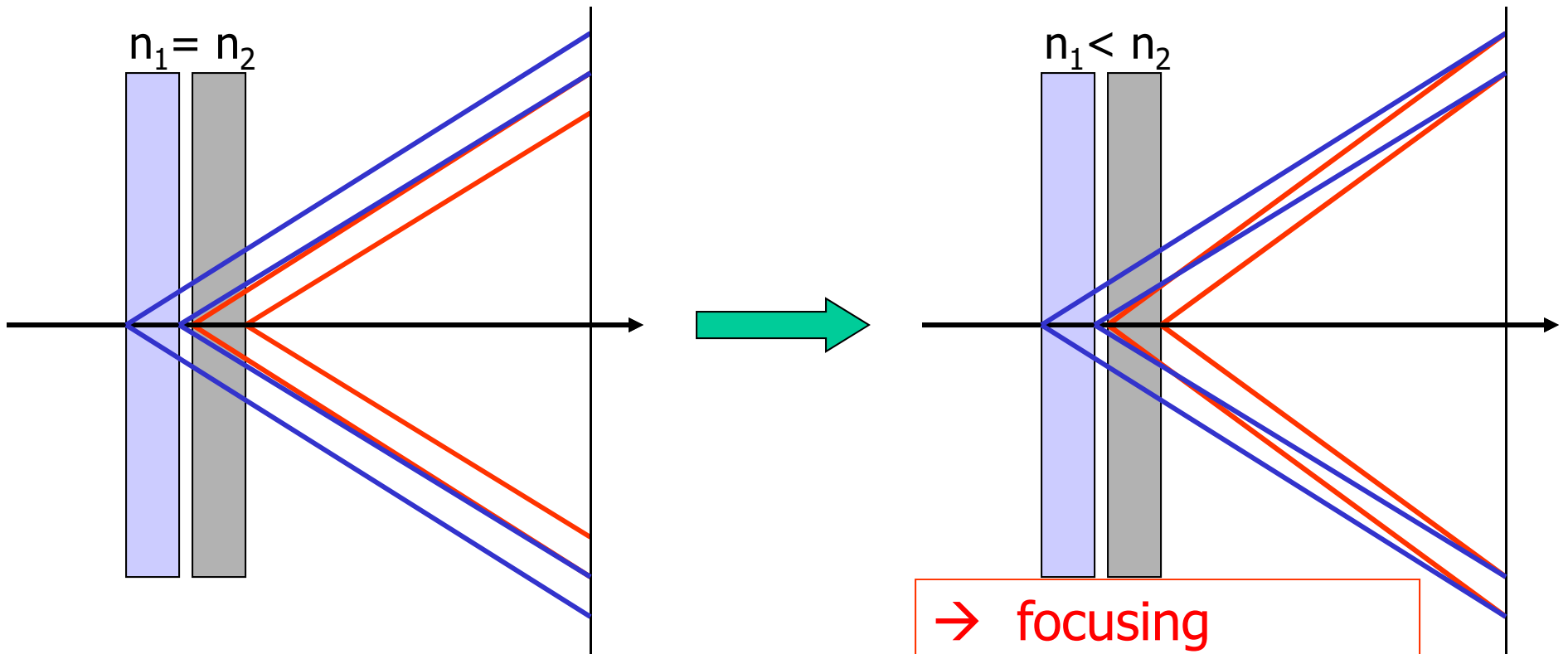


Radiator with multiple refractive indices

How to increase the number of photons without degrading the resolution?

→ stack two tiles with different refractive indices:
“focusing” configuration

normal



→ focusing

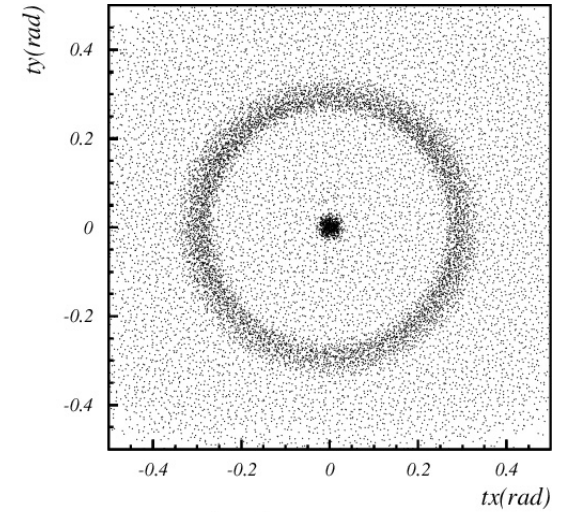
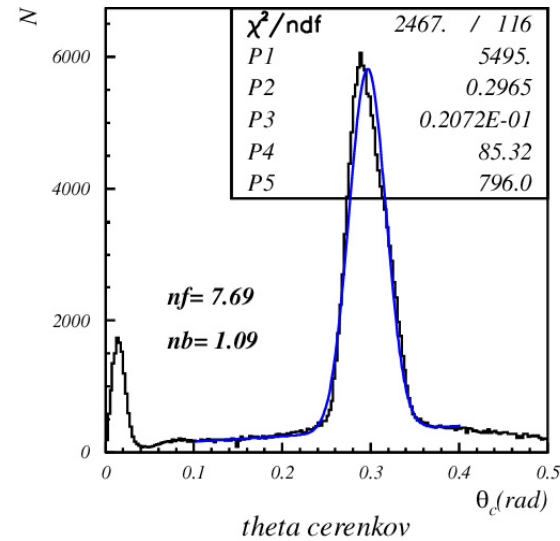
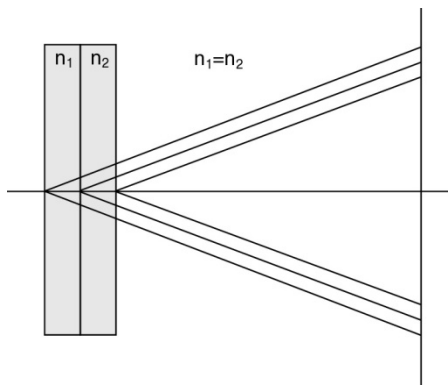
Such a configuration is only possible with aerogel (a form of Si_xO_y)
– material with a tunable refractive index between 1.01 and 1.13.



Focusing configuration – data

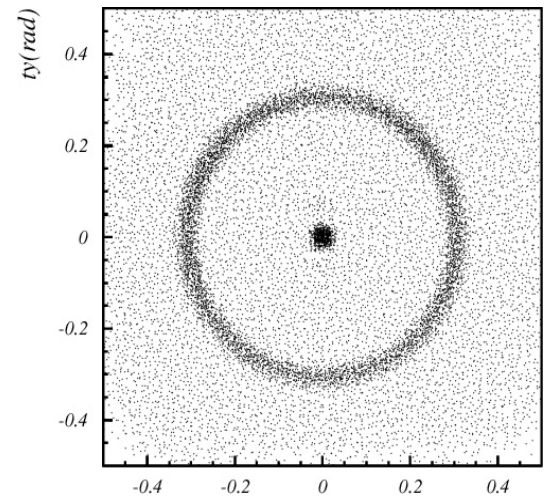
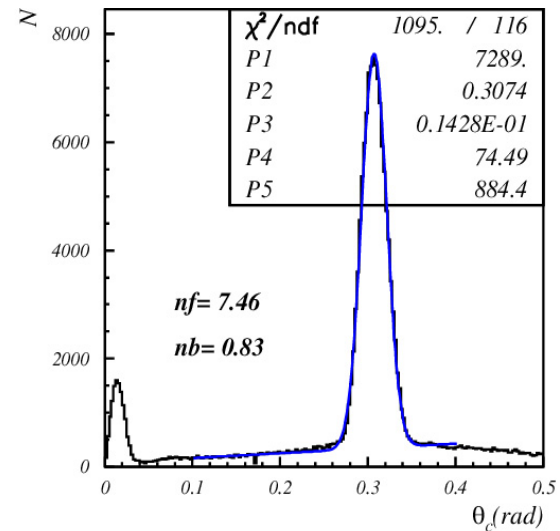
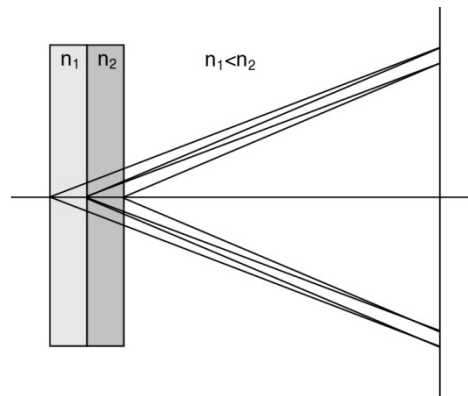
Increases the number of photons without degrading the resolution

4cm aerogel single index



ring in cerenkov space

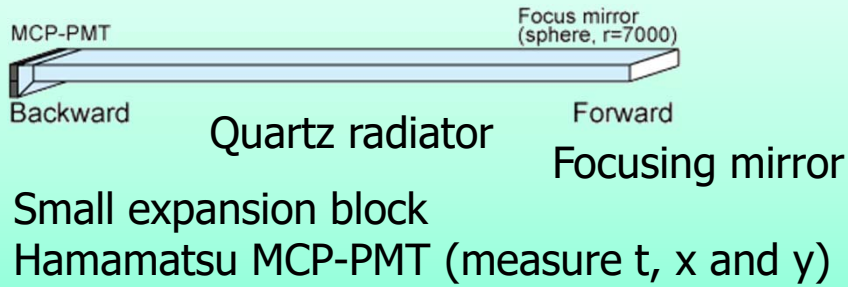
2+2cm aerogel



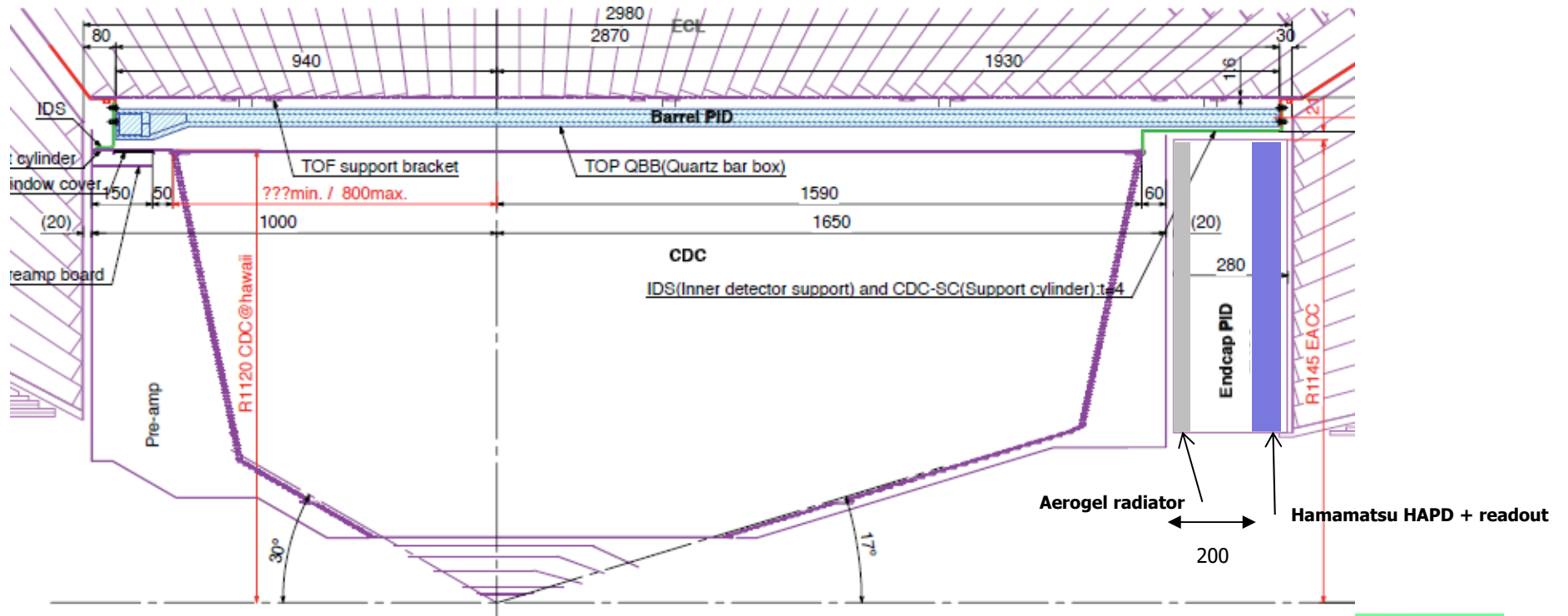
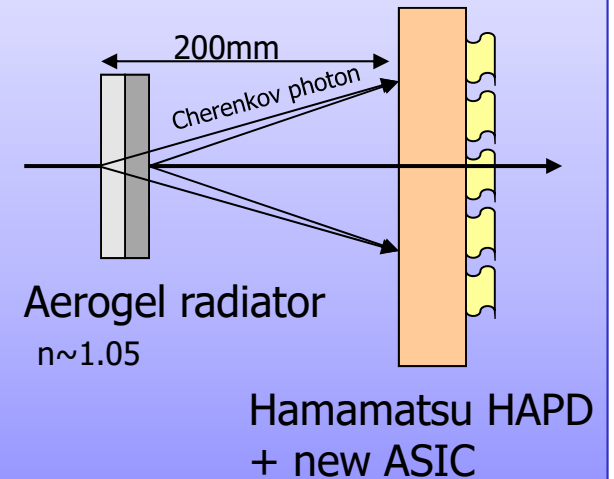
→ NIM A548 (2005) 383

Cherenkov detectors

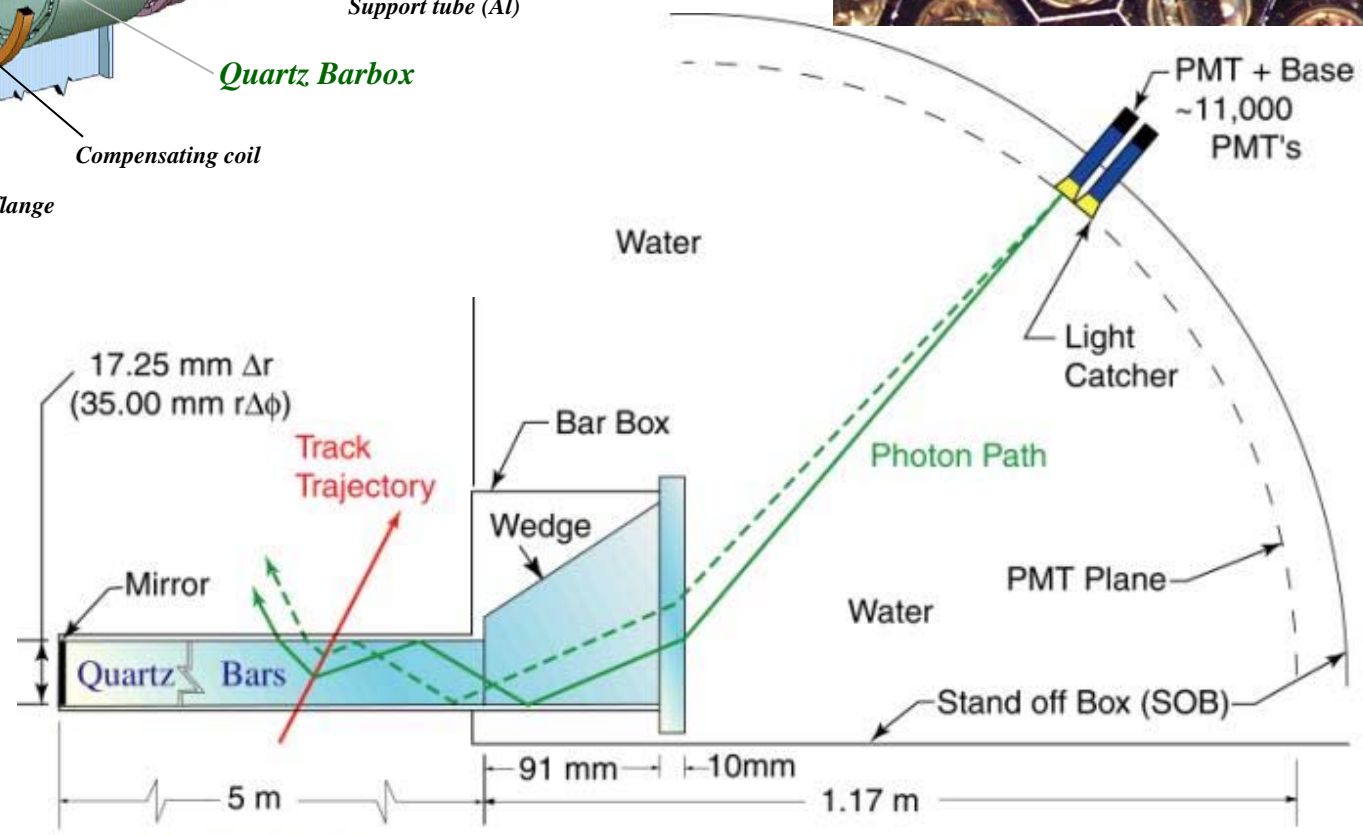
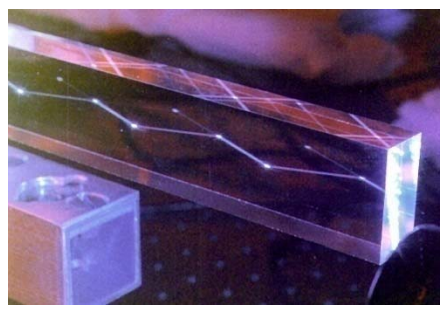
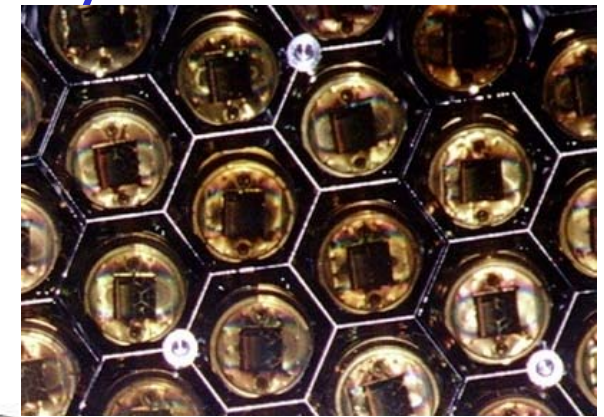
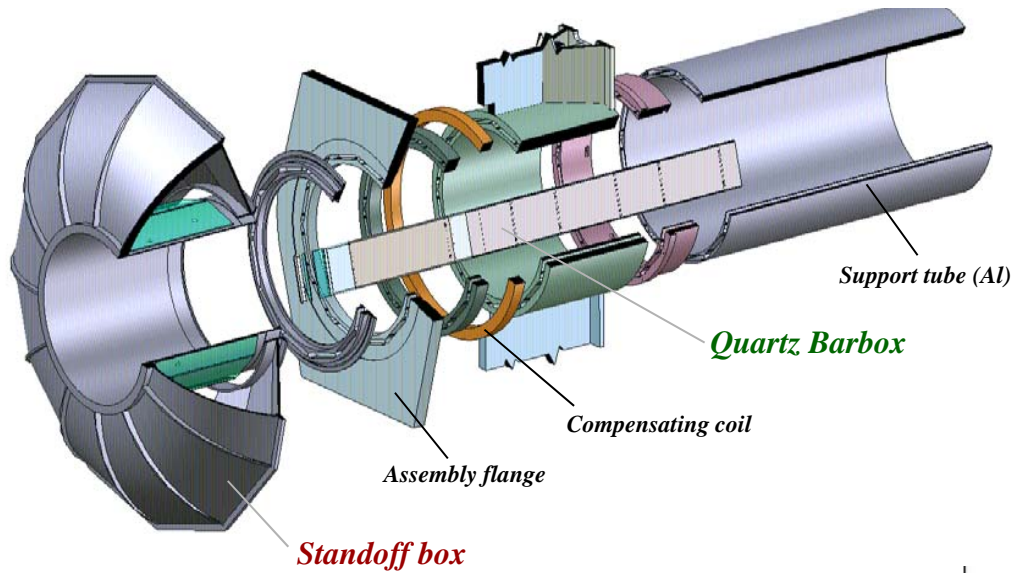
Barrel PID: Time of Propagation Counter (TOP)



Endcap PID: Aerogel RICH (ARICH)

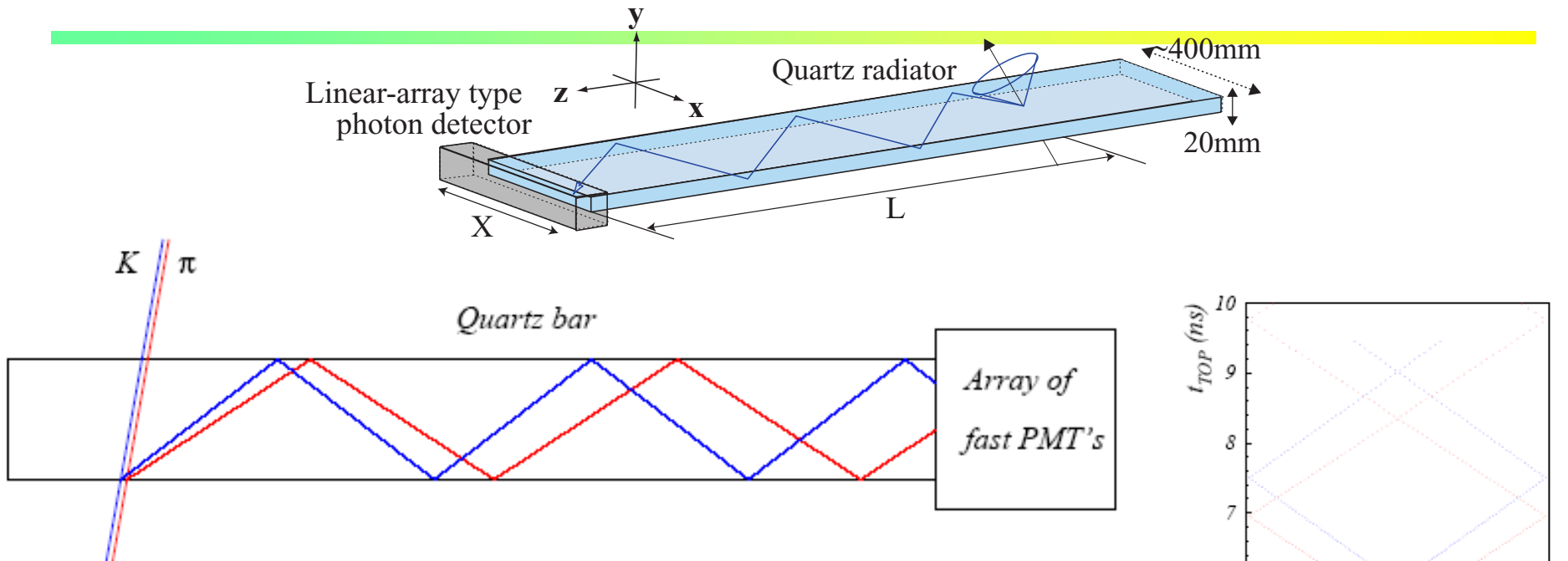


DIRC (@BaBar) - detector of internally reflected Cherenkov light

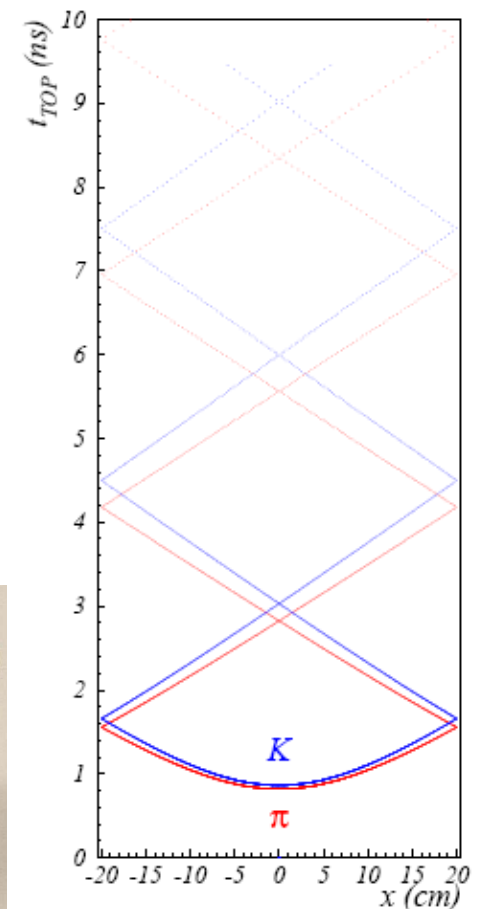
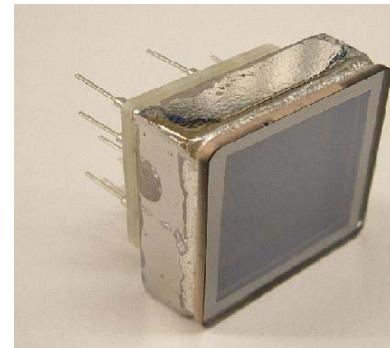


4 x 1.225 m Bars
 glued end-to-end

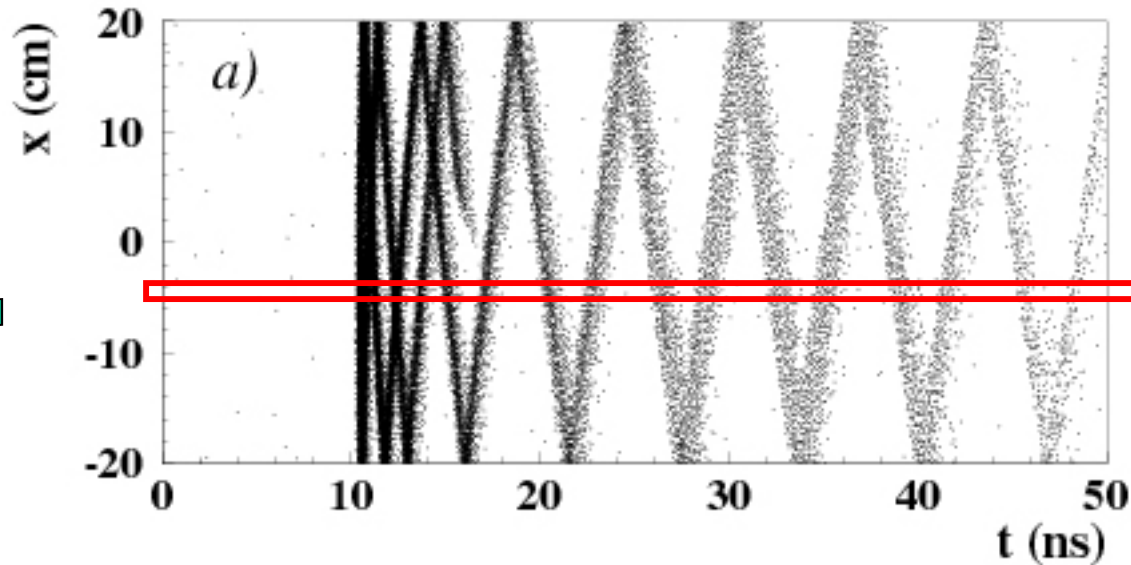
Belle II Barrel PID: Time of propagation (TOP) counter



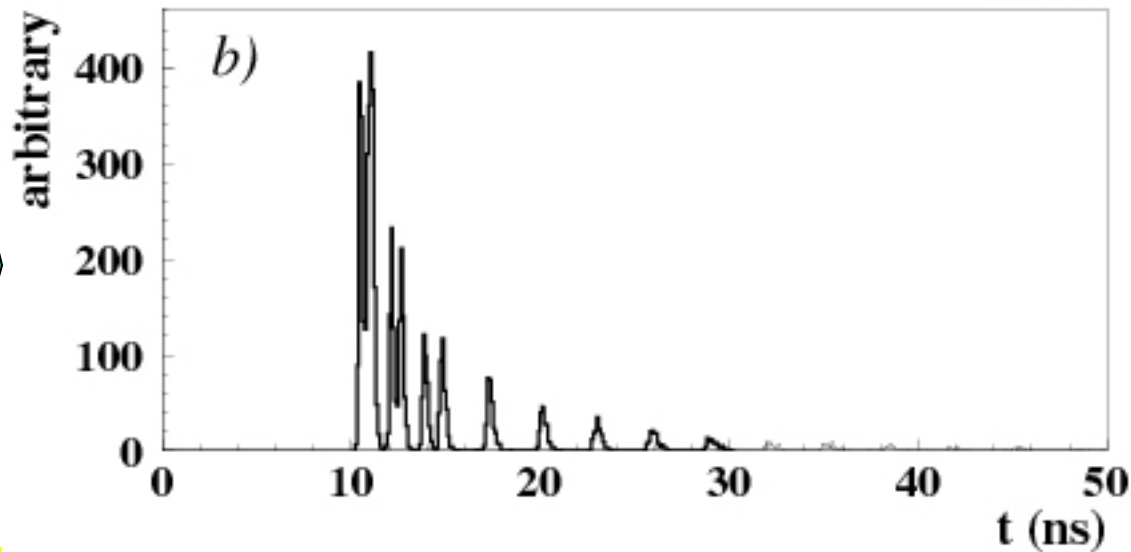
- Cherenkov ring imaging with **precise time measurement**.
- Device uses internal reflection of Cherenkov ring images from quartz like the BaBar DIRC.
- Reconstruct Cherenkov angle from two hit coordinates and the time of propagation of the photon
 - Quartz radiator (2cm)
 - **Photon detector (MCP-PMT)**
 - Excellent time resolution ~ 40 ps
 - Single photon sensitivity in 1.5



TOP image



Pattern in the coordinate-time space ('ring') of a pion hitting a quartz bar with ~ 80 MAPMT channels



Time distribution of signals recorded by one of the PMT channels: different for π and K (\sim shifted in time)

Muon (and K_L) detector

Separate muons from hadrons (pions and kaons): exploit the fact that muons interact only e.m., while hadrons interact strongly \rightarrow need a few interaction lengths (about 10x radiation length in iron, 20x in CsI)

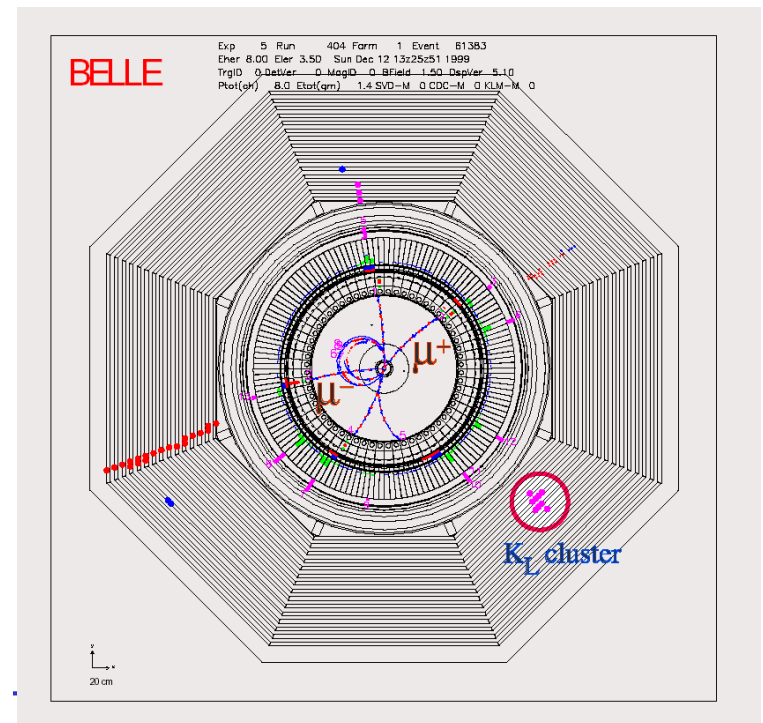
Detect K_L interaction (cluster): again need a few interaction lengths.

\rightarrow Put the detector outside the magnet coil, and integrate into the return yoke

Some numbers: 3.9 interaction lengths (iron)

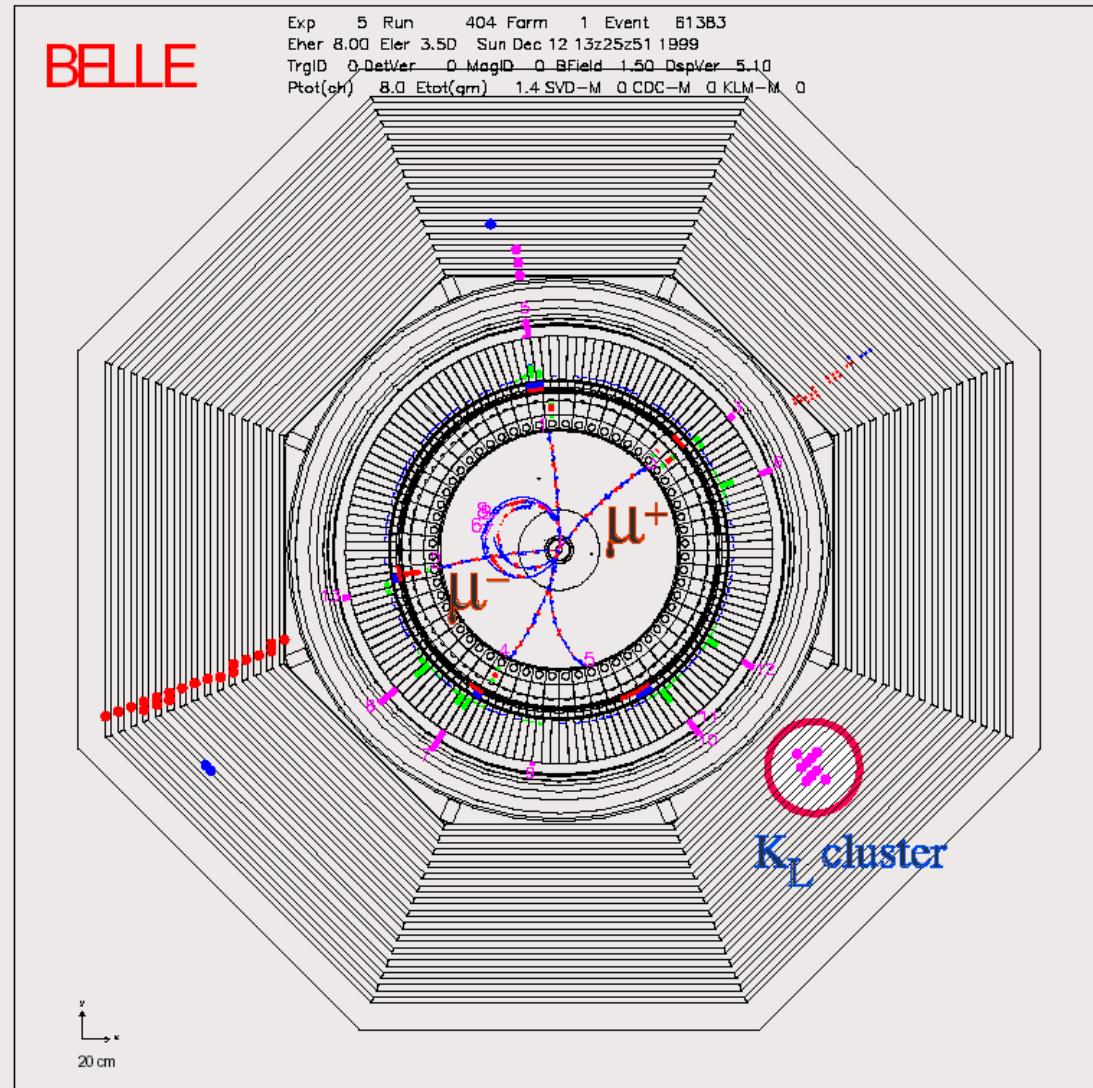
Interaction length: iron 132 g/cm², CsI 167 g/cm²

$(dE/dx)_{\min}$: iron 1.45 MeV/(g/cm²), CsI 1.24 MeV/(g/cm²) $\rightarrow \Delta E_{\min} = (0.36+0.11)$ GeV = 0.47 GeV \rightarrow identification of muons above ~ 600 MeV



Muon and K_L detector

- Example:**
- event with**
- two muons and a K_L
- and a pion that partly penetrated**



Muon and K_L detector performance

Muon identification >800 MeV/c

efficiency

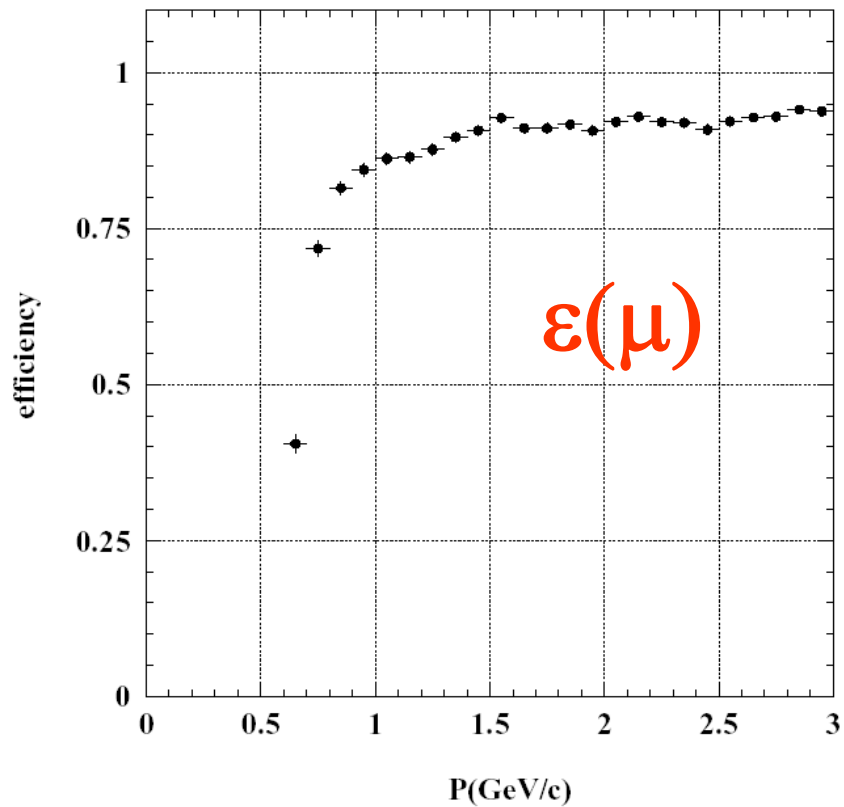


Fig. 109. Muon detection efficiency vs. momentum in KLM.

fake probability

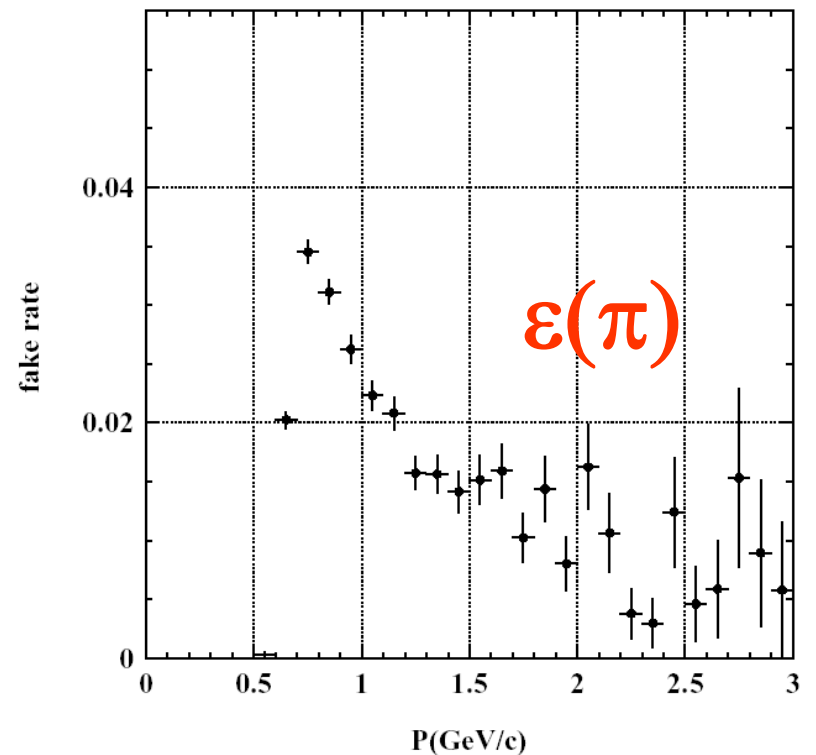


Fig. 110. Fake rate vs. momentum in KLM.

Muon and K_L detector performance

K_L detection: resolution in direction →

K_L detection: also with poss with electromagnetic calorimetry (0.8 interaction lengths)

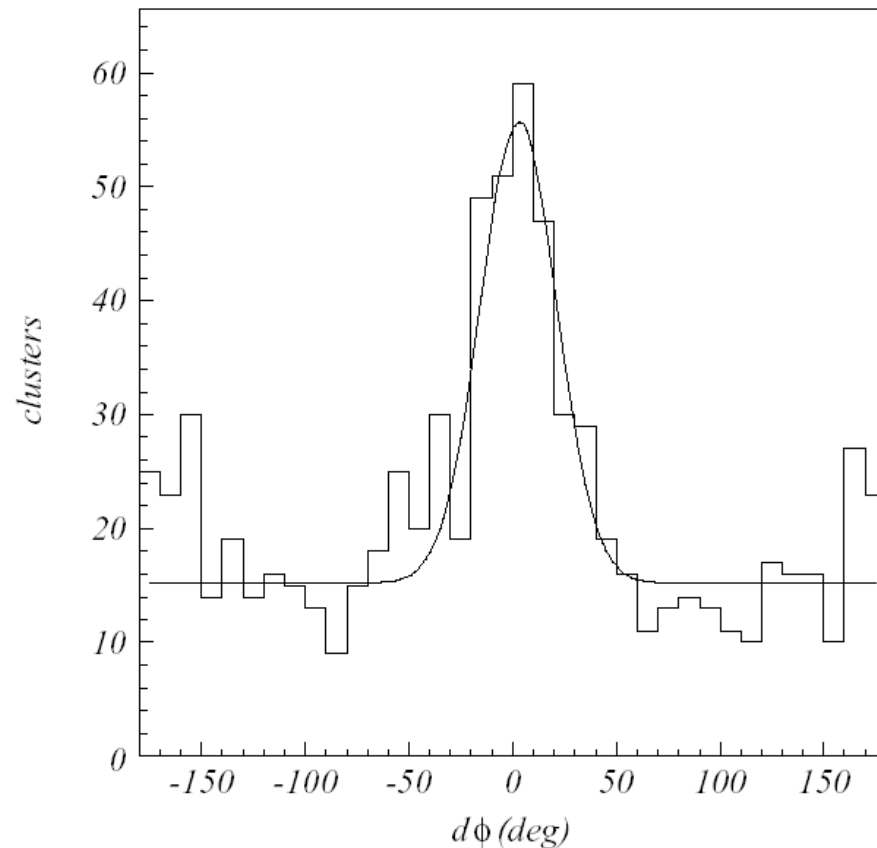
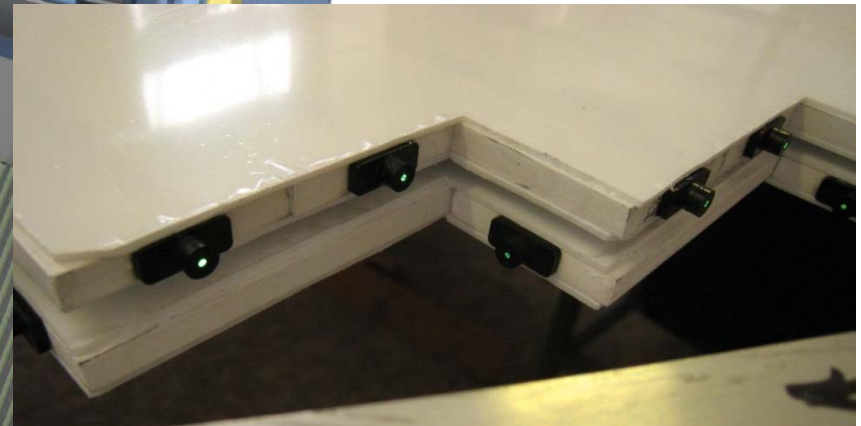
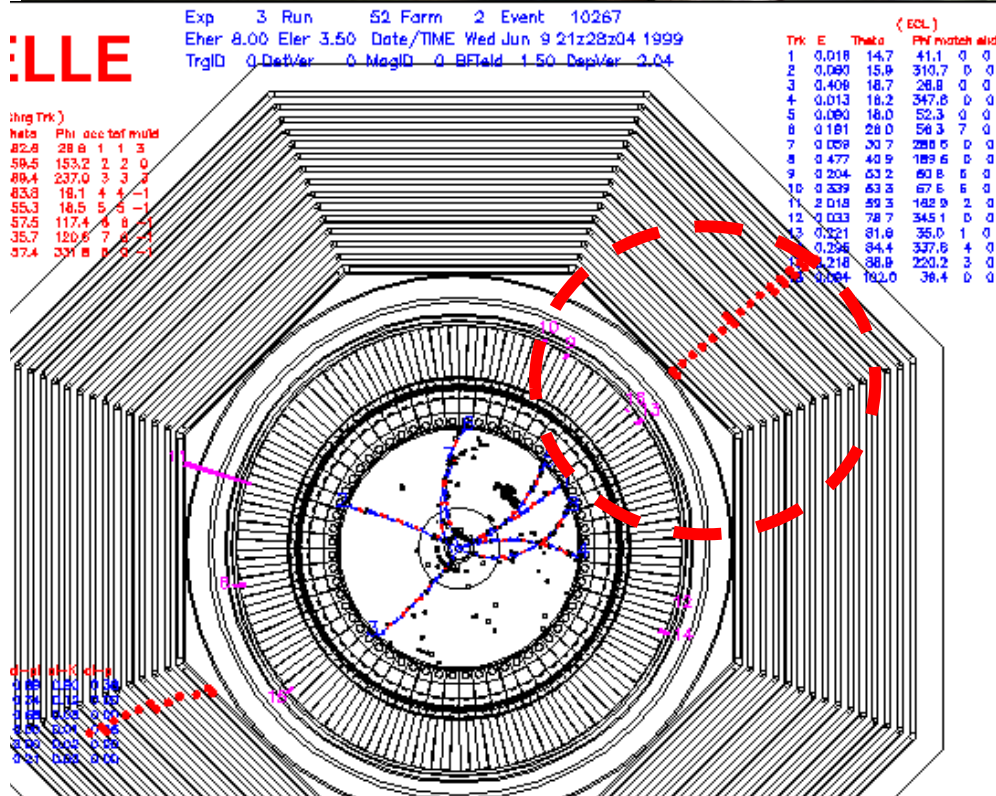
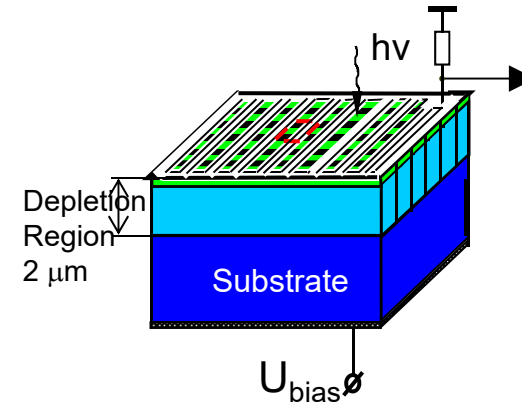
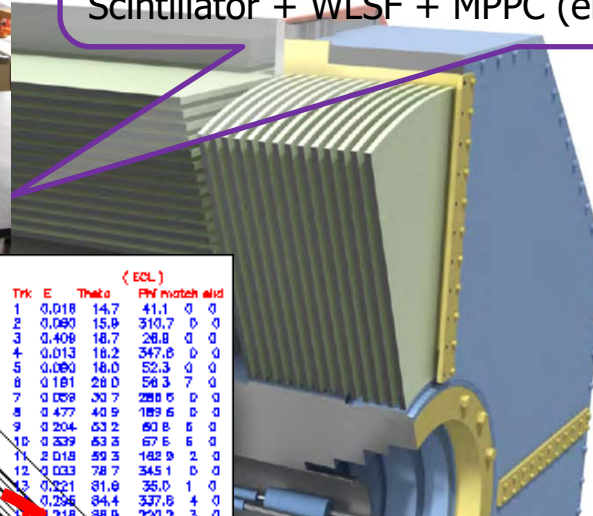
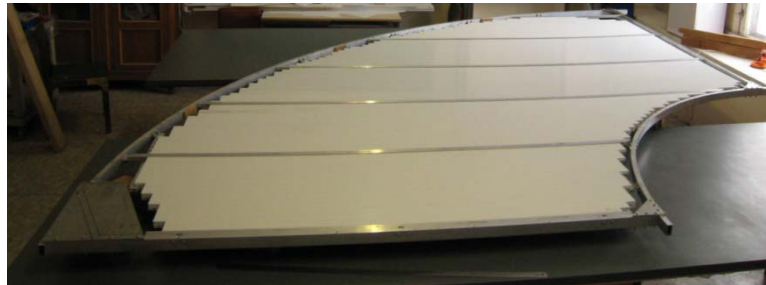


Fig. 107. Difference between the neutral cluster and the direction of missing momentum in KLM.

Belle II, detection of **muons and K_L s**: Parts of the present RPC system have to be replaced to handle higher backgrounds (mainly from neutrons).

K_L and muon detector:
Resistive Plate Counter (barrel)
Scintillator + WLSF + MPPC (end-caps + barrel 2 inner layers)

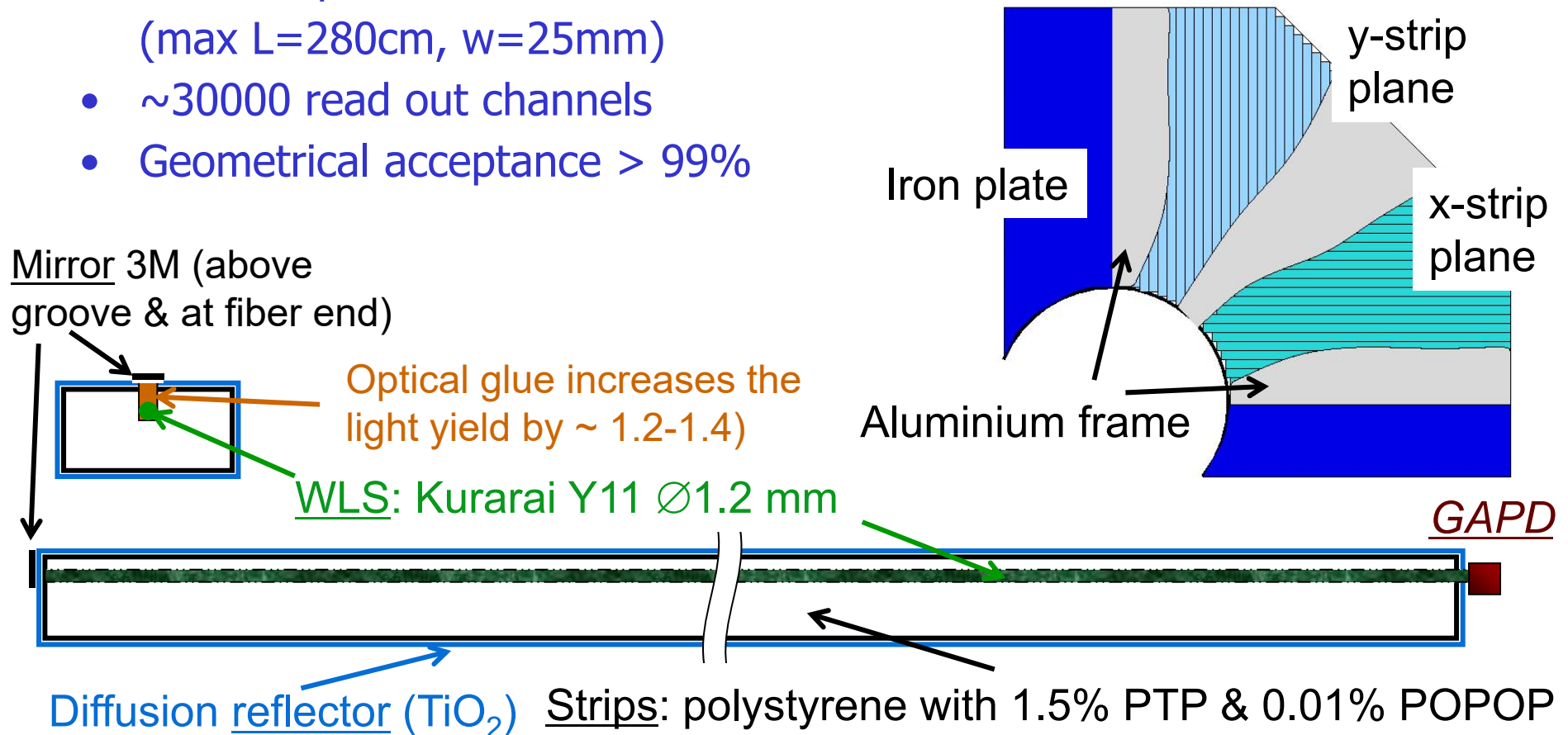


ljana

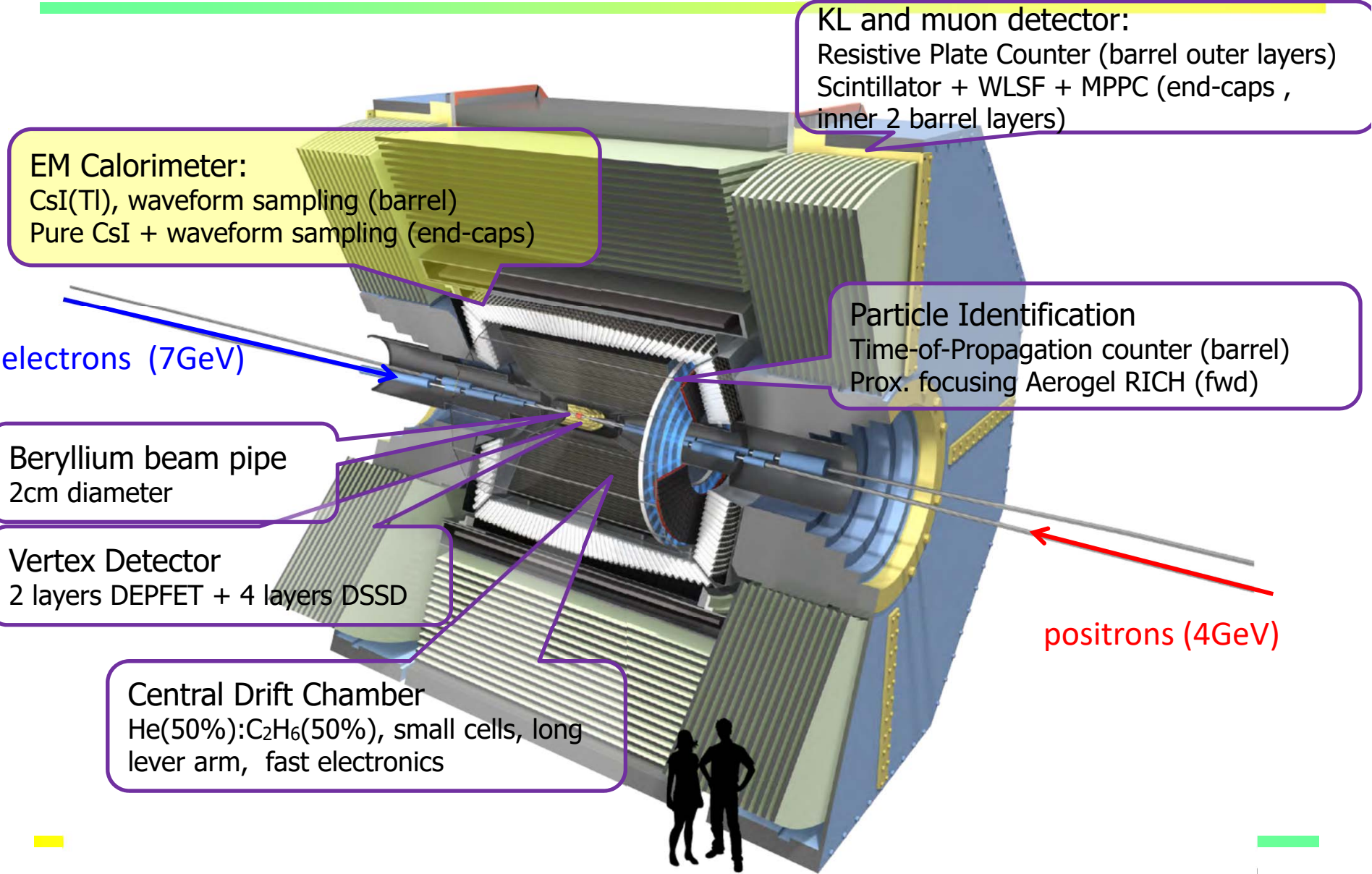
Muon detection system upgrade in the endcaps

Scintillator-based KLM (endcap and two layers in the barrel part)

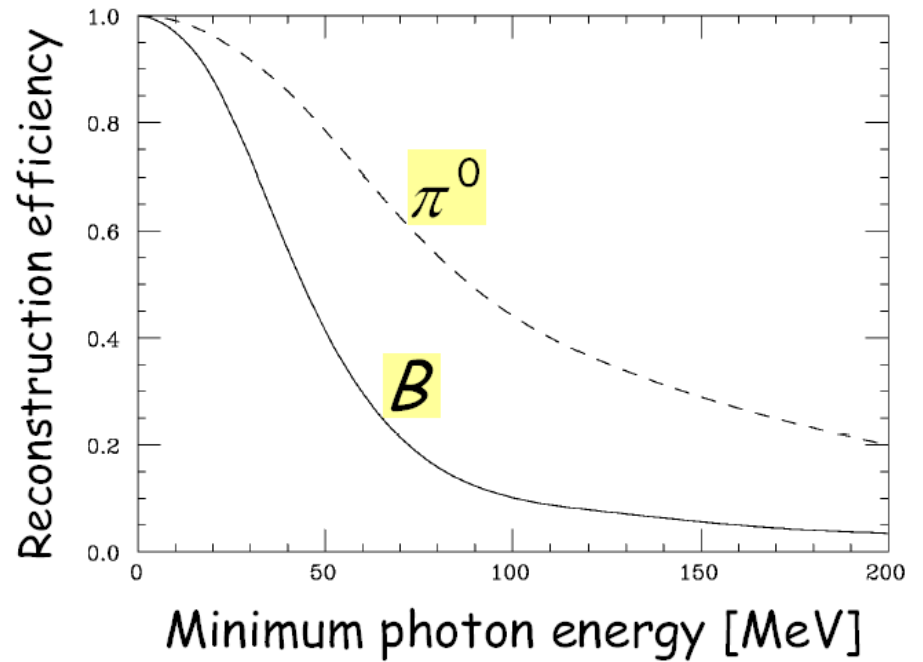
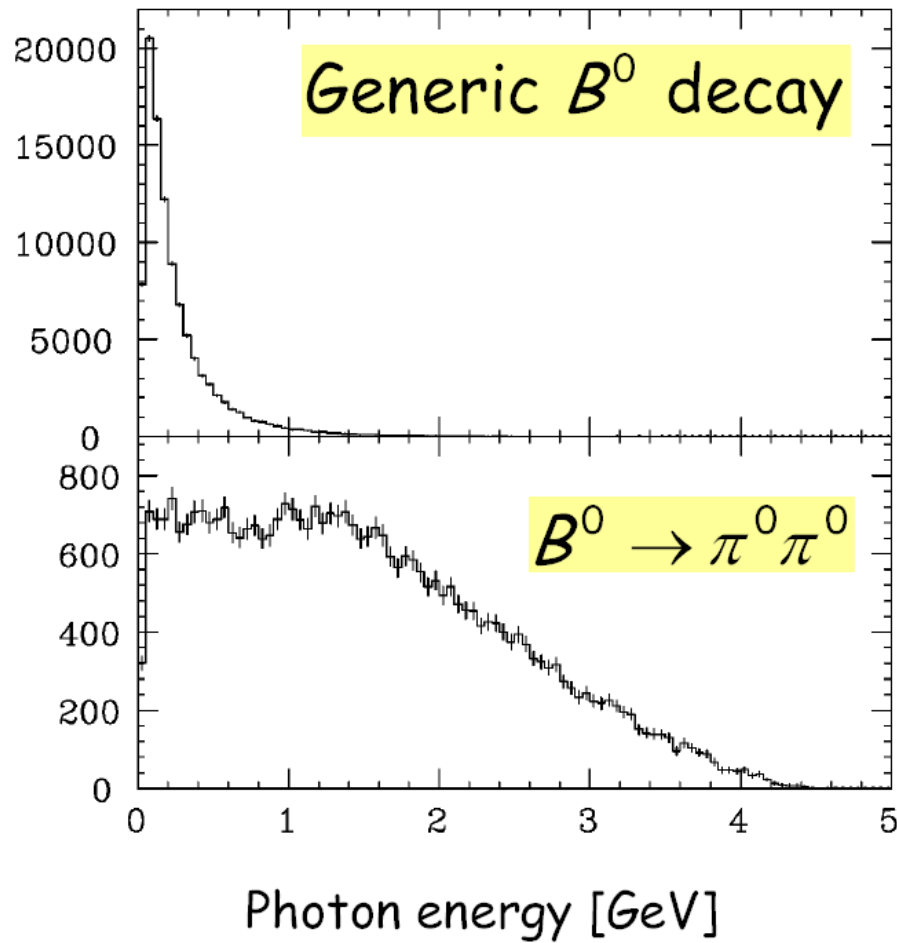
- Two independent (x and y) layers in one superlayer made of orthogonal strips with WLS read out
- Photo-detector = avalanche photodiode in Geiger mode (SiPM)
- ~ 120 strips in one 90° sector (max $L=280\text{cm}$, $w=25\text{mm}$)
- ~ 30000 read out channels
- Geometrical acceptance $> 99\%$



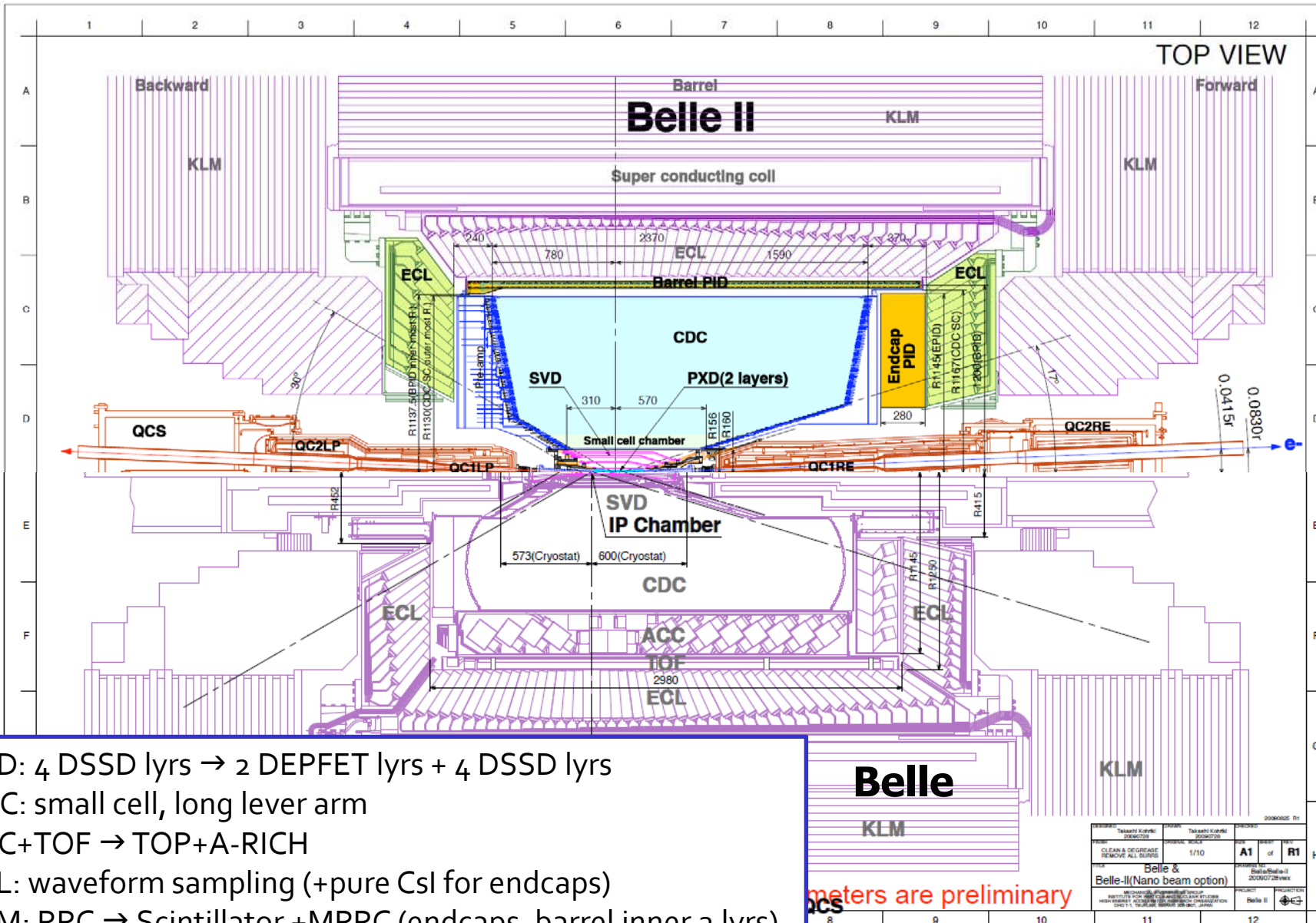
Calorimetry in Belle II



Requirements: Photons



Belle II Detector (in comparison with Belle)



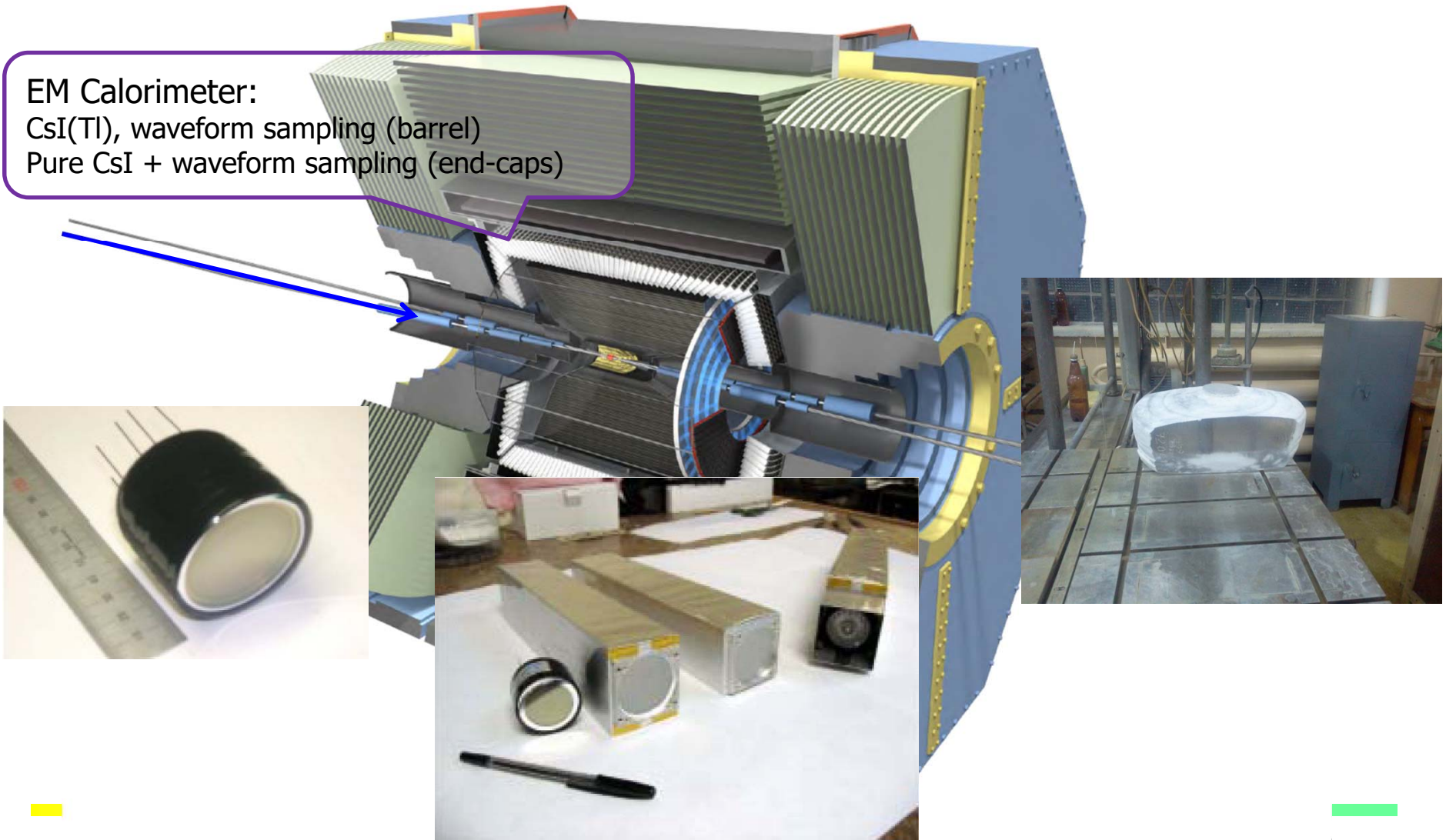
SVD: 4 DSSD lyrs → 2 DEPFET lyrs + 4 DSSD lyrs
 CDC: small cell, long lever arm
 ACC+TOF → TOP+A-RICH
 ECL: waveform sampling (+pure CsI for endcaps)
 KLM: RPC → Scintillator +MPPC (endcaps, barrel inner 2 lyrs)

meters are preliminary

Scintillator material	Density (g/cm ³)	Radiation length	Refractive index	Wavelength at peak	Decay time	Light yield (Y/MeV)
Nal (TI)	3.67	2.59 cm	1.78	410 nm	230 ns	4.1 x10 ⁴
Csl (TI)	4.51	1.86 cm	1.85	550 nm	800–6000 ns	6.6 x10 ⁴
Csl (Na)	4.51	1.86 cm	1.80	420 nm	630 ns	4.0 x10 ⁴
LaBr ₃ (Ce)	5.3	1.88 cm	1.9	358 nm	35 ns	6.1 x10 ⁴
Bi ₄ Si ₃ O ₁₂ BSO	6.8	1.15 cm	2.06	480 nm	100 ns	0.2 x10 ⁴
Bi ₄ Ge ₃ O ₁₂ BGO	7.1	1.12 cm	2.15	480 nm	300 ns	0.9 x10 ⁴
CdWO ₄	7.9	1.1 cm	2.25	495 nm	5000 ns	2.0 x10 ⁴
YAlO ₃ (Ce) YAP	5.5	2.9 cm	1.94	350 nm	30 ns	2.1 x10 ⁴
Lu ₃ Al ₅ O ₇ (Ce) LuAG	7.4	1.4 cm	1.84	420 nm	40 ns	2.6 x10 ⁴
Gd ₂ SiO ₅ (Ce) GSO	6.7	1.4 cm	1.87	440 nm	60 ns	0.8 x10 ⁴
PbWO ₄	8.3	0.89 cm	1.82	425 nm	25 ns	0.05 x10 ⁴

EM calorimeter: upgrade needed because of **higher rates**
(barrel: **electronics**, endcap: **electronics** and CsI(Tl) → **pure CsI**), and **radiation** load (endcap: CsI(Tl) → **pure CsI**)

EM Calorimeter:
CsI(Tl), waveform sampling (barrel)
Pure CsI + waveform sampling (end-caps)

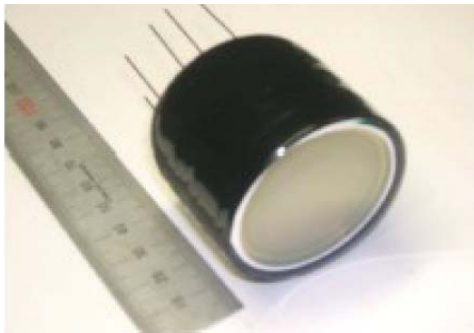


EM calorimeter: upgrade needed because of

- higher rates (barrel: **electronics**, endcap: **electronics** and CsI(Tl) → **pure CsI**), and
- radiation load (endcap: CsI(Tl) → **pure CsI**)

Pure CsI is faster, but has a smaller light yield...

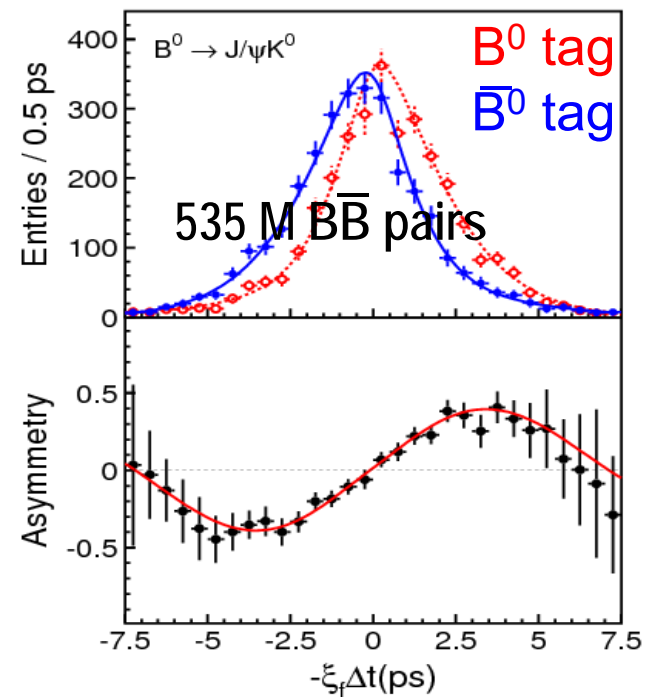
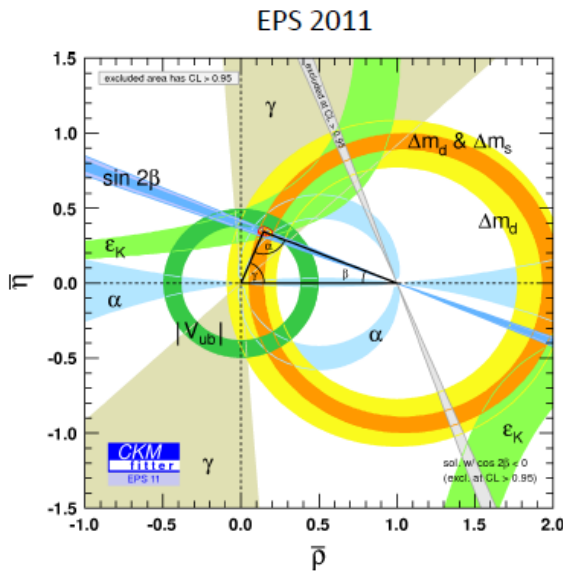
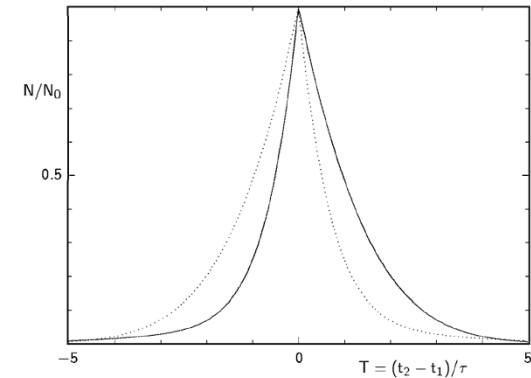
→ replace photodiodes with a special kind of PMT (photopentode) that can be operated in magnetic field



B factories main result: CP violation in the B system

CP violation in B system: from
the **discovery** (2001) to a
precision measurement

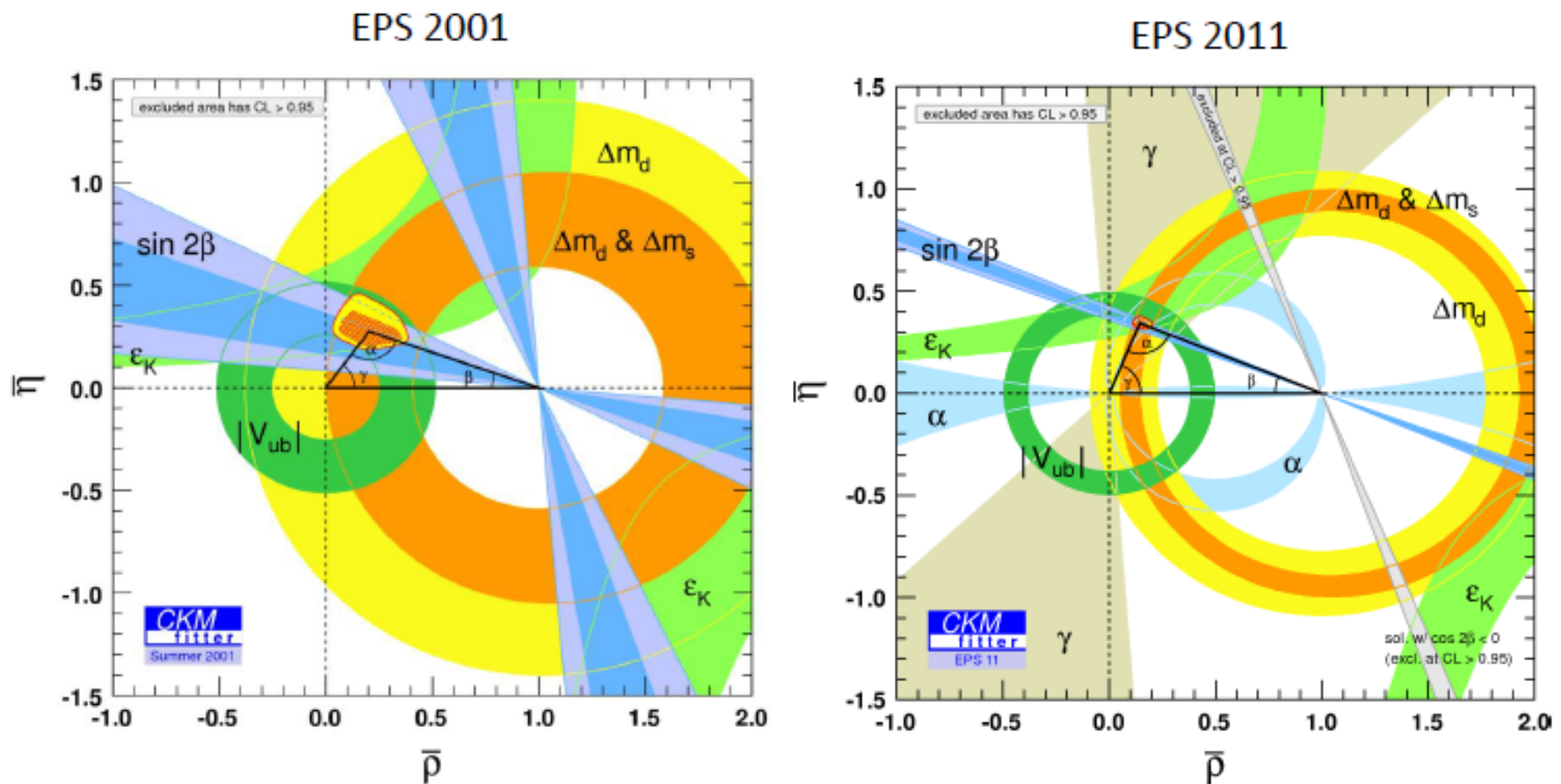
$\sin 2\phi_1 / \sin 2\beta$ from $b \rightarrow cc\bar{s}$



Constraints from measurements of angles and
sides of the unitarity triangle \rightarrow **Remarkable
agreement**

Unitarity triangle – 2011 vs 2001

CP violation in the B system: from the **discovery** (2001) to a **precision measurement** (2011).

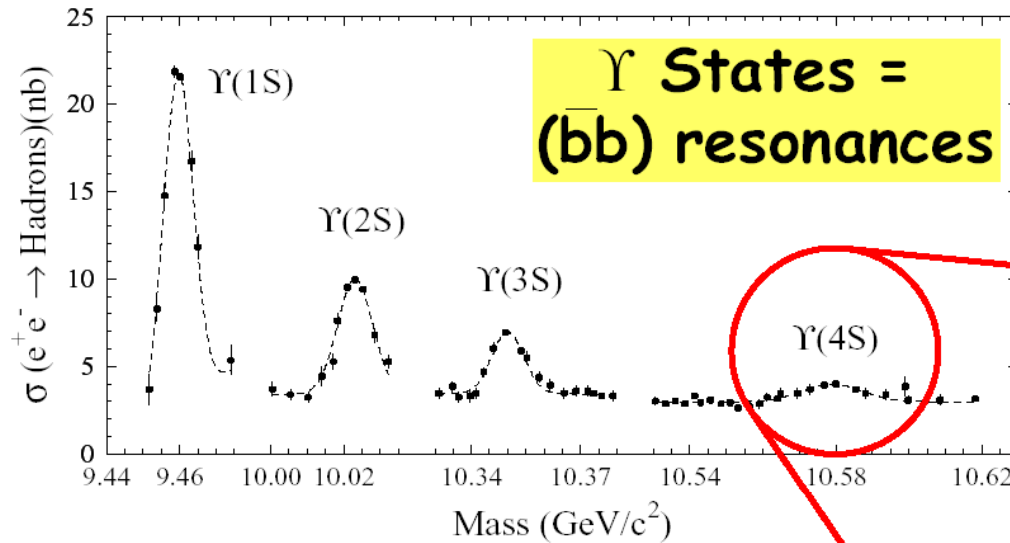


B factories: a success story

- Measurements of CKM matrix elements and angles of the unitarity triangle
- Observation of direct CP violation in B decays
- Measurements of rare decay modes (e.g., $B \rightarrow \tau \nu$, $D \tau \nu$)
- $b \rightarrow s$ transitions: probe for new sources of CPV and constraints from the $b \rightarrow s \gamma$ branching fraction
- Forward-backward asymmetry (A_{FB}) in $b \rightarrow s l^+ l^-$ has become a powerful tool to search for physics beyond SM.
- Observation of D mixing
- Searches for rare τ decays
- Observation of new hadrons

More slides...

Systematic studies of B mesons: at $\Upsilon(4S)$



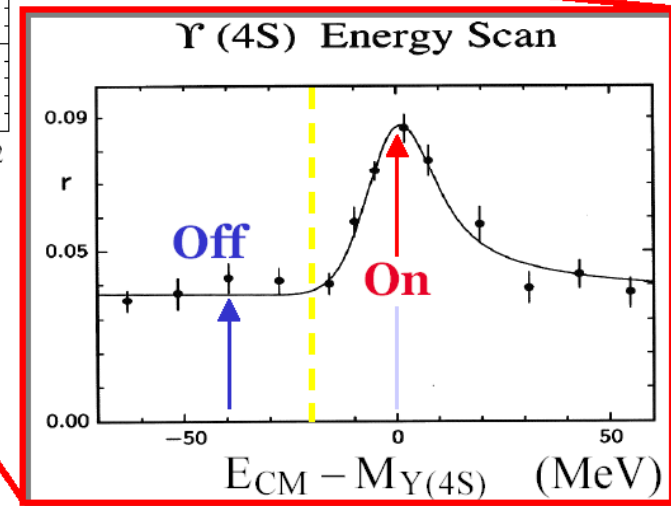
Cross Sections at $\Upsilon(4S)$:

$b\bar{b} \sim 1.1$ nb

$c\bar{c} \sim 1.3$ nb

$d\bar{d}, s\bar{s} \sim 0.3$ nb

$u\bar{u} \sim 1.4$ nb



$e^+e^- \rightarrow \Upsilon(4S) \rightarrow B\bar{B}$
 $L = 1$ state

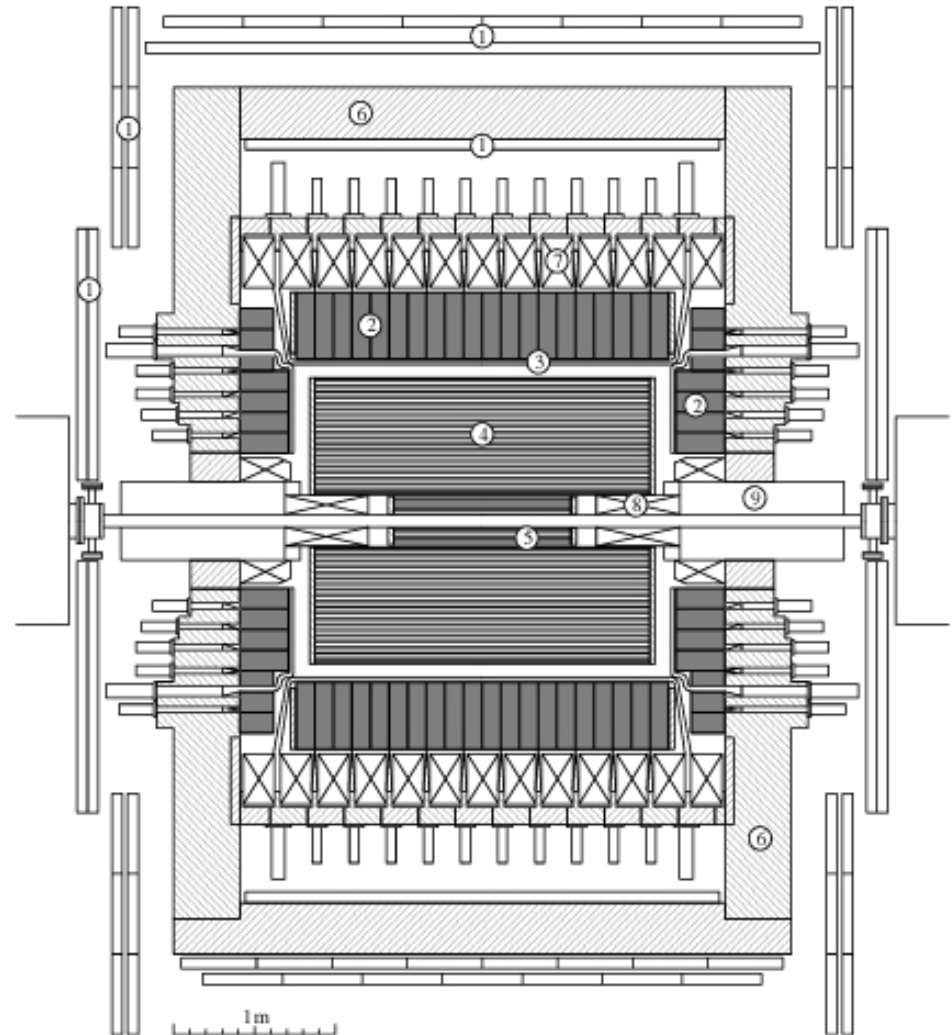
Systematic studies of B mesons at $Y(4s)$

80s-90s: two very successful experiments:

- **ARGUS** at DORIS (DESY)
- **CLEO** at CESR (Cornell)

Magnetic spectrometers at e^+e^- colliders (5.3GeV+5.3GeV beams)

Large solid angle, excellent tracking and good particle identification (TOF, dE/dx , EM calorimeter, muon chambers).



Mixing in the B^0 system

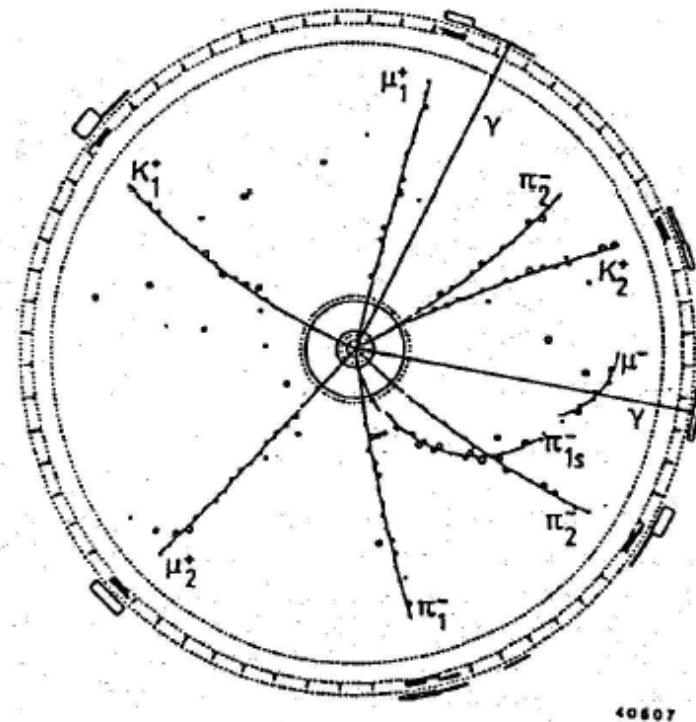
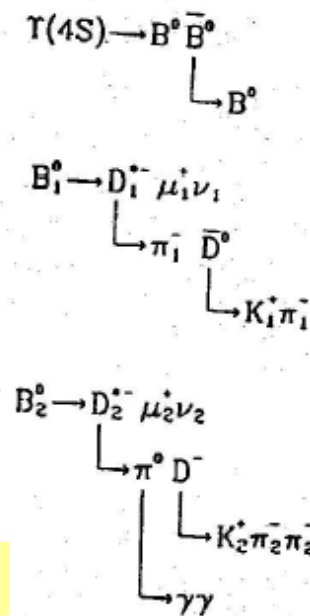
1987: ARGUS discovers BB mixing: B^0 turns into anti- B^0

Reconstructed event

$$\chi_d = 0.17 \pm 0.05$$

ARGUS, PL B 192, 245 (1987)

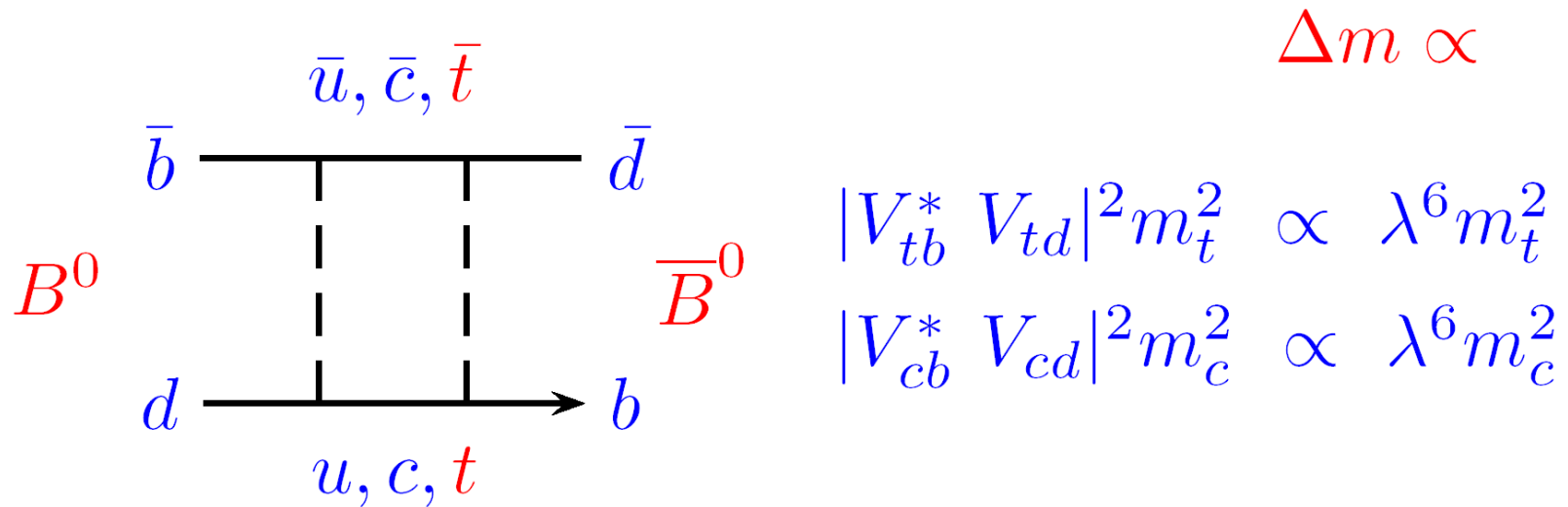
cited >1000 times.



Time-integrated mixing rate: 25 like sign, 270 opposite sign dilepton events

Integrated $\Upsilon(4S)$ luminosity 1983-87: $103 \text{ pb}^{-1} \sim 110,000 \text{ B pairs}$

Mixing in the B^0 system



Large mixing rate \rightarrow high top mass (in the Standard Model)

The top quark has only been discovered seven years later!

Time evolution in the B system

An arbitrary linear combination of the neutral B-meson flavor eigenstates

$$a|B^0\rangle + b|\bar{B}^0\rangle$$

is governed by a time-dependent Schroedinger equation

$$i\frac{d}{dt}\begin{pmatrix} a \\ b \end{pmatrix} = H\begin{pmatrix} a \\ b \end{pmatrix} = \left(M - \frac{i}{2}\Gamma\right)\begin{pmatrix} a \\ b \end{pmatrix}$$

M and Γ are 2x2 Hermitian matrices. CPT invariance $\rightarrow H_{11}=H_{22}$

$$M = \begin{pmatrix} M & M_{12} \\ M_{12}^* & M \end{pmatrix}, \Gamma = \begin{pmatrix} \Gamma & \Gamma_{12} \\ \Gamma_{12}^* & \Gamma \end{pmatrix}$$

diagonalize \rightarrow

Time evolution in the B system

The light B_L and heavy B_H mass eigenstates with eigenvalues $m_H, \Gamma_H, m_L, \Gamma_L$ are given by

$$|B_L\rangle = p|B^0\rangle + q|\bar{B}^0\rangle$$

$$|B_H\rangle = p|B^0\rangle - q|\bar{B}^0\rangle$$

With the eigenvalue differences

$$\Delta m_B = m_H - m_L, \Delta\Gamma_B = \Gamma_H - \Gamma_L$$

They are determined from the M and Γ matrix elements

$$(\Delta m_B)^2 - \frac{1}{4}(\Delta\Gamma_B)^2 = 4(|M_{12}|^2 - \frac{1}{4}|\Gamma_{12}|^2)$$

$$\Delta m_B \Delta\Gamma_B = 4 \operatorname{Re}(M_{12} \Gamma_{12}^*)$$

The ratio p/q is

$$\frac{q}{p} = -\frac{\Delta m_B - \frac{i}{2} \Delta \Gamma_B}{2(M_{12} - \frac{i}{2} \Gamma_{12})} = -\frac{2(M_{12}^* - \frac{i}{2} \Gamma_{12}^*)}{\Delta m_B - \frac{i}{2} \Delta \Gamma_B}$$

What do we know about Δm_B and $\Delta \Gamma_B$?

$\Delta m_B = (0.502 \pm 0.007) \text{ ps}^{-1}$ well measured

$$\rightarrow \Delta m_B / \Gamma_B = x_d = 0.771 \pm 0.012$$

$\Delta \Gamma_B / \Gamma_B$ not measured, expected $O(0.01)$, due to decays common to B and anti-B - $O(0.001)$.

$$\rightarrow \Delta \Gamma_B \ll \Delta m_B$$

Since $\Delta\Gamma_B \ll \Delta m_B$

$$\Delta m_B = 2|M_{12}|$$

$$\Delta\Gamma_B = 2 \operatorname{Re}(M_{12}\Gamma_{12}^*)/|M_{12}|$$

and

$$\frac{q}{p} = -\frac{|M_{12}|}{M_{12}} = \text{a phase factor}$$

or to the
next order

$$\frac{q}{p} = -\frac{|M_{12}|}{M_{12}} \left[1 - \frac{1}{2} \operatorname{Im} \left(\frac{\Gamma_{12}}{M_{12}} \right) \right]$$

B^0 and \bar{B}^0 can be written as an admixture of the states B_H and B_L

$$|B^0\rangle = \frac{1}{2p} (|B_L\rangle + |B_H\rangle)$$

$$|\bar{B}^0\rangle = \frac{1}{2q} (|B_L\rangle - |B_H\rangle)$$

Time evolution

Any B state can then be written as an admixture of the states B_H and B_L , and the amplitudes of this admixture evolve in time

$$a_H(t) = a_H(0)e^{-iM_H t} e^{-\Gamma_H t/2}$$

$$a_L(t) = a_L(0)e^{-iM_L t} e^{-\Gamma_L t/2}$$

A B^0 state created at $t=0$ (denoted by B^0_{phys}) has

$$a_H(0) = a_L(0) = 1/(2p);$$

an anti-B at $t=0$ ($\text{anti-}B^0_{\text{phys}}$) has

$$a_H(0) = -a_L(0) = 1/(2q)$$

At a later time t , the two coefficients are not equal any more because of the difference in phase factors $\exp(-iMt)$

→ initial B^0 becomes a linear combination of B and anti-B

→ mixing

Time evolution of B's

Time evolution can also be written in the B^0 in \bar{B}^0 basis:

$$\left| B_{phys}^0(t) \right\rangle = g_+(t) \left| B^0 \right\rangle + (q/p) g_-(t) \left| \bar{B}^0 \right\rangle$$

$$\left| \bar{B}_{phys}^0(t) \right\rangle = (p/q) g_-(t) \left| B^0 \right\rangle + g_+(t) \left| \bar{B}^0 \right\rangle$$

with

$$g_+(t) = e^{-iMt} e^{-\Gamma t/2} \cos(\Delta m t / 2)$$

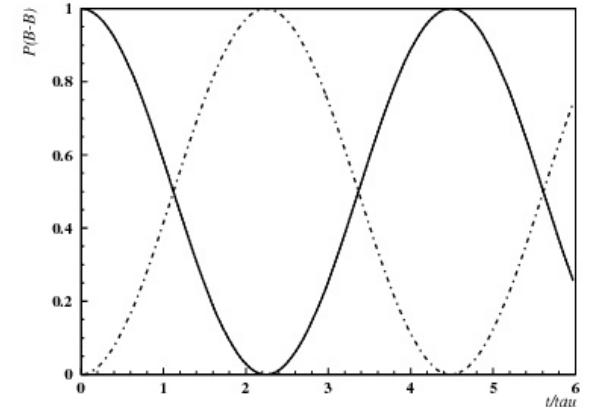
$$g_-(t) = e^{-iMt} e^{-\Gamma t/2} i \sin(\Delta m t / 2)$$

$$M = (M_H + M_L) / 2$$

If B mesons were stable ($\Gamma=0$), the time evolution would look like:

$$g_+(t) = e^{-iMt} \cos(\Delta mt / 2)$$

$$g_-(t) = e^{-iMt} i \sin(\Delta mt / 2)$$



→ Probability that a B turns into its anti-particle

→ beat in classical mechanics

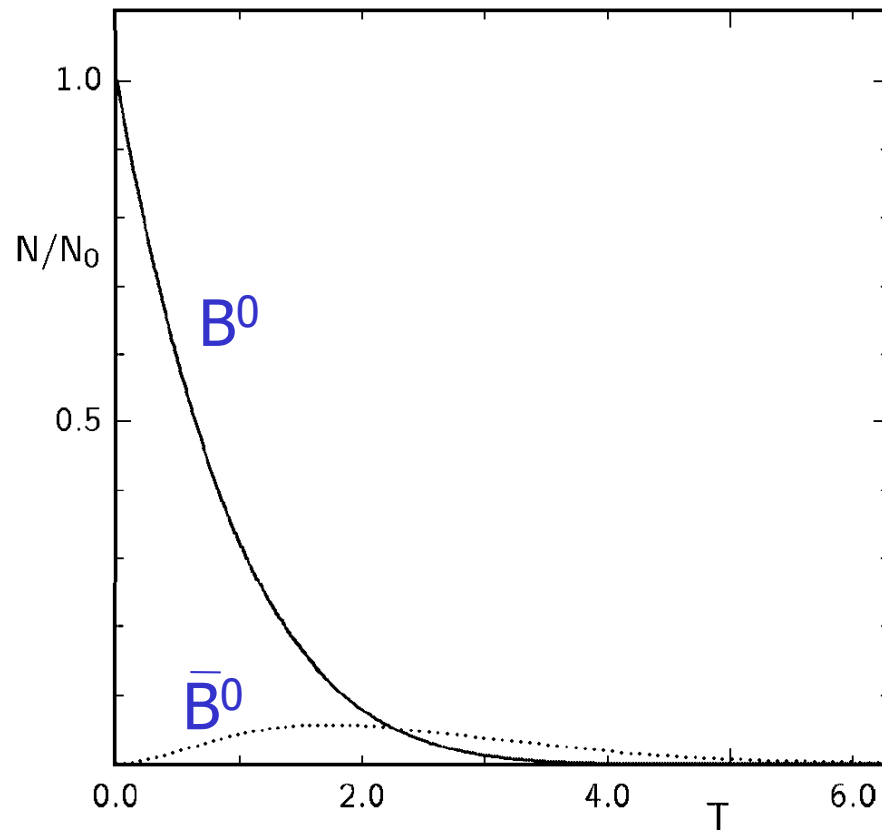
$$\left| \langle \bar{B}^0 | B_{phys}^0(t) \rangle \right|^2 = |q/p|^2 |g_-(t)|^2 = |q/p|^2 \sin^2(\Delta mt / 2)$$

→ Probability that a B remains a B

$$\left| \langle B^0 | B_{phys}^0(t) \rangle \right|^2 = |g_+(t)|^2 = \cos^2(\Delta mt / 2)$$

→ Expressions familiar from quantum mechanics of a two level system

B mesons of course do decay →



B^0 at $t=0$

Evolution in time

• Full line: B^0

• dotted: \bar{B}^0

T : in units of $\tau=1/\Gamma$

Decay probability

Decay probability $P(B^0 \rightarrow f, t) \propto \left| \langle f | H | B_{phys}^0(t) \rangle \right|^2$

Decay amplitudes of B and anti-B to the same final state f

$$A_f = \langle f | H | B^0 \rangle$$

$$\bar{A}_f = \langle f | H | \bar{B}^0 \rangle$$

Decay amplitude as a function of time:

$$\begin{aligned} \langle f | H | B_{phys}^0(t) \rangle &= g_+(t) \langle f | H | B^0 \rangle + (q/p) g_-(t) \langle f | H | \bar{B}^0 \rangle \\ &= g_+(t) A_f + (q/p) g_-(t) \bar{A}_f \end{aligned}$$

... and similarly for the anti-B

CP violation: three types

Decay amplitudes of B and anti-B
to the same final state f

$$A_f = \langle f | H | B^0 \rangle$$

$$\bar{A}_f = \langle f | H | \bar{B}^0 \rangle$$

Define a parameter λ

$$\lambda = \frac{q}{p} \frac{\bar{A}_f}{A_f}$$

Three types of CP violation (CPV):

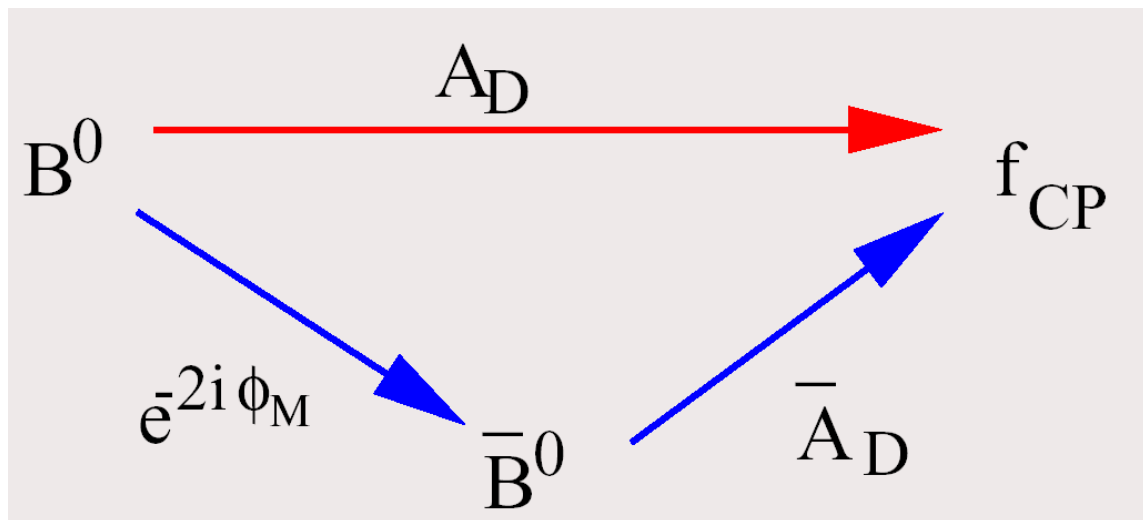
$$\left. \begin{array}{l} \cancel{\text{CP}} \text{ in decay: } |\bar{A}/A| \neq 1 \\ \cancel{\text{CP}} \text{ in mixing: } |q/p| \neq 1 \end{array} \right\} |\lambda| \neq 1$$

$\cancel{\text{CP}}$ in interference between mixing and decay: even if
 $|\lambda| = 1$ if only $\text{Im}(\lambda) \neq 0$

CP violation in the interference between decays with and without mixing

CP violation in the interference between mixing and decay to a state accessible in both B^0 and anti- B^0 decays

For example: a CP eigenstate f_{CP} like $\pi^+ \pi^-$



$$\lambda = \frac{q}{p} \frac{\bar{A}_f}{A_f}$$

We can get CP violation if $\text{Im}(\lambda) \neq 0$, even if $|\lambda| = 1$

CP violation in the interference between decays with and without mixing

Decay rate asymmetry:

$$a_{f_{CP}} = \frac{P(\bar{B}^0 \rightarrow f_{CP}, t) - P(B^0 \rightarrow f_{CP}, t)}{P(\bar{B}^0 \rightarrow f_{CP}, t) + P(B^0 \rightarrow f_{CP}, t)}$$

Decay rate: $P(B^0 \rightarrow f_{CP}, t) \propto \left| \langle f_{CP} | H | B_{phys}^0(t) \rangle \right|^2$

Decay amplitudes vs time:

$$\langle f_{CP} | H | B_{phys}^0(t) \rangle = g_+(t) \langle f_{CP} | H | B^0 \rangle + (q/p) g_-(t) \langle f_{CP} | H | \bar{B}^0 \rangle$$

$$= g_+(t) A_{f_{CP}} + (q/p) g_-(t) \bar{A}_{f_{CP}}$$

$$\langle f_{CP} | H | \bar{B}_{phys}^0(t) \rangle = (p/q) g_-(t) \langle f_{CP} | H | B^0 \rangle + g_+(t) \langle f_{CP} | H | \bar{B}^0 \rangle$$

$$= (p/q) g_-(t) A_{f_{CP}} + g_+(t) \bar{A}_{f_{CP}}$$

$$\begin{aligned}
a_{f_{CP}} &= \frac{P(\bar{B}^0 \rightarrow f_{CP}, t) - P(B^0 \rightarrow f_{CP}, t)}{P(\bar{B}^0 \rightarrow f_{CP}, t) + P(B^0 \rightarrow f_{CP}, t)} = \\
&= \frac{\left| (p/q)g_-(t)A_{f_{CP}} + g_+(t)\bar{A}_{f_{CP}} \right|^2 - \left| g_+(t)A_{f_{CP}} + (q/p)g_-(t)\bar{A}_{f_{CP}} \right|^2}{\left| (p/q)g_-(t)A_{f_{CP}} + g_+(t)\bar{A}_{f_{CP}} \right|^2 + \left| g_+(t)A_{f_{CP}} + (q/p)g_-(t)\bar{A}_{f_{CP}} \right|^2} = \\
&= \frac{(1 - |\lambda_{f_{CP}}|^2) \cos(\Delta mt) - 2 \operatorname{Im}(\lambda_{f_{CP}}) \sin(\Delta mt)}{1 + |\lambda_{f_{CP}}|^2} \\
&= C \cos(\Delta mt) + S \sin(\Delta mt)
\end{aligned}$$

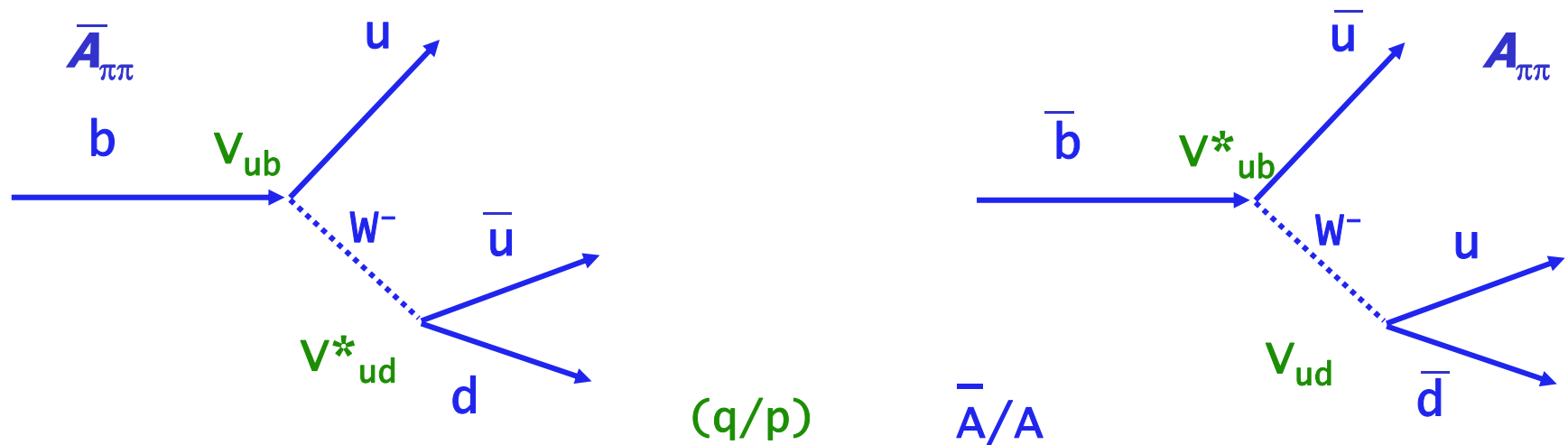
$$\lambda = \frac{q}{p} \frac{\bar{A}_f}{A_f}$$

Non-zero effect if $\operatorname{Im}(\lambda) \neq 0$,
even if $|\lambda| = 1$

If $|\lambda| = 1 \rightarrow$

$$a_{f_{CP}} = -\operatorname{Im}(\lambda) \sin(\Delta mt)$$

Decay asymmetry predictions – example $\pi^+ \pi^-$



$$\lambda_{\pi\pi} = \eta_{\pi\pi} \left(\frac{V_{tb}^* V_{td}}{V_{tb} V_{td}^*} \right) \left(\frac{V_{ud}^* V_{ub}}{V_{ud} V_{ub}^*} \right) \quad \bar{A}/A$$

$$\text{Im}(\lambda_{\pi\pi}) = \sin 2\phi_2 \quad (q/p)$$

$$\alpha \equiv \phi_2 \equiv \arg \left(\frac{V_{td} V_{tb}^*}{V_{ud} V_{ub}^*} \right)$$

N.B.: for simplicity we have neglected possible penguin amplitudes (which is wrong as we shall see later, when we will do it properly).

Decay asymmetry predictions – example $J/\psi K_S$

$b \rightarrow c\bar{c}s$:

Take into account that we measure the $\pi^+ \pi^-$ component of K_S – also need the $(q/p)_K$ for the K system

$$\begin{aligned}
 \lambda_{\psi K_S} &= \eta_{\psi K_S} \left(\frac{V_{tb}^* V_{td}}{V_{tb} V_{td}^*} \right) \left(\frac{V_{cs}^* V_{cb}}{V_{cs} V_{cb}^*} \right) \left(\frac{V_{cd}^* V_{cs}}{V_{cd} V_{cs}^*} \right) = \\
 &= \eta_{\psi K_S} \left(\frac{V_{tb}^* V_{td}}{V_{tb} V_{td}^*} \right) \left(\frac{V_{cb}}{V_{cb}^*} \frac{V_{cd}}{V_{cd}^*} \right) \\
 \text{Im}(\lambda_{\psi K_S}) &= \sin 2\phi_1 \qquad \beta \equiv \phi_1 \equiv \arg \left(\frac{V_{cd} V_{cb}^*}{V_{td} V_{tb}^*} \right)
 \end{aligned}$$

BELLE

Exp 3 Run 21 Farm 2 Event 7854
 Eher 8.00 Eler 3.50 Date/TIME Tue Jun 1 14z37z44 1999
 TrgID 0 DetVer 0 MagID 0 BField 1.50 DspVer 2.01

$$p_t \sim 1 \text{ GeV}/c$$

$$B = 1.5 \text{ T}$$

$$L \sim 1 \text{ m}$$

$$N \sim 50$$

$$X_0 \sim 2.9 \cdot 10^5 \text{ cm}$$

estimate:

$$\sigma_{pt}/p_t \sim \sqrt{[(8 \cdot 10^{-3})^2 + (0.6 \cdot 10^{-3})^2]}$$

\uparrow \uparrow
 3 p_t^2

measured:

$$\sigma_{pt}/p_t \sim \sqrt{[(3 \cdot 10^{-3})^2 p_t^2 + (3 \cdot 10^{-3})^2]}$$

how to measure?

→ calibration!

